



## FLOOD RISK IN SZEGED BEFORE RIVER ENGINEERING WORKS: A HISTORICAL RECONSTRUCTION

Csaba Szalontai

University of Szeged, Department of Geology and Palaeontology, Egyetem u. 2-6, H-6720 Szeged, Hungary

\*Corresponding author, e-mail: csaba.szalontai@gmail.com

Research article, received 3 May 2016, accepted 10 September 2016

### Abstract

Szeged situated at the confluence of the Tisza and the Maros Rivers has been exposed to significant flood risk for centuries due to its low elevation and its location on the low floodplain level. After the Ottoman (Turkish) occupation of Hungary (ended in 1686), secondary sources often reported that the town was affected by devastating floods which entered the area from north, and a great part of the town or its whole area was inundated. Natural and artificial infill reduced the flood risk to some extent after the town had been founded, but in the 19<sup>th</sup> century flood risk was mitigated by river engineering and the reconstruction of the town. The town relief was raised by a huge amount of sediment, which makes it difficult to determine the elevation of the original relief as well as the exact flood risk of the study area. However, some engineering surveys originating from the 19<sup>th</sup> century contain hundreds of levelling data in a dense control point network making possible to model the relief of the whole town preceding its reconstruction and ground infill. Based on these data, we prepared a relief model which was compared with the known data of the 1772 flood peak, from which we deduced that 60% of the town must have been inundated before it was filled up. As there could have been 50–100 cm thick natural or artificial ground infill since the 11<sup>th</sup> century, the original natural relief can be gained by deducting these data. Based on this deduction, the extent of inundation centuries ago could reach 85%, which means almost total flooding.

**Keywords:** Szeged, relief, flood, inundation map, settlement history

### INTRODUCTION

Szeged was the third most important town in the medieval Kingdom of Hungary, right after Buda and Fehérvár. The town was founded at the mouth of two big rivers (the Tisza and the Maros), so its most important potential was being an ancient junction of trading and military routes. This potential was well-utilised by its inhabitants. The economic and urban development of the town starting in the 11<sup>th</sup> and 12<sup>th</sup> centuries resulted in being granted certain privileges by the king, and Szeged became a free royal town by the 14<sup>th</sup> century.

A common principle in urban geography and in archaeology is that river mouths are one of the most important urban settlement factors. Rivers do not only provide an active connection with other parts of the world, but they also have other important features, for example, according to biogeography, rivers may guarantee tranquillity for the inhabitants of the surrounding area.

The confluence of the Tisza and the Maros Rivers exhibits similar advantages. Their valleys have been important routes connecting the Middle East through the Balkan with the central and the northern parts of Europe, and as such, they made the travel of ancient people and the spread of different economies, raw materials, lifestyles, and material cultures easier. This advantageous geographical situation should have enabled the foundation of significant human settlements at the mouth of the two rivers or the nearby riverside in different archaeological periods, which would also have meant several significant and big archaeological sites. As opposed to this,

the lack of archaeological findings and sites points to the fact that the area was mainly uninhabited before the 11<sup>th</sup> century. Neither archaeology, nor history have researched its reasons in detail so far, the presented ambiguity has not been resolved.

We finished a complex land use evaluation some years ago, which also enabled us to add a new approach to settlement history (Szalontai, 2014). Our findings indicated that the reasons for the area staying unpopulated for such a long time must be connected to the disadvantageous physical geographical features of the Tisza-Maros confluence.

A detailed analysis of archaeological sites and road networks proved that the Tisza-Maros confluence was not controlled by the ancient people directly on the riverside, but from a bit farther away. While the river mouth proved to be rather unfavourable, the water system situated 8 km farther away from the Tisza, which we are going to describe later, provided more favourable conditions. The ancient routes crossing the Carpathian Basin met here, too. By controlling the fords, the confluence of the two rivers could be overseen every period, and the more favourable physical geographical features of these places provided more peaceful life than the river mouth. High flood risk and low elevation were those two unfavourable features that hindered human settlement here the most before the 11<sup>th</sup> century.

The research of historical floods has been boosted by new findings both in national and international studies for two decades. Climate and environmental history research as well as flood research have gained more and more attention. Our primary aim was to reconstruct floods events

by the systematic analysis of primary and secondary sources as well as architectural monuments. In addition, flood-induced environmental, economic, social, architectural, and settlement historical effects and consequences of certain flood sites were studied in detail (Brázdil and Kotyza, 1995; Kiss, 2011; Rohr, 2007; Glaser, 2008).

Our previous researches aimed at identifying and classifying those landscape characteristics of Szeged which help us understand the history of Szeged and its surrounding area. We also intended to provide the basics for the development of a great and comprehensive settlement history of Szeged and its neighbourhood that is based on a new approach developed by the combined efforts of different sciences.

The present study is the continuation of the previous work (Szalontai, 2014a). Our current research questions are the followings: 1) What was the degree of flood risk at the Tisza-Maros confluence and Szeged in the centuries (and millennia) preceding the reconstruction of the town and the beginning of the river engineering works at the end of the 19<sup>th</sup> century? 2) What was the flood risk extent of medieval Szeged? 3) What influence did it have on the habitation of the area? 4) How often was the area inundated by the Tisza? 4) Where were those higher grounds that remained dry even during floods so they could ensure survival chances? 5) How did all these features influence human settlement?

The above mentioned questions are closely connected to the research interests of archaeology and settlement history as the structure of the inhabited parts of Szeged was basically determined by the connections between surface water and topography. These two features designated those morphological sites that were suitable for permanent settlement. By answering the above mentioned questions, we can identify those places that are suitable for human settlement.

We also aimed at studying why the area of the present-day town was not populated before the 11<sup>th</sup> century (in the so-called Hungarian Middle Ages), and why there are no such archaeological findings and sites that would signify the presence of permanent or, at least, frequently-populated settlements at the strategic point of the Tisza-Maros confluence. Our previous research proved that the centre of the settlement was not situated along the Tisza before the Hungarian Middle Ages, but it was situated on

the high floodplain areas of the water system surrounding the town in an 8-km diameter (Maty-ér/Maty Creek, Fehértó/White Lake, Fertő-lápos/Fertő Marsh, etc.). More significant human settlements were founded on the banks of the Tisza only from the 11<sup>th</sup> century (Szalontai, 2014b).

Finally, we also aimed at finding out whether there are hills in the area which are usually not affected by floods, but they are so close to the surrounding surface water that they can support life.

## STUDY AREA

Szeged is the county seat of Csongrád County, the largest city and the regional centre of Southern Hungary. It is closely situated to the Hungarian-Serbian border, and it is located on the boundary of two microregions: the Southern Tisza Valley and the Dorozsma-Majsa Sand Ridge (Fig. 1). The area is the lowest-lying region of Hungary, its geomorphology is characterised by the relatively small number of macro- and mesoforms (Mezősi, 1984). Its surface forms have relatively small relief (0-2 m/km<sup>2</sup>), and they are mainly of fluvial origin. The average relief is between 77-79 m asl, flood-free areas can only be found at a height of 81-82 m asl on the natural levees and the edges of Fehértó. A greater part of the area belongs to the low floodplain of the Tisza, which also surrounds the city of Szeged. The three small islands of the city rise above the surroundings as residual surfaces.

Basically, the hydrography of the study area is determined by the Tisza and the Maros Rivers as well as some smaller streams along the Tisza (Szillér, János-ér/János Creek, Tápai-ér/Tápai Creek). The River Maros hardly affected the features of the right bank of the Szeged landscape, except when its flood dammed up the water of the Tisza. The Tisza is characterised by two annual floods, which are often likely to last for half a year because they subside slowly. It also means that the land along the river is inundated almost continuously. As the medieval part of Szeged lies in a basin-like area, the somewhat higher ridges along the Tisza prevent floodwater from flowing back into the main river channel, which results in longer floodings. The second important water network around Szeged (Maty-ér, Fehértó, Baktó) has an 8-to-10-km-wide

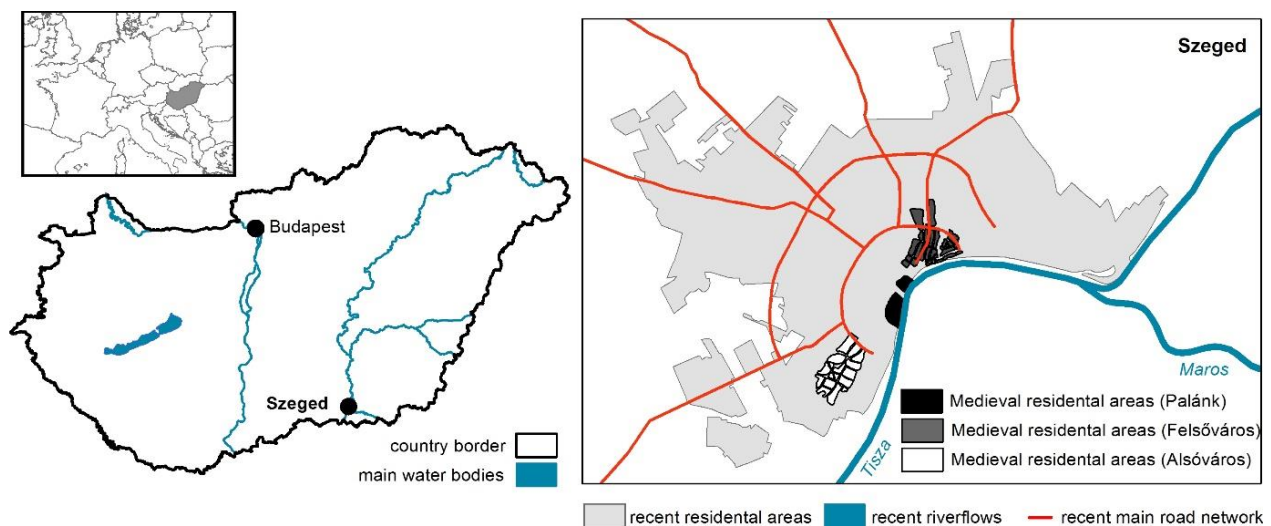


Fig. 1 The location and map of the study area, demonstrating the recent and the medieval residential areas

diameter, and it totally surrounds Szeged. The two water networks have different flood risk characteristics. The Maty-ér, Fehértó, and Fertő-láposza receive water input from the Kiskunság Sand Ridge (Homokhátság) lying between the Danube and the Tisza. This water input includes both surface and subsurface water flows, which fill the pools, basins, and channels along the boundaries of the Sand Ridge. These water flows are slow, static, and of little or no dynamics, they reach the Tisza from beneath Szeged, and they cross the natural stream channels without any obstacles. They have no flood risks in general. This water network is accompanied by unflooded ridges, and the arable lands found here are of the best quality.

As opposed to this, the water network situated on the east is connected to the dynamically changing gauge height of the Tisza, and its parts pose a regular and devastating flood risk due to the two annual floods of the Tisza. The relationship of Szeged and the Tisza is totally different from the usual river-settlement relationship, where every change occurring on the river affects the structure and the safety of the accompanying settlement. Secondary sources documenting floods in Szeged have never reported that the Tisza would have flooded the town by stepping over its banks in the city. Some documents say that the embankment situated on the outer arch of the city-side of the river was washed away, and they also mention that the eastern wall of the fortress standing directly on the riverbank was destroyed by a flood. But there is no data proving that the city would have been totally flooded.

The Tisza always floods the city from the north. The right bank of the Tisza to the north of Szeged is accompanied by a 30-km-long and 2-to-4-km-wide low floodplain which used to carry flood flows downstream. The three small islands where the oldest parts of Szeged were founded are situated on the low floodplain with an average height of 1-1.5 m. Floods usually flowed around these islands: one part of the flood flow passed round from the eastern area of the town, the other part passed round the islands from the north and the west, and they returned to the main channel of the Tisza beyond the town further downstream. In addition, the island of Felsőváros (Upper Town), which is one of the ancient city parts, was divided by several smaller streams which carried water from the low floodplain downstream into the Tisza. These streams also allowed bigger floods to inundate even these older parts of the city. The above mentioned characteristic of the city's location meant a relatively high flood risk, which was further strengthened by unusually high floods.

## DATA AND METHODS

### *Methodology*

In order to answer our research questions, we had to reconstruct the hydrographic and geomorphologic environment preceding the land use changes that occurred in the 19<sup>th</sup> century. By reconstructing the original natural circumstances, we could also get an insight into the circumstances that characterised the different archaeological periods.

A detailed study of the original relief and geomorphology is greatly complicated by the fact that the number of the sources is very scarce, which makes the research object very difficult to investigate. It is obvious that our

primary task is not the investigation of historical sources, instead we have to focus on preparing geological surveys/bores that cover the entire area of the city in the greatest possible number, and we have to prepare the model of the original terrain based on these data, and, finally, we have to display historical changes with the help of the so-prepared model. Since such a model is not available for us at present, we are forced to make use of historical data and reconstruct the original relief of the city with the complex analysis of the available historical sources.

Although the historical sources provide useful general information about the structure and the relief of the city, they do not abound with accurate data. Even the great number of available secondary (written) sources (certificates, travel literature, military reports, etc.) do not contain data on topography. In case they do, they usually emphasise the lowland character of the landscape, and they rarely mention the "Öthalom" hills (literally Five Hills) which are residual surface elements with an average of 12-15 meters. The geographical names of the area may contain names with the word "mount", but they are not of morphological origin, they refer to former vineyards. Flood descriptions often mention flood free (dry) islands as well as floods flowing through most of the town without any obstacles.

The research was made further difficult by another characteristic of Szeged. The city was completely destroyed in the 1879 flood, and, during the rebuilding of the city, its residential areas were filled up with a considerable amount of land lifting the relief but also forever concealing any traces of the original terrain. Therefore, in order to investigate our questions concerning settlement history, we have to reconstruct the geomorphology characterising the area before 1879. Then, we will be able to identify those city parts which were inundated or usually dry by analysing flood data.

Filling up the inhabited parts of Szeged and the basins between them with soil was a known practice before the 19<sup>th</sup> century, which resulted in a gradual decrease in the size of the flooded areas. However, the enormous work that began in 1879 surpassed all previous landscape-changing work and was considered a rare and unique process both in Hungary and in Europe. Its primary purpose was to reduce flood risk, and in order to do so, the ground level of the Downtown area was going to be raised to the height of 822 cm compared to the 0 cm of the stream gauge of the Tisza, which corresponds to 81.92 metres above the Baltic Sea level. There is no doubt, however, that the entire area of the Downtown was not intended to be covered by a homogenous layer. The final version realized was even simpler, in fact, only roads and streets were filled in while the gardens and yards of the houses were no, so there were level differences up to a meter within relatively small distances, such as a house and the street in front of it, which has characterised Szeged since then. So, while the streets are artificially infilled and lifted terrains, the elevation of the gardens and yards of the houses did not change essentially (Kuklay, 1880; Lechner, 2000).

A 3-4-meter-thick or even thicker layer was filled in only into former pools and surface streams, but the entire area is characterized by a 1-2-meter-thick layer (Kaszab, 1987). The thickest infill in the three ancient parts of Szeged can be found in Palánk (City), while the thickness of the infill is not significant in Alsóváros (Lower Town) and

Felsőváros (Upper Town). A new city structure was developed during the reconstruction. The new structure was characterized by a network of boulevards and avenues, all of which lay higher than their surroundings, the ideal infill height was only kept along the road network. As a result, all side streets rise toward the main streets even nowadays.

The natural or artificial lifting of the terrain level of populated areas is not an unknown phenomenon in European towns. It was a well-known practice even in different archaeological periods, which practice resulted in distinctive, interdependent settlements built on each other. It is a natural phenomenon that settlements, especially cities, having been inhabited for centuries or millennia, have several meters thick infill layers (Puskás, 2008). In Moscow, for example, this layer is 2-5 meters thick, but natural depressions may also have a 20-meter-thick infill. Thus, three typical geomorphological forms can be created in cities: excavated (hollow, negative), graded (levelled) and accumulative (cumulative, positive) (Puskás, 2008; Farsang and Puskás, 2009). The resulting infill can be sediment of natural origin, or soil-like material, and can be artificial material (debris, gangue, waste, etc.).

Due to the infill of the city, we have to look for maps that were prepared before the reconstruction. It led us to investigate the topographical data of those handwritten or printed maps that were created before the end of the 19<sup>th</sup> century, which finally helped us to prepare the topographical reconstruction of the historical town centre. Our previous research did not make use of these maps, although more of these scaled city maps that were prepared before the 1879-1890 city reconstruction contain elevation data. Their importance is also great, because only these maps contain exact data about the original (i.e. preceding the reconstruction of the city) topographical features of the area so they are essential for the topographical reconstruction.

Reducing flood risk was a regularly recurring need and demand in the 19<sup>th</sup> century Szeged, but to plan this, a general survey of the area had to be done first, with a special attention to surveying elevation. Otherwise it was not possible to start planning river engineering. Thus, the first such map was created in 1830 (Map 1, Buday 1830), but the overall survey took place only a few decades later when, due to the 1879 flood, the destroyed city had to be completely rebuilt (Maps 2-4, Barilari et al., 1879, Heller, 1880, Kuklay, 1879). The consistent and accurate use of elevation data was made easier by 45 iron rods that had been installed as fixed points, and which were intended to promote mapping and rebuilding the city (Map 5, Halácsy, 1879) (Halácsy, 1879; Bertalan, 1884).

After digitizing the maps having been collected during the research, they were georeferenced, then their elevation data were visualized in an EOVS system using a GIS program, and they were also recalculated to the present value of meters above the Baltic Sea level (m asl). No compiled city maps depicting the iron rods were made, but each iron rod had a very accurately drawn on-site sketch, which made it possible for us to identify their position as accurately as possible. Therefore, we could locate each reference point and its elevation on the georeferenced city map.

When identifying the original terrain characteristics of the area before the reconstruction and the infill, we also had to pay attention to determine the ground level associated with

the elevation data, because elevation data were measured in meters above the Adriatic at the end of the 19<sup>th</sup> century. The Baltic baseline is 0,675 meters higher than that of the Adriatic baseline, i.e. the absolute values of the Baltic heights are that much smaller than the values of the Adriatic heights. There was one independent reference point in Szeged, to which all architectural plans were aligned: it was the 0 point of the stream gauge of the Tisza River (73.70 m asl) (Vágás, 1991). The reason why it is important to emphasise 0 as a reference point is that, for example, when giving the thickness of the infill layer, this thickness was given compared to the 0 point of the stream gauge. Six meters of infill does not mean six meters of soil, it means that compared to the 0 reference point of the Tisza, the level of the terrain was lifted with 6 meters. That is, the Tisza 0 point + 6 m + 74.37 m above Adriatic sea level -0.675 m = 79.7 m above Baltic sea level.

After the terrain reconstruction, the collected elevation data were compared to the peak values of the floods, then by depicting them on a map we were able to locate those areas which were more likely to be inundated when a higher flood occurred. To do so, we utilized the flood data which were less influenced by landscape-changing human activities. It means using those data which originate from the time when floods occurred in a natural (non-engineered) riverbed, flood control works did not hinder flood flow, and floodwater returned to the original river channel naturally. These requirements are necessary because archaeological and historical flood risk cannot be compared to such floods of which causes or flow were influenced by significant human activities. Therefore, useful and credible data can only be gained from the times preceding river engineering. Thus, we used the data of the 1772 flood as our standard flood level data, which peaked with 630 cm (80 m asl above the 0 point of the Tisza stream gauge in Szeged). It was not the biggest flood Szeged had to suffer, but it was one of the last floods which was neither caused nor influenced by human activities, and there were accurate data on the highest flood level. There were bigger floods in the 18<sup>th</sup> and 19<sup>th</sup> centuries (1851: 80.61 m), and there were even higher average flood peaks between 1772 and 1850 (80.11 m asl), but we deliberately underestimated the extent of the potential risks a little bit (Fig. 2).

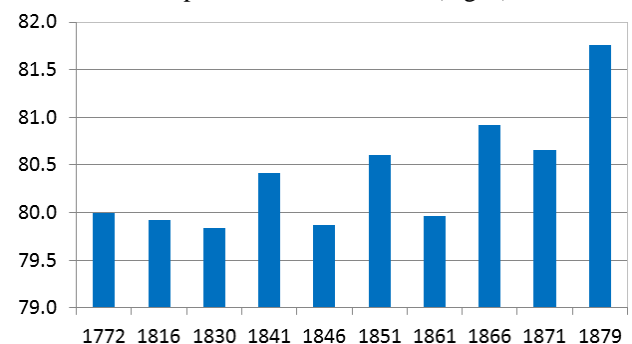


Fig. 2 Data of the highest floods on the Tisza (m asl) (Vágás, 1991)

We carried out the following analyses with the data of the studied maps. We indicated the elevation data on the original and the georeferenced maps one by one. We divided the measured points into 3 groups on the basis of

the highest flood water level in 1772 (630 cm over the 0 point of the Tisza stream gauge = 80.00 m asl):

- inundated points;
- saturated points, which are situated 20 cm higher than flood level;
- flood-free (dry) points.

Subsequently, we performed the same process, but we subtracted 50 cm from the 19<sup>th</sup> century elevation data assuming that it equals with the amount of natural infill of the area between the 11<sup>th</sup> and the 19<sup>th</sup> centuries. Based on these data, we divided the elevation data into three groups again.

Finally, we simultaneously visualized all data of the five maps by copying them into one file, then we carried out the above mentioned classification again. We also carried out an analysis where we calculated with a 100-cm-thick infill since the 11<sup>th</sup> century settlement. In order to provide easier orientation, we indicated the contemporary major road network (avenues

and boulevards) as well as the earliest settlement structure of Szeged on the original map.

#### *The detailed description of the applied historical maps*

Map 1 (Buday, 1830) is one of the most accurate and detailed maps from the first half of the 19<sup>th</sup> century, which depicted the outline of all surface water on the town structure, and both the height of water level and that of the walking level were given everywhere. The data were given in Viennese feet / inch units, and the then highest flood peak data of the year 1770 were also given in the same units. A total of 70 elevation data were recorded, 44 of which were numbered. Data measured in the streets, on the water level of Eugenius Ditch and its trench are also included in the elevation data (Fig. 3a,b).

Map 2 (Barilari et al., 1879) depicts the entire area of the city, its street network, street names, all houses, and the data of 203 measured points. The survey was carried out mainly during and after the flood receded. Slope calculations

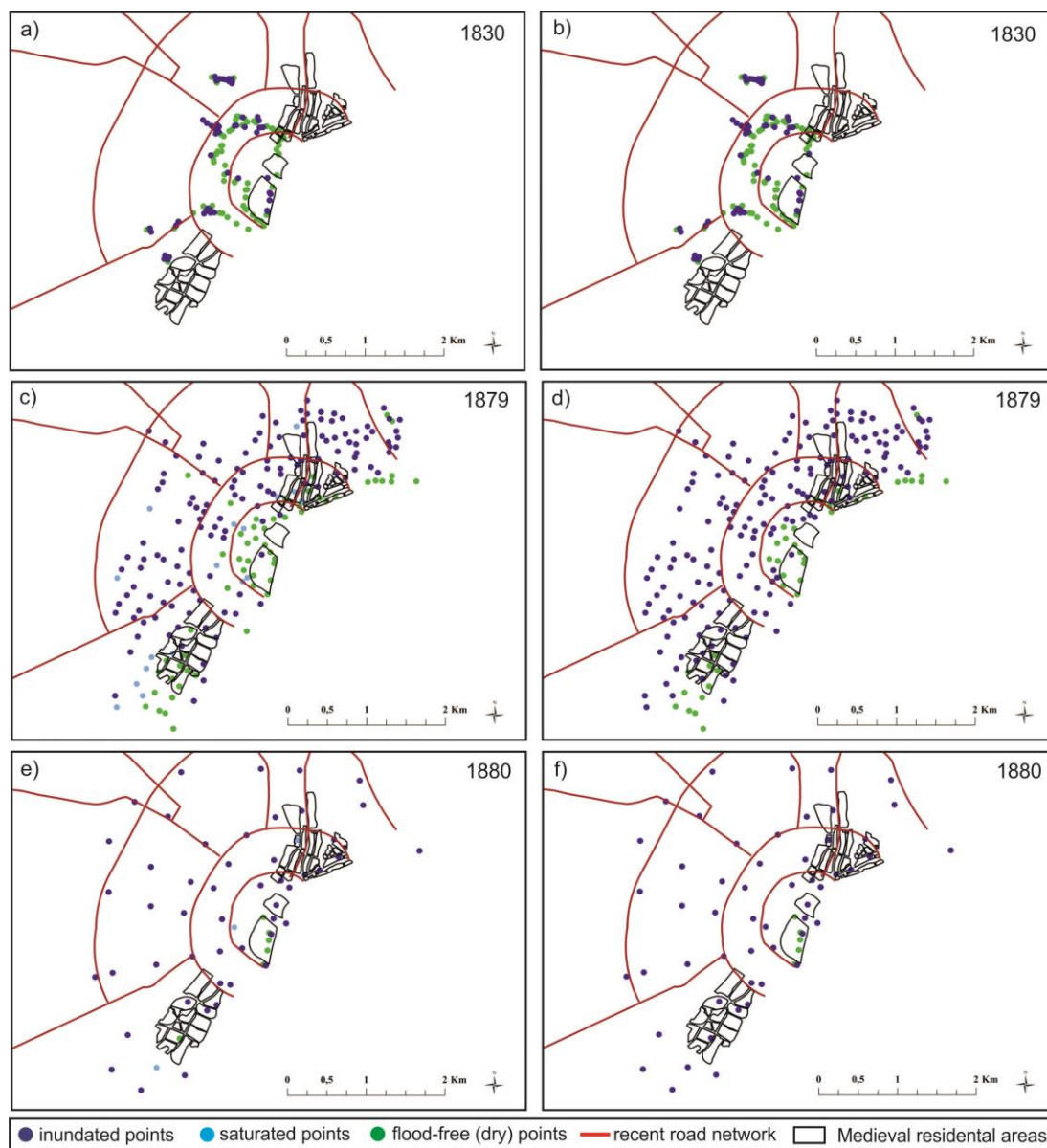


*Fig. 3* Location of inundated and flood-free points in the city a) on the basis of Buday (1830); b) on the basis of Buday (1830), calculated with 50 cm infill; c) on the basis of Barilari et al. (1879); d) on the basis of Barilari et al. (1879), calculated with 50 cm infill; e) on the basis of Heller's map depicting boring sites (1880); f) on the basis of Heller's map boring sites (1880), calculated with 50 cm infill

were done in the inner area of the city to determine elevation differences, and the elevation layer plan of the city was developed on the basis of these calculations (Kulinyi, 1901). Elevation values were given compared to the 0 point of the Tisza stream gauge (Fig. 3c,d).

Map 3 (Heller, 1880) depicts the ground-plan of Szeged as it was before the flood. The works were organized by B. Kuklay, a royal assistant engineer appointed to help the Royal Commissioner of Szeged, and B. Zsigmondy engineer, who also evaluated the data (Bertalan, 1884). There are 63 boring points on the map, which were drilled with augers between April 4, 1879 and December 15, 1880. Measuring points were designated to gather data about the entire area of the city, but first of all the three major city parts, especially the central squares. Additional data were collected on such sites which had hydrographic, topographic, or town-planning importance (e.g. Mars Square and vicinity). The map also includes the drilling profile of the "Geological Cross-section of Lajos Tisza Boulevard artesian fountain 1: 2500" as well as the section drawings of the "Geological layer plan of the Royal town of Szeged". The eight sections have scales, the elevation of the surface (above the Tisza 0 point marked with a line and text as well) is also written on the surface (e.g. +6.75) (Fig. 3 e,f).

Map 4 (Szeged, 1879) depicts the entire area of the city, street network, street names, all buildings and land lots. Areas covered by water were indicated with blue colour. Elevation values were given compared to the 0 point of the Tisza stream gauge. The data come from the 1879-survey of Kuklay, in which a total of 110 points were measured. In several cases, it happened that he measured at the same location

as the data indicated on Map 3 (e.g. at the two corners of the same street), but the values did not correspond to each other. As a point definition of these places is no longer possible, we treated both values as authentic and included them into our database (Fig. 4a,b).

Finally, Map 5 (Halácsy, 1879) depicts the points (87 pieces) that were placed out for triangulation in order to help mapping and rebuilding the city, among which 45 pieces were cast iron rods and 42 were marked wooden posts (Halácsy, 1879; Bertalan 1884). The iron rods were marked with Roman numbers from I to XLV, and each of them had two designated elevation data: one indicated the elevation above the 0 point of the Tisza stream gauge, the other one indicated meters above the Adriatic (Fig. 4c,d). A number of outskirts points were also designated by elevation data. The work was carried out in July-August 1879, when the city was still partly inundated, and there were lots of ruins.

Each rod and post had an own data sheet which contained a few lines in handwriting about their exact location, the property where they were placed out or they were the closest to, and each property was marked with the number of the respective rod or post. In addition, a 1: 1000 scale sketch was also prepared depicting all of the important landmarks, rods, and posts as in a plan.

We continued to survey the extent of flood risk on the basis of the maps mentioned above. We know a lot of floods from the history of the city, so we have to classify the area as having high flood risk on the basis of its historical data already. However, only a detailed analysis of the data can answer the question whether it was always true for the entire city or there were dry, flood-free spots in the flooded area.

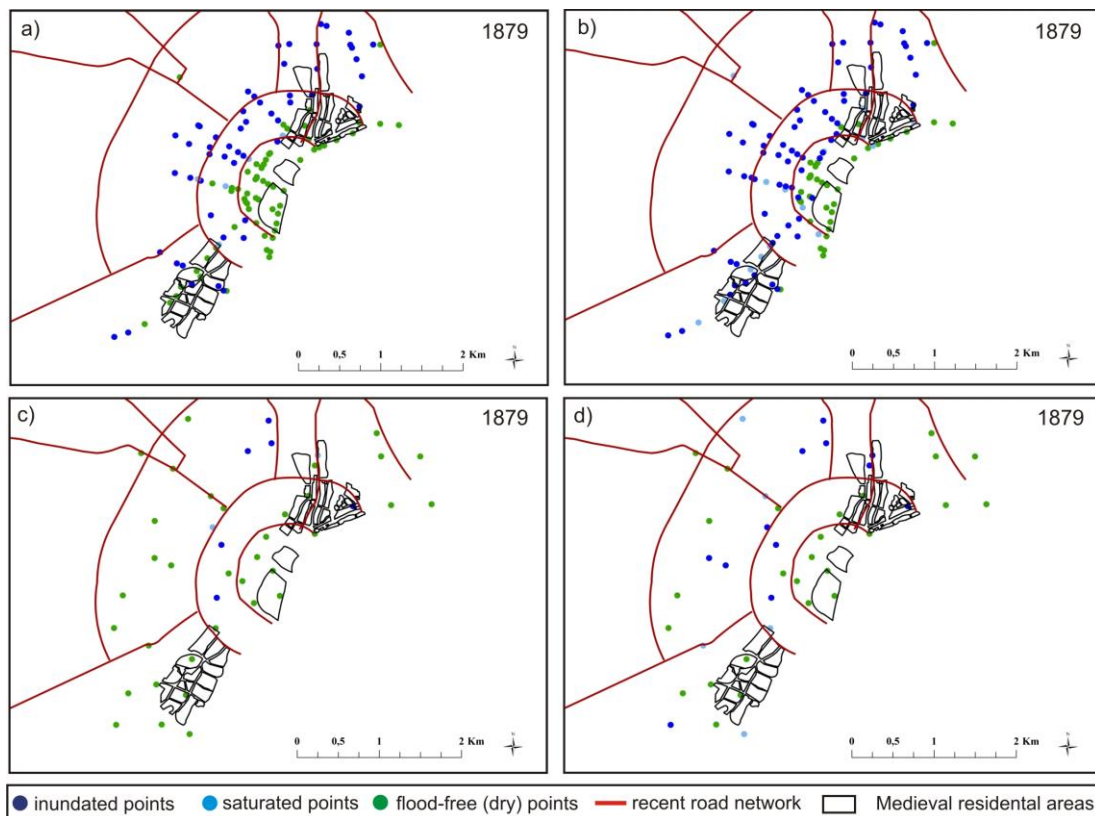


Fig. 4 Location of inundated and flood-free points in the city a) on the basis of Kuklay's map (1879); b) on the basis of Kuklay's map (1879) calculated with 50 cm infill; c) location of inundated and flood-free points in the city based on the number of iron survey posts a) based on Halácsy's map (1879); d) on the basis of Halácsy's map (1879), calculated with 50 cm infill

## RESULTS

### *The topography of Szeged*

Those anthropogenic activities that shape the downtown area of contemporary Szeged have been present for nearly a thousand years. Landscape transformation is likely to have begun in the early settlement times when people started to change the terrain in order to securely possess central areas. It was not a major influence on the landscape back then because it was not a primary goal to change the functioning of the natural environment. The inhabitants' will to adapt to nature was still stronger than the force to change the environment.

The second phase is the post-Ottoman city-forming period when two types of landscape changing activities took place. First, there was a conscious and significant reconstruction of the city structure (e.g. building Eugenius Ditch which was a fortification system around the inhabited parts of the city). Second, there was an increasing demand for more and more area which also facilitated stronger landscape changing activities. This period had a stronger impact already but it had little impact on the landscape and topography yet. However, former depressions around the islands were started to be infilled, and the surface of the islands was also subject to levelling.

In the third phase, the settlement structure became stable by the middle of the 19<sup>th</sup> century, and, in addition to the already existing landscape changing activities, the city experienced a significant external impact in the form of recurring floods of the Tisza River. Hundreds of houses collapsed in the inundated city, and after the flood retreated, the ruins were certainly used locally for grading, for example, or for levelling elevation differences. The 1867 flood had the greatest influence on the city: this period saw the reconstruction and the infill of the city's inhabited areas to reach the ideal level as well as the infill of the inner part of the city.

By analysing the database of the five maps previously described, we can see that the elevation values varied between 77 and 83 m asl (Fig. 5) by the 19<sup>th</sup> century. One of the outstandingly high data among the 83 m asl values definitely refers to the height of a flood control dam, so it is not a relevant data.

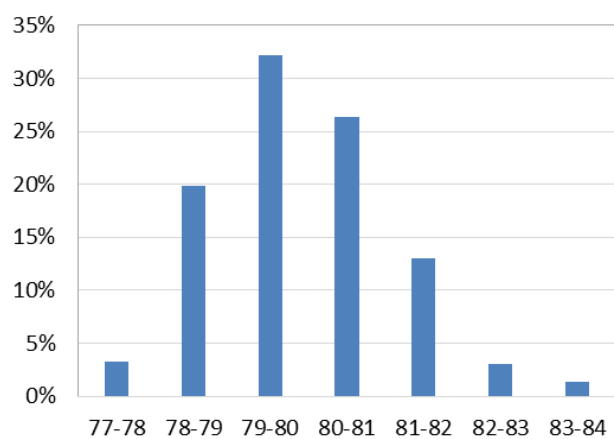


Fig. 5 Height distribution of the survey points (m asl) in the database

Only a few data were included in the extreme range, 55.24% of the points were shorter than 80 meters (the flood peak of the Tisza was 80 meters in 1772). If we also add those data which are in the high-risk data range of 80-81 m, then we can see that a significant part of the city, i.e. 81.59 % of the measured points can be found under the critical 81 m asl. The highest values (above 82 m asl) typically occur in a narrow stripe along the Tisza, which values clearly indicate initial bank dikes and natural levees. In addition, these high values often appear along the Eugenius Ditch (an earth trench built as fortification at the end of the 17<sup>th</sup> century) too. The mean of all points is 79.85 m asl (Fig. 6).

Unfortunately, the elevation data of Map 1 cannot be used here as its lowest points indicate such channels and pools that were either temporarily or permanently covered by water. The purpose of its creation was not the levelling of the city, but the survey of the water-filled pools, therefore the measuring points do not show the relief of the city. The highest points of the survey can be found either along the Tisza or on the city side of Eugenius Ditch, which points designate artificial dikes along the water.

The results correspond to the known data of the topography of the city well. Earlier reconstructions (Reizner, 1899; Kaszab, 1987; Blazovich, 2002) reached the same essential conclusion. J. Reizner proved very early that Szeged was founded on those three islands which we knew as Palánk (City), Alsóváros (Lower Town) and Felsőváros (Upper Town) later. He was the first to utilize scientifically the results of the drillings that had been carried out 20 years earlier, and he evaluated the data not only from a geological point of view, but also in terms of settlement history.

Topographic data (Fig. 7) also show that the different parts of the city and the area between them were divided into several small pools that were permanently covered by water (called as "csöpörke" in Szeged). They were regularly filled with water during floods, and it took a long time for them to dry up completely, so it was very difficult to utilize the suitable parts of the islands.

All three islands are residual surfaces located directly on the riverfront. Their slightly higher surfaces by the river can be defined as narrow natural levees which are characteristic of meandering channels (Kohán, 2003; Molnár, 2011). The edges of the islands that are farther away from the Tisza gradually sink toward the direction of the lower terrains, so the area beyond the islands becomes deeper, and closed pools do not let flood water flow back to the river. Those parts of the city that are situated even more distant from the Tisza may lie even deeper, the elevation difference may reach up to 1-2 meters compared to the levees.

This drainless area character was the reason for the 1879 flooding to downflow so slowly; it took a half year to get rid of the water in the inhabited parts of the city, and even then steam pumps had to be used. But this nature was the cause of another common phenomenon: several-day-long rainfall could cause serious aerial floods in the city (Lechner, 2000).

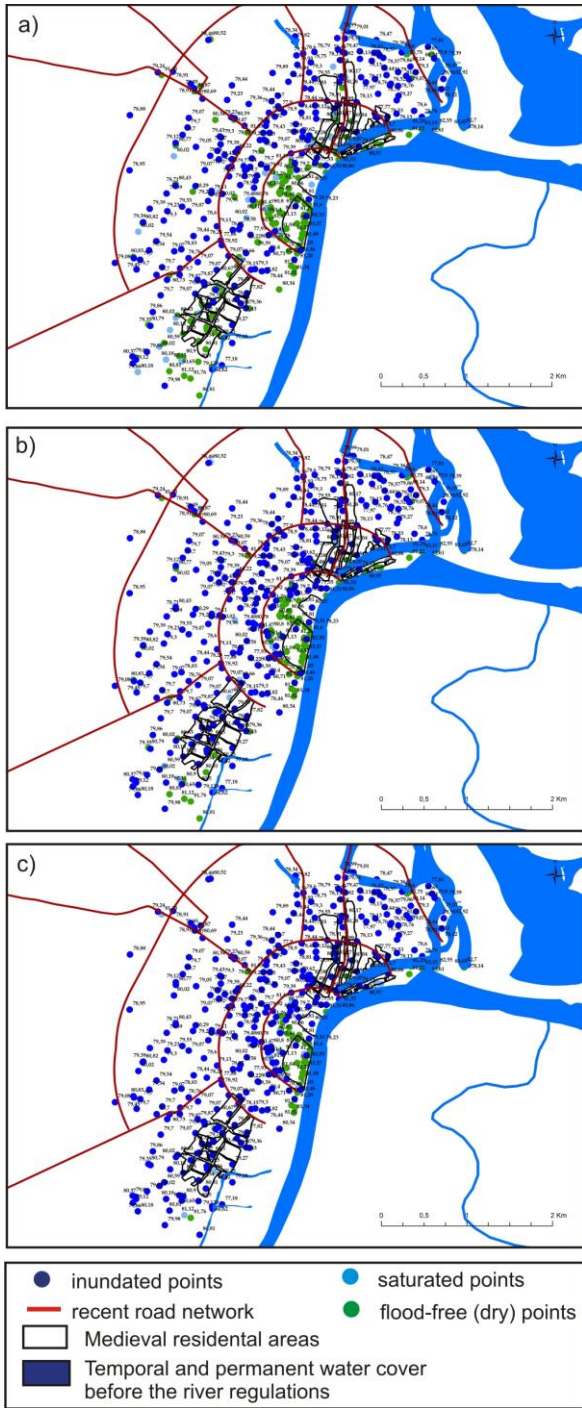


Fig. 6 Location of inundated and flood-free points a) on the basis of all height points depicted on the map; b) calculated with 50 cm infill; c) calculated with 100 cm infill

The geomorphological features of the islands were also different. The middle island (Downtown) was the highest of the three islands. Other parts of the city which are usually situated farther away from the central part of Felsőváros (Upper Town) lie lower than the rest of the city. Obviously, it also means that these parts of the city were inundated first when flood waves from the north arrived. Present day Rókus and Makkosháza are also characterized by lower terrain, but they were not inhabited in the Middle Ages. A significant part of Alsóváros (Lower Town) is also considered to be low-lying save its southern end where the elevation of the surface reaches that of the Palánk (Fig. 7).

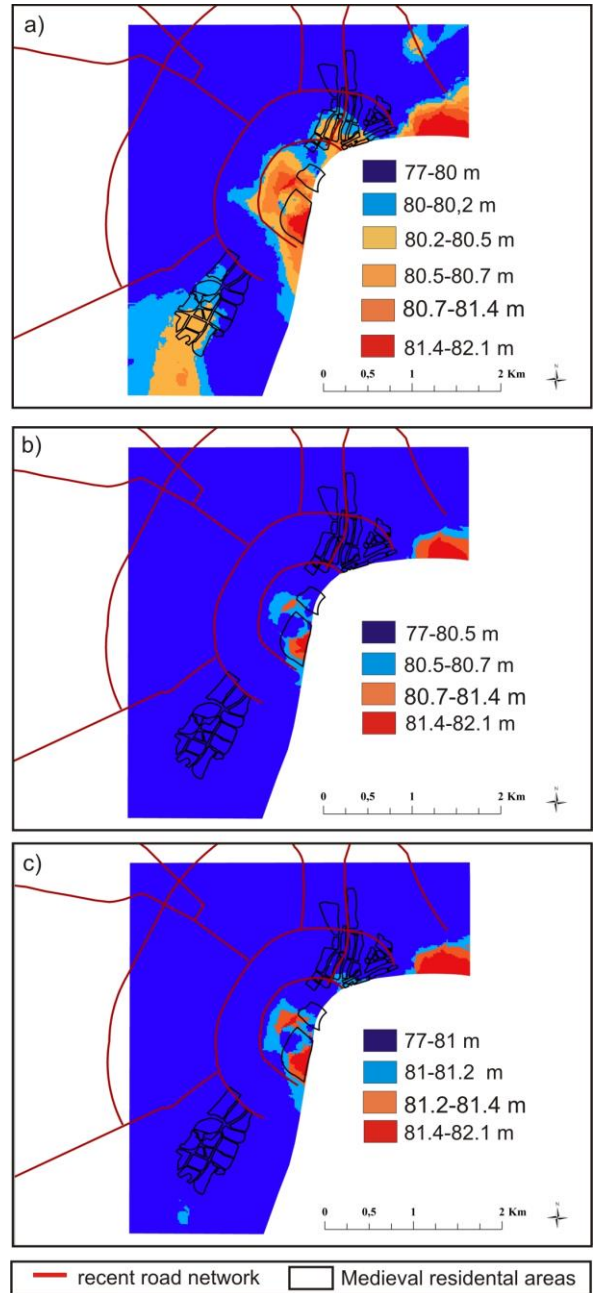


Fig. 7 Relief models of Szeged before the great flood a) on the basis of map data; b) calculated with 50 cm infill; c) calculated with 100 cm infill

*Flood risk of Szeged*

According to scientific literature, flood-proof settlement level is marked at 6 meters above the 0 point of the Tisza stream gauge (Nagy, 1957), which is 79.70 m asl in the case of Szeged. For this reason, the research assumes that prior to 1879 those parts of Szeged which lay below 77.32 m asl were hardly habitable, while large areas of the city lay either at or below 75.32 m asl (Vágás, 1991).

The newly processed data clearly show that a high flood would not inundate about half of the city by the end of the 19<sup>th</sup> century. However, it is clear that it could hardly have been valid in previous centuries or millennia, and already in the early Middle Ages the city had very high flood risk. If we do not take the 50-100 cm thick infill originating from urban



planning into account, the elevation of the measured points reduces, and, therefore, the number of inundated points greatly increases.

These data and results spectacularly demonstrate that the low-lying terrain of Szeged, which characterized the city before the reconstruction, meant extremely high flood risk, and virtually the entire territory of the city was equally affected. However, this risk continues to grow if remember the simple fact that it is not just inundation that causes damage, but also those seemingly dry city parts are greatly affected where the soil is saturated from beneath, furthermore the waves caused by the wind could also pose further damages on the dry surfaces. Flood damage does not end at the water level, however, we had to define damaged area in our present study so we considered those area damaged which lay 10 to 20 cm above the highest flooded water level. Saturated areas also become totally useless, life is limited here for a while, too. So, if we examine flooded and saturated areas together, an even higher proportion of the inhabited parts of the city is affected by the flood.

Visualizing the processed data on a map meant important new results, as it was the first time that we could assess the extent of flood on the basis of accurate figures (Fig. 6-7). However, if we subtract the values of the assumed 0.5-1 meters thick infill layer from the data gained from the map analyses, it is even more clearly visible which parts of the city were affected by a high flood.

This result also indicates that in climate cycles similar to the 18<sup>th</sup> and 19<sup>th</sup> centuries the extent of inundated areas might have been the same. It also became clear that before the foundation of the town, 86% of the measured points was certainly inundated when a higher flood occurred on this low-lying terrain, which was due to the absence of a thick, either natural or artificial infill layer (Fig. 8). It means an almost total inundation actually.

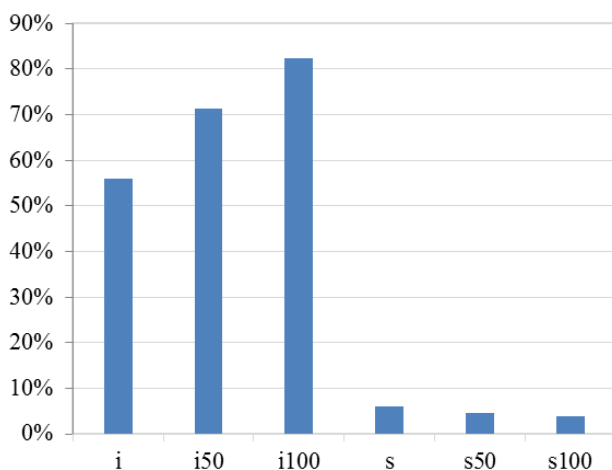


Fig. 8 Normal inundation extent of the points in database (i: inundated, s: saturated), as well as calculated with 50 cm infill (i50, s50) and 100 cm infill (i100, s100)

The reliability of our method can be checked easily. We marked the elevation points on the inundation map of the 1879 flood, and they obviously indicated a total overlay with the inundation of the city which means that our results are correct (Fig. 9).

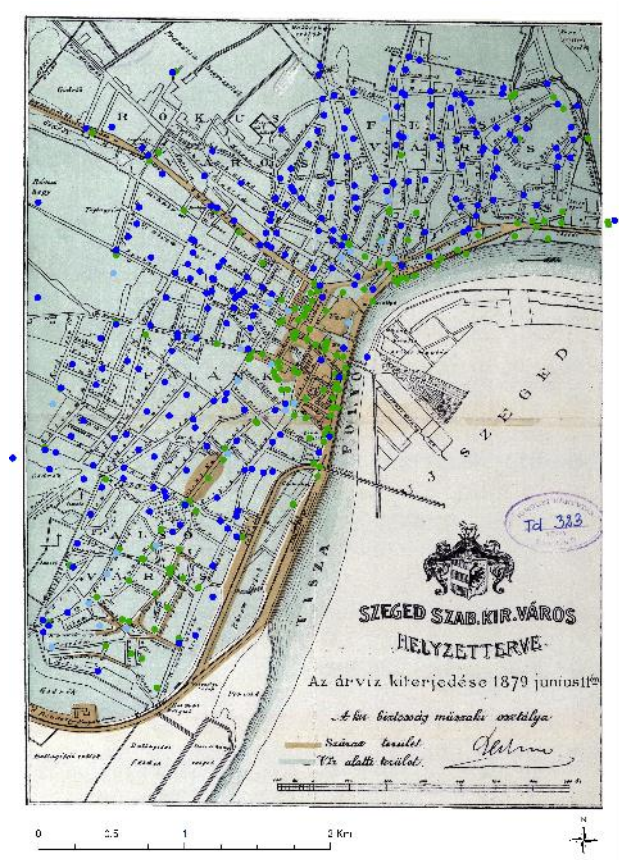


Fig. 9 a) Location of the studied points on an inundation map dating from 11 June 1879 (Action Plan, 1879); b) Medieval city structure on an inundation map dating from 24 July 1879 (Action Plan, 1879)

Since the primary purpose of our present study was to analyse the flood risk of the study area during a much longer time period, we must also emphasize that the highest flood was compared to the levels measured in 1879. In addition, we also found data that supports our hypothesis that the elevation of the original terrain was different centuries ago, or, for example, in archaeological times. Unfortunately, we do not have precise and useful drilling data about it, but if we presume that a minimum of 50-cm-thick layer was formed at certain measuring points, we must be close to the truth. I. Puskás measured a 50-cm-thick layer in the former fortress, which was formed before the 19<sup>th</sup> century, and there are other excavation proofs of 50 to 100 cm thick infill layers from other parts of the city, which layers originated in the Middle Ages or the modern era (Puskás, 2008). We cannot find as thick an infill layer in an empty room inside of a fortress as in residential areas, there are no ruins of former buildings there, no sign of purposeful infill, and floods were not able to deposit a significant amount of mud due to the fortress walls. Based on these observations and data, we are right to presume that there was a minimum of 50-cm-thick infill from the foundation of the city to the end of the 19<sup>th</sup> century. Moreover, even higher values, up to a 100-cm-thick infill, are also likely to have occurred, but we must also emphasize that it still has to be researched in the near future.

We cannot finish our investigation without commenting on the real destruction of the flood. The earliest measured data about the flood peak of the Tisza in Szeged originates in 1770 (Buday, 1830). Although there are older secondary sources describing the devastating effects of major floods, they do not contain any accurate

data about flood peaks. For this reason, we do not know where the flood peak of the Tisza was before the 18<sup>th</sup> century. It is certain that the end of the 18<sup>th</sup> century was characterized by a cooler and more humid climate both in European and Hungarian history, which meant that river flow rates must have increased and resulted in higher floods. However, it also means that drier climate periods (e.g. the Roman Age, or the 10<sup>th</sup> to the 13<sup>th</sup> centuries) witnessed smaller floods, which also reduced the high flood risk of the city.

As to settlement history, the most important issues concerning the Tisza are related to the floods. The most important settlement historical issue of the frequently flooded areas was the population's ability to adapt to the changing stages and discharges of the river, to what extent they were able to use the excess water of the floods, or how they could mitigate flood damage (Molnár, 2011). The Tisza has two characteristics that distinguish it from other large rivers. One of them is that the river floods the low floodplain already at middle water level surface elevation, and its environment is gradually flooded. The other one is that the two annual flood cycles make life unbearable along the Tisza due to the elongated time of river downflow and slow drying out of the flooded areas (Fig. 10). It has been made even more difficult by the fact that the populated area of the city is of basin-like, and the slightly higher ridges along the river prevent the free flow of flood water from the deeper pools that are farther away from the river. So the whole process takes much longer than elsewhere. Flood damage, isolation and all negative effects are extremely important in terms of settlement history, because they complicate life as well as land use (Kiss, 2011).

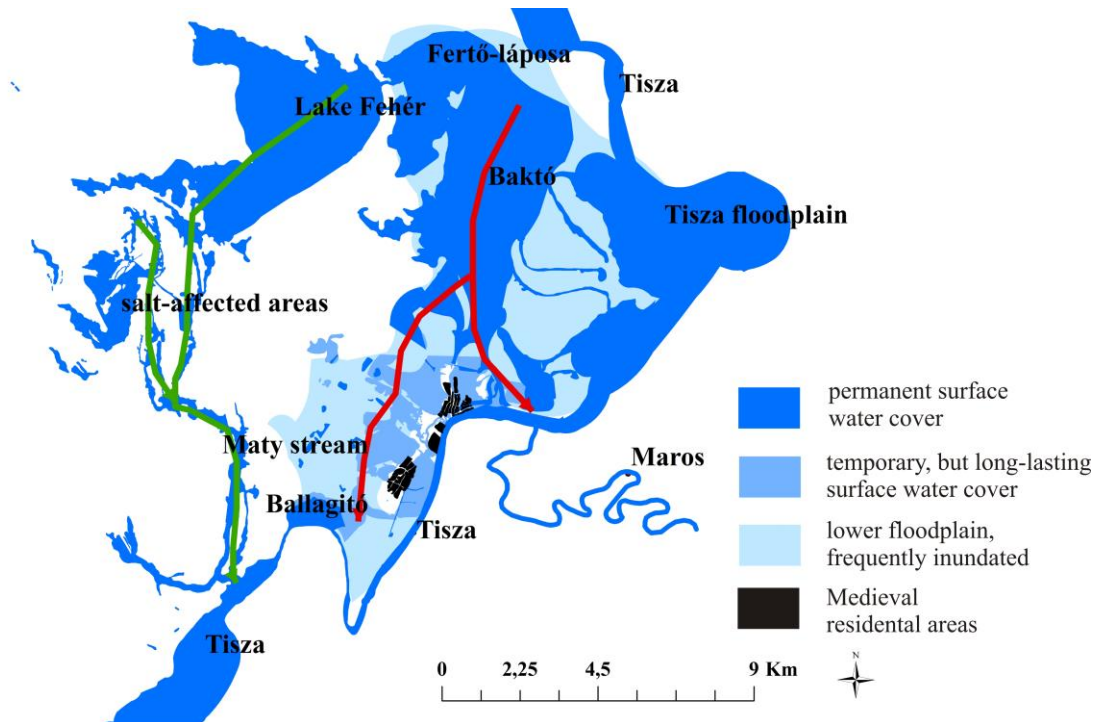


Fig. 10 Map of the catchment area of the river-system in and near Szeged, and map of the permanent and temporary surface water cover before river engineering (Szalontai, 2014b). Green arrow: waterflow from the Kiskunság Sand Ridge (Homokhátság) without flood risk; red arrow: Tisza floods posing significant flood risk and damages

It cannot be accurately determined which areas were flooded in Szeged and in its vicinity. We know about a flood that reached even the pool of Fehértó from the west (in 1801), but floods usually inundated the areas that lie to the east of the highway leading to Csongrád today. In the late Middle Ages, of all populated areas it was the northern part of the city, Felsőváros (Upper Town) that experienced the most floods or was directly threatened by them. Nevertheless, it was also common that Alsóváros (Lower Town) was also flooded, for example in 1712 (Reizner, 1899), when the flood arrived from the north and inundated the inhabited parts from that direction (Fig. 11)

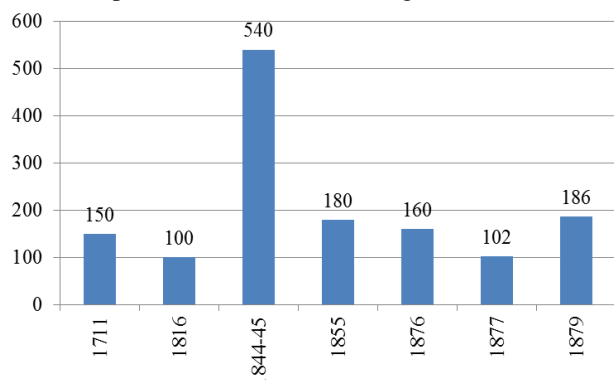


Fig. 11 Length of inundations (number of days) (Vágás 1991)

From landscape assessment point of view it is also important to know where were dry surfaces where the inhabitants could move in case of a flood inundating the whole city. It is known that in 1689 and in April 1712 the whole city was inundated except for Palánk due to the earth trenches. In these cases the surrounding vineyards and the “Óthalom” hills were surely dry, which could be approached by boats (Reizner, 1899; Kardos, 1979). In 1770 Szilléri hills, the highest situated small island (79.5-80 m) were also inundated, which meant that all other lower-lying areas were flooded for that time and the loess-covered “islands” were also inundated. Engineering maps from 1830 demonstrate that these flooded areas extended to the Óthalom hills and Ballagító areas; water covered low-lying arable lands, thus, the city was fully surrounded by Tisza floods from the north.

If we study the flood exposure of Szeged, we have to take into account another important aspect. Today we can state precisely where there used to be streams, pools in the populated parts of the city (Szalontai, 2014a). These surface waters were not of temporary nature, but permanent, their riverbed was always visible and meaningful to the community, as long as it was not concealed (or destroyed) artificially. Their long-lasting (sometimes persisting for centuries) presence is best proved by the fact that street and ground-plot structure was developed in harmony with the then-present subsurface water bodies, and thus the people living there adapted to their channels and water influx.

But what is even more surprising is that not only the permanent hydrological elements trace out the possible settlement sites, but temporarily flooded areas as well. We can come to this conclusion also when we overlay the medieval town structure to the city map that was prepared five months after the great flood. In 1879, the deepest

parts of the city were still covered by floodwater in July, after the March flood. These areas indicate those pools which were characterized by temporary inundation before the river was engineered. It can be noticed very well that these pools almost completely surround the earliest parts of the city, and they literally complement the blank spaces between the separated units.

These urban wetlands were not built in with houses and remained empty until the 20<sup>th</sup> century. Their single city structure utilization was the building of Eugenius Ditch after the Turkish occupation as the southern end of the ditch was built by using these wetlands and pools as a security system. The stream that once ran along the northern wall of the former fortress had similar effects on the settlement structure, as there was a large wetland there that separated the two parts of the city for centuries, and this situation did not change over time, not even after losing the border fortification role it previously had.

The low-lying areas were not inhabited, and they were usually swamplands with recurring inundation. The area is likely to have had aquatic or hydrophobic plants as the predominant vegetation. In the modern era, they were low-lying arable lands (so-called “nyomásföldek”) which served mainly for grazing.

It is a complex water system, which received significant flood water supply on each occasion when the inhabited parts of the city were flooded. Its pools are likely to have always been filled with water. Due to the significant water supply of these pools, their infill or drying out became significantly difficult, which can also be considered as flood damage, similarly to the physical destruction caused by water.

## CONCLUSION

Concluding the results of our study, we can say that, compared to the 19<sup>th</sup> century city, the inhabited parts of Szeged were situated on lower-lying terrains for centuries or millenia before the foundation of the city. For this reason, particularly during periods of cooler and wetter climate, the Tisza floods coming from the north inundated the entire area of the later city. The flood covered the low floodplain and the low-lying basins to be filled with water, thus creating an actual sea around the city with several kilometers of diameter. This huge amount of water made life as well as entering or leaving the settlement impossible. These conditions significantly limited the location of residential areas and therefore before the Hungarian Middle Ages the center of settlement was found farther away from the banks of the Tisza, and not along it, on the flood-free areas of the surroundings.

The 10<sup>th</sup> and 11<sup>th</sup> centuries were characterized by a gradual warming, and the coming drier climate (medieval climate optimum) significantly improved this unfavorable hydrological feature, and must have reduced flood risk to a great extent (Lamb, 1982; Rácz, 2001). These changes led to the possibility of using the economic benefits of Maros salt trade to start the development of the city, which finally turned Szeged into one of Hungary’s most important and flourishing cities.

## References

- Bertalan, A. 1884. Szeged szab. kir. város földrajzi és meteorológiai viszonya. (Geology and meteorology at Szeged) Szeged. 70 p. (In Hungarian)
- Blazovich, L. 2002. Városok az Alföldön a 14–16. században. Dél-Alföldi évszázadok 17. (Cities of the Great Hungarian Plain in the 14th-16th centuries) Szeged. 271 p. (in Hungarian)
- Brázdil, R., Kotyza, O. 1995. History of Weather and Climate in the Czech Lands I (Period 1000–1500). Zürcher Geographische Schriften 62, Zürich. 260 p.
- Farsang, A., Puskás, I. 2009 A talajok sajátosságai a városi ökoszisztémában — Szeged talajainak átfogó elemzése. (Soil attributes in urban ecosystems – The detailed assessment of soils in Szeged) *Földrajzi Közlemények* 133, 397–409. (In Hungarian)
- Glaser, R. 2008 *Klimagesichte Mitteleuropas. 1200 Jahre Wetter, Klima, Katastrophen.* Darmstadt, Primus Verlag, 227 p.
- Halácsy, S. 1879. Szab. kir. Szeged városa beltelkeiben háromszögített elsőrendű főalappontok kiszámításának jegyzőkönyve (Report on the calculations on the main geodesic points in Szeged). Szeged, kézirat. Somogyi Library (in Hungarian)
- Kardos, I. 1979. Szeged árvízvédelmi rendszerének kialakulása az 1879. évi katasztrófa előtt és után. (Flood protection in Szeged before and after the flood in 1879). *Hidrologiai Közöny* 59, 252–260. (in Hungarian)
- Kasab, I. 1987 *Építésföldtani összefüggések Szeged és környéke felszínközeli üledékeiben.* (Engineering Geology of near-surface sediments of Szeged and its neighborhood). Budapest. 113 p. (In Hungarian)
- Kiss, A. 2011. Floods and Long-Term Water-Level changes in Medieval Hungary. PhD dissertation. Budapest. 323 p.
- Kohán, Z. 2003. A tradicionális középkori ártéri gazdálkodás geomorfológiai környezete (Geomorphological environment of traditional (medieval) floodplain farming). *Földrajzi Értesítő* 52, 5–21. (In Hungarian)
- Kuklay, B. 1880. Talajfűréskek Szegeden. (Soil surveys in Szeged) Kézirat. 4 p. (In Hungarian)
- Kulinyi, Zs. 1901. Szeged új kora. A város újabb története (1879–1899) és leírása. (The new history of Szeged (1879-1899) Szeged, 690 p. (In Hungarian)
- Lamb, H. H. 1982. *Climate, history and the modern world.* London and New York. 387 p.
- Lechner, L. 2000. Szeged újjáépítése. (The reconstruction of Szeged) Reprint, Szeged. 92 p. (In Hungarian)
- Máté, Zs. 1989. Szeged XIV. századi helyrajza. (Szeged in the 14th Century) *TCsMT* 14, 5–75. In Hungarian
- Mezősi, G. 1984. Szeged környékének negyedkori és recens felszínfejlődésének néhány kérdése a részletes geomorfológiai elemzés tükrében. (Quaternary and recent surface development in the vicinity of Szeged based on a detailed geomorphological assessment) In: *Az Alföld gazdaságföldrajzi kutatásának eredményei és további feladatai. II. Természeti környezet.* Békéscsaba 1984, 203–212. (In Hungarian)
- Molnár, S. 2011. Environmental historical research of floodplain management demonstrated through two sampling sites on the Great Plain of Hungary. PhD Theses, University of Szeged, 125 p.
- Nagy, M. 1957. Szeged földrajzi energiái és a város hatásterülete. (Geographical energies and the affected areas in Szeged) *A Szegedi Pedagógiai Főiskola Évkönyve*, 137–170. (In Hungarian)
- Ozsváth, G. 2003. Három, a közelmúltban visszakertült 19. századi kézirat Szeged térkép. (Újabb malomadatokkal). (Three maps recently became available from the 19th century on Szeged including new mill data). *MKCsM 2002* (Szeged 2003), 81–93. (in Hungarian)
- Puskás, I. 2008. Urban soils: complex evaluation and classification of soils in Szeged. PhD Theses, University of Szeged, 153 p.
- Rácz, L. 2001. Magyarország éghajlattörténete az újkor idején (Climate history of Szeged in the Modern Age). *Juhász Gyula Felsőoktatási Kiadó*, Szeged. 303 p. (In Hungarian)
- Reizner, J. 1899. Szeged története I. (The history of Szeged) Szeged, 398 p. (In Hungarian)
- Rohr, Ch. 2007. *Extreme Naturereignisse im Ostalpenraum. Naturerfahrung im Spätmittelalter und am Beginn der Neuzeit.* Köln-Weimar-Wien, Böhlau Verlag, 201–398.
- Szalontai, Cs. 2014a. The role and significance of the Maty creek and the connected hydrological system in the settlement history of the vicinity of Szeged. PhD Theses, University of Szeged, Doctoral School of Earth Sciences, Geoarcheology, Szeged, 131 p.
- Szalontai, Cs. 2014b. Két víz között. Hatalmi és stratégiai központ váltás Szeged környékének településtörténetében. (Between two floods. Political and strategic centre changes in the settlement history of the vicinity of Szeged). In: Horváth, G. K. (ed.) *Vízhasználat, vízszabályozás és társadalom a 13–20. századi Magyarországon.* Balassi Kiadó, Budapest, 37–78. (In Hungarian)
- Vágás, I. 1991. A Tisza szabályozása. (River regulation works of the River Tisza) In: Gaál, E. (ed.) *Szeged története 3/1. 1849–1919*, Szeged, 133–139. (In Hungarian)

## Maps

- Buday 1830. Buday Mihály város főmérnök által jegyzett térkép Rajzolat mely Szabad Kir. Szeged városának belsőbb részeiben található Motsáros víz állásoknak házhelyekre való felosztását mutattya. 1830. Magyar nyelvű, színes kézirat térkép. Mérete: 950x600. Méretarány: 2” Bétsi hüvelk=100 öl. (Ozsváth, 2003; Szalontai, 2014) MFM jelzet nélkül.
- Barilari et al. 1879. Situation de la ville de Szeged. Szeged szab. kir. városának átnézeti vázlatrajza. Másolva és kiegészítve a k. biztosság műszaki osztálya által. Barilari, P. Gros, L. Jacquet, L. Waldorp, J. Kozłowski, Th, Szegeden 1879. évi július havában. Magyar és francia nyelvű könyvomasz árvízvédelmi térkép. Méret: 78x122 cm. Méretarány: 1:7200. MNL S068 V Ny (Részlet).
- Heller 1880. Szeged sz. kir. város Földtani réteg-terve. A Tisza 0 pontja alatt 4 méter mélységben képzelt vízszintes metszet. Plan géologique de la ville de Szeged. Coupe horizontale prise au niveau du zéro fleuve de Tisza. Heller Lajos mérnök térképe. 1:10000. 1880. Sk Td 329, Td 381 (Kuklay, 1880).
- Kuklay 1879. Szeged szab. kir. városának átnézeti vázlatrajza. A jelenlegi városi lejt mérési adatok. 1879. Másolva és kiegészítve a k. biztosság műszaki osztálya által, Szegeden 1879. évi július havában. Endrényi Lajos nyomdájából. Mérték 1”=100 méter 33,5x42 cm. CsML T102, Sk Td 319, Tm 343, Tm 73, Tm 74.
- Action Plan 1879. június Szeged szab. kir. város helyzetterve. A kir. biztosság műszaki osztálya által. Mértékmérővel. Sk Td 323a
- Action Plan 1879. július Szeged szab. kir. város helyzetterve.. A kir. biztosság műszaki osztálya által. Mértékmérővel. Sk Td 322

## Abbreviations

- CsML Archives of Csongrád County /Csongrád Megyei Levéltár/, Szeged  
 MFM Móra Ferenc Museum /Móra Ferenc Múzeum/, Szeged  
 MNL National Archives of Hungary Magyar/Nemzeti Levéltár/, Budapest  
 Sk Somogyi Library/Somogyi Könyvtár/, Szeged



## IMAGE BASED SURFACE TEMPERATURE EXTRACTION AND TREND DETECTION IN AN URBAN AREA OF WEST BENGAL, INDIA

**Sk Ziaul\*, Swades Pal**

Department of Geography, University of Gour Banga, Malda 732103, West Bengal, India

\* Corresponding author, e-mail: skziaul87@gmail.com

Research article, received 2 June 2016, accepted 25 October 2016

### Abstract

Rapid urbanization and change of landuse/landcover results in changes of the thermal spectrum of a city even in small cities like English Bazaar Municipality (EBM) of Malda district. Monitoring the spatio-temporal surface temperature patterns is important, therefore, the present paper attempts to extract spatio-temporal surface temperature from thermal band of Landsat imageries and tries to validate it with factor based Land Surface Temperature (LST) models constructed based on six proxy temperature variables for selected time periods (1991, 2010 and 2014). Seasonal variation of temperature is also analyzed from the LST models over different time phases. Landsat TIRS based LST shows that in winter season, the minimum and maximum LST have raised up 2.32°C and 3.09°C in last 25 years. In pre monsoon season, the increase is much higher (2.80°C and 6.74°C) than in the winter period during the same time frame. In post monsoon season, exceptional situation happened due to high moisture availability caused by previous monsoon rainfall spell. Trend analysis revealed that the LST has been rising over time. Expansion and intensification of built up land as well as changing thermal properties of the urban heartland and rimland strongly control LST. Factor based surface temperature models have been prepared for the same period of times as done in case of LST modeling. In all seasons and selected time phases, correlation coefficient values between the extracted spatial LST model and factor based surface temperature model varies from 0.575 to 0.713 and these values are significant at 99% confidence level. So, thinking over ecological growth of urban is highly required for making the environment ambient for living.

**Keywords:** Land Surface Temperature, Landsat TIRS, factor based LST models

### INTRODUCTION

Knowledge of Land Surface Temperature (LST) and its temporal and spatial variations within a city environment is of prime importance to the study of urban climate and human–environment interactions (Stathopoulou and Cartalis, 2009; Sharma and Joshi, 2013; Singh and Grover, 2014; Alavipanah et al., 2015). The retrieval of the LST from remotely sensed TIR data has attracted much attention, and its history dates back to the 1970s (McMillin, 1975). Urban heat island (UHI) and magnitude of the difference in observed ambient air temperature between cities and their surrounding rural regions have been a concern for more than 60 years (Landsberg, 1981). Nichol and Hang (2012) reported that there is a clear cut difference of temperature between rural and urban region and this gap is usually 3–4°C. One of the earliest UHI studies was conducted in 1964 (Nieuwolt, 1966) in the urban southern Singapore. Extensive urbanized surfaces modify the energy and water balance processes and influence the dynamics of air movement (Nichol and Hang, 2012). Afterward, many scientists (Giridharan et al., 2004; Neteler, 2010; Schwarz et al., 2011; Xiong et al., 2012; Zhang et al. 2013; Li et al. 2014; Kuang et al., 2015b; Alavipanah et al., 2015) have worked in this field emphasizing different cognitive issues.

LST is a key factor in physical dispensation of land surface at different spatial scale, and it generalizes the results of the interaction between land surface and atmosphere, exchange of matter and energy (Wan and Dozier, 1996; Alavipanah et al, 2015). In the general assessment model of sustainable development and LST change, the change of LST is regarded as an important criterion upon which the evaluation of environmental quality and social and economic development policy can be based (Keller, 2008; Dai et al., 2010). Dynamic variability of LST seasonally and diurnally encouraged scholars to address this fact. Seasonal variation is well documented by Yuan and Bauer (2007) and Deosthali (2000) and they found that at night, the center of the city appeared as both heat and moisture island whereas at the time of sunrise as heat and dry island.

In 2008 more than half of the world's population were urban dwellers and the urban population is expected to reach 81% by 2030 (UNFPA, 2007). This acceleration of urbanization is very high both in intensity and area in developing countries like India. So, studying of the environmental conditions is necessary for proper planning or policy review. At the same time, it is already established that low population density is associated with lower LST values (Li et al., 2014) and conversely it is true that higher temperatures are associated with densely populated urban areas.

Intensity of LST is related to patterns of land use/cover changes (LULC), e.g. the composition of vegetation, water and built-up and their changes (Ding and Shi, 2013; Li et al. 2014; Grover and Singh, 2015; Kuang et al, 2015 a, b). Both horizontal and vertical urban expansion, spacing between buildings, building materials, location of public places, bus stoppage, railway station, major and minor industrial hubs etc. influence temperature concentration (Park, 1986; Alavi-panah et al., 2015). Rising population and building density are also accelerating factors of LST (Schwarz et al., 2011; Peng et al., 2012). The spatial extent of concrete cover and material composition is another major vector of spatial pattern of LST (Xiong et al., 2012; Kuang et al., 2015b). Growing population density, greater consumption of energy etc. can also aggravate temperature condition (Zhang et al, 2013; Li et al., 2014).

Clearly, the built-up land exhibited the highest LST, followed by bare soil, water body, and vegetation in all three periods as reported by Weng (2001), Weng and Yang (2004) and Chen et al. (2006). In forested area, temperature is almost 4.5-5°C lower than bare land (Buyantuyev and Wu, 2010).

It has been shown from both a theoretical and a practical point of view that the Normalized Difference Vegetation Index (NDVI) derived from satellite data is a good indicator of vegetation density (Grover and Singh, 2015; Gulácsi and Kovács, 2015). Vegetation can reduce LST by 13°C and considered one of the dominant factors for better health condition and a positive human comfort (Gémes et al., 2016). Both directionality of values (positive and negative) carry important role for regulating surface temperature. Positive and negative respectively indicate high vegetation density and high moisture which can help to reduce surface temperature (Choudhury, 1987; Kibert, 2012). In most cases, a negative correlation between NDVI and LST is found (Xiao et al., 2007; Zhang et al., 2013), although high canopy cover area is not a prime determinant because plant species, leaf area, soil background, and shadow can all contribute to the NDVI variability (James and Charles, 2014). Yuan and Bauer (2007), Li et al. (2012) revealed that the relationship between NDVI and LST varies seasonally. James and Charles (2014) also established that water bodies exhibits minimum land surface temperature than other landuse/land cover.

Normalized Difference Building Index (NDBI) indicates built up area concentration over space. Most of the previous studies recorded high surface temperature in the urban built up areas (Chen et al., 2006; Liu and Zhang, 2011; Essa et al., 2012) although its magnitude varies significantly due to variability in composition of building materials and density of buildings. Vertical growth is also responsible for intensifying LST (Park, 1986). Yuan and Bauer (2007) suggested that the percentage impervious surface cover as a more reliable metric for quantitative analysis of LST over different seasons for urbanized areas. Major road axes and railway station are characterized by high traffic and population concentrations and often have a higher temperature (Weng et al., 2004).

For preparing multi criteria approach based spatial modeling in different sector, the use of GIS has received valued reputation (Carver, 1991; Eastman, 1997). The Boolean overlay operations (no compensatory combination rules) and

the weighted linear combination (WLC) methods (compensatory combination rules) are two major dimensions of multicriteria suitability modeling. They have been the most often used approaches for different sorts of landuse suitability analysis (Malczewski, 2004). All the previous work in this approach is based on weighted additive average of the data layers selected for the suitability models. But the way of providing weight to the data layers according to their importance are different. For weighting the data layers PCA based approach (Khatun and Pal, 2016), analytic hierarchical approach (AHP) (Satty, 1980) etc. are used.

Ground measurement cannot provide wide spread data of different places at a time therefore contribution of satellite-based thermal infrared data is applied frequently in the developed nations. In India, this advanced method for spatial surface temperature extraction is not often applied. Growing urbanization rate, intra-urban density etc. require such study for rethinking about renewal of urban planning based on satellite data based temperature analysis at different spatio-temporal scale. In the Third World Countries like India, the density of meteorological stations is so sparse over space (average density of meteorological station is 1/500 km<sup>2</sup>, in plain region it is 1/520 km<sup>2</sup>, in elevated land it is 1/260-390 km<sup>2</sup> and in hilly region it is 1/130 km<sup>2</sup> (Raghunathan, 2010) that there is no other alternative than to use TIR satellite data based temperature extraction. Another major advantage of this data is that it provides pixel to pixel temperature information and produces micro level variation of temperature over space. Such data also helps to predict the local driving factors of surface temperature. Kawashima et al. (2000) documented a relation between mean air temperature and mean surface temperature. Also they rightly mentioned that this relation varies with altitude. They recorded that mean air temperature is 7° to 9.6°C larger than the mean surface temperature and obviously difference is higher at lower elevation. Adjusted R<sup>2</sup> ranges from 0.91 to 0.98 when regression is carried out between spatial air temperature and LST distribution models because of their high spatial association.

Present paper attempts to capture spatio-temporal variation of land surface temperature over the English Bazar Municipality (EBM) and its peripheral areas of West Bengal state of India. Furthermore, a factor based LST model was developed for understanding the relative variation of temperature over the region. Comparison of the actual land surface temperature data extracted from TIR is done in response to the factor based LST models constructed using major controlling factors. Main motive behind the factor based modeling is to find out it can substitute TIR satellite data based LST model. Also it aims to investigate whether the selected factors are effective for explaining spatial LST patterns. Priority analysis of the local level driving factors of temperature variation is carried out to understand the dominant driving factor of LST. Seasonal variation of temperatures at each time period (pre-monsoon, monsoon and winter) is analyzed to show seasonal extremities in this sub humid urban region. Trend analysis of temperature in different seasons over the temporal scale is also carried for identifying changing degree and intensity of LST. In brief, two sets of LST models have applied in this work. First approach is Landsat TIR based LST modeling and second approach is proxy factor based LST

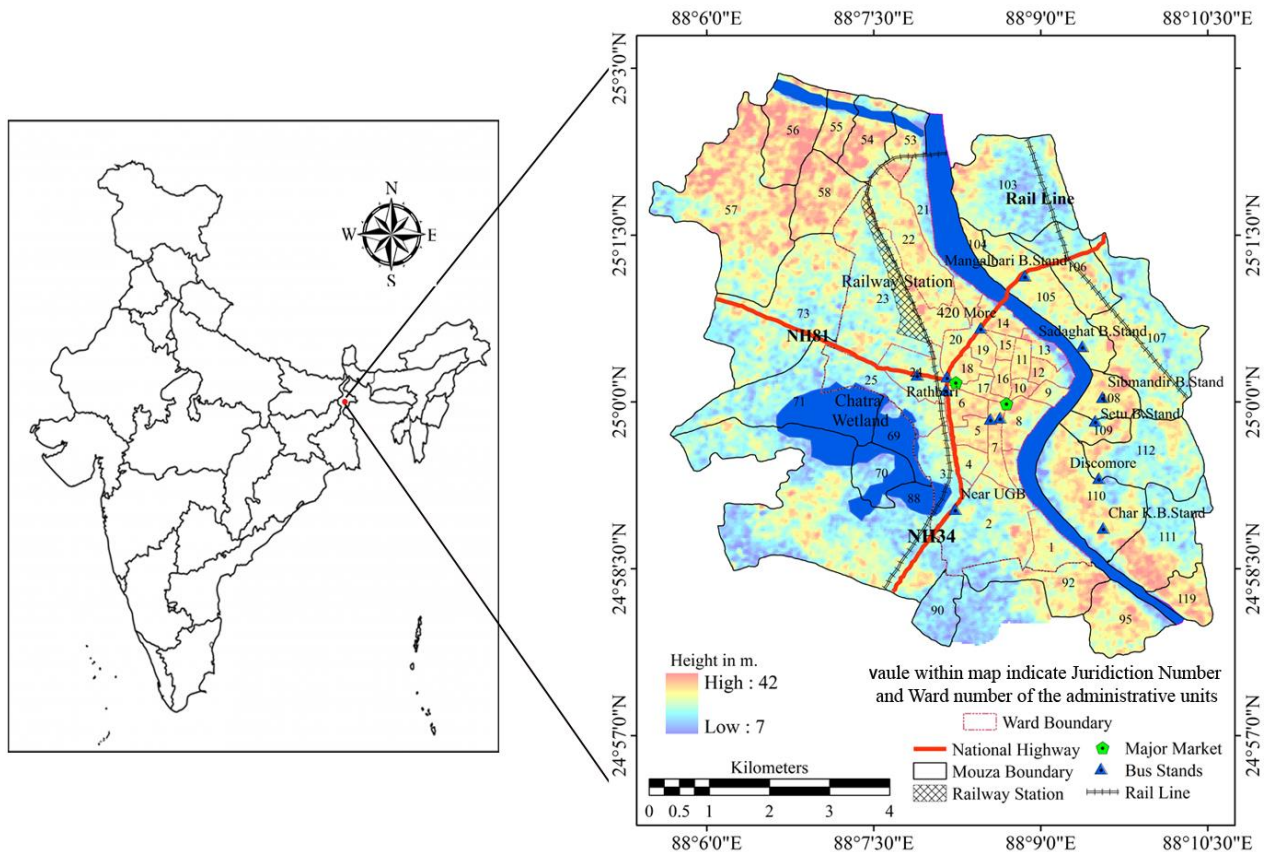


Fig. 1 Study sites showing selected mouzas, rivers, wetland, NH34, railway line, station and major market points

modeling for the same phases. Ultimately, spatial correlation coefficient between two sets of models have been calculated to test the accuracy of the factor based models.

## STUDY AREA

The present study area consists of 29 wards of English Bazar Municipality (EBM), 16 surrounding mouzas (smallest administrative or land revenue unit) from English Bazar block and 11 mouzas from Old Malda block (relatively larger administrative unit composed with several mouzas) covering an area of about 5500 ha (Fig. 1). The entire study area comes under Diara tract of West Bengal with fertile fine grain silty clay carried out by river Ganga and its distributary Kalindri River and Mahananda River, located at the northern and eastern margins of the study area. The average elevation of the region is 17m above MSL.

The water table is moderately deep (5 m to 10 m under surface) with moderately high seasonal fluctuation (2-4m). (Central Ground Water Board, 2010) and it may control evaporation as well as land surface temperature.

North western part of the present study area is covered with mango orchards. Chattra wetland (perennial) is considered the lungs of the town, and is located at the boundary zone of the town. Over time, this wetland area is captured by built up area. Climate of this region is characterized by sub tropical monsoon with seasonal wet and dry spell of rainfall, cold and hot spell of temperature. The year is sub divided by four major seasons: (1) winter season (January and February), (2) pre-monsoon season (March to May) with little rain and high temperature and evaporation, (3) monsoon season (June to mid-October) with maximum (about 82% of total rain) rain and high temperature and (4) post-monsoon season (mid-October to mid-December) with steady decline of rainfall and temperature. The post monsoon effect is less distinct. Average annual rainfall of this basin as gauged by Malda meteorological station is 1444 mm. Monthly variation of rainfall and temperature is noticeable (Table 1). The average potential evaporation, being one of the controlling factors of surface temperature, was 73 mm/year between 1901 and 2014 in the area.

Table 1 Average monthly temperature and rainfall conditions between 1991 and 2014

Climatic indicator	January	February	March	April	May	June	July	August	Sept.	Oct.	Nov.	Dec.
Tmax (°C)	23	26.7	32.3	35	34.7	33.7	32.2	32.2	31.7	30.8	28.5	24.8
Tmin (°C)	10.1	12.1	16.5	21.7	24.3	25.7	25.9	26	25	22	16.9	11.9
Rainfall (mm)	10.9	10.8	11	39.1	117.5	229.4	353.1	302.4	296.6	91.8	12.3	10.3

The town possesses a good infrastructure and facilities. Two railway stations e.g. GourMalda and Malda town are located at southern and northern part of this area. Railway line and National High way (NH) 34 perforate the town from south to north. Two main markets, Netaji market/Rathbari market and Chittaranjan market are located at the heart of the town and are considered as Central business district (CBD) of this commercially improved town (see Fig. 1).

The total number of population and house hold in the study area are 291612 people and 61803 households respectively according to the census of 2011. Additionally, it is also needed to mention that apart from these, the amount of people in the city is more than 50 % higher due to people from outside the city. The town is the main market town of the larger catchment of the Malda, Murshidabad and Dinajpur districts of West Bengal and Larger part of Eastern Jharkhand state of India. Most of the cases, spacing between houses is about to 45-60cm, exemplifying the dense building pattern.

**MATERIALS AND METHODS**

*Data and image pre-processing*

Landsat 5 and Landsat 8 are used for both landuse/land-cover mapping and LST modeling (path/row 139/43; spatial resolution for TIR band of Landsat 5 is 120m and for

Landsat 8 it is 100m.; spatial resolution for other bands is 30m in Landsat 5 and band 1 to 7 for Landsat 8). The extraction of LST is based on Landsat satellite images acquired through the USGS Earth Resource Observation Systems Data Center, which are corrected for radiometric and geometrical distortions of the images to an acceptable quality level before delivery. The Landsat image is further rectified to a common Universal Transverse Mercator coordinate system. Noise diminution is essential for the thermal sensed satellite images, particularly for the thermal infrared (TIR) band. The inherent noise may affect the retrieval of brightness temperature or LST.

*Methods*

The methodology consists of three sections (Fig 2): extraction of LST from Landsat images, multicriteria LST modelling, spatial association between Landsat based LST model with multicriteria LST (McLST) model. The first section adopted two approaches for LST modeling. 1) Landsat TIR based extraction of LST and 2) Proxy temperature factor based multicriteria LST modeling. First approach is entirely based on thermal band of landsat images of different time periods and the second approach is based on six proxy temperature factors as indicated in Table 2. Entire methodological work flow is illustrated in Figure 2.

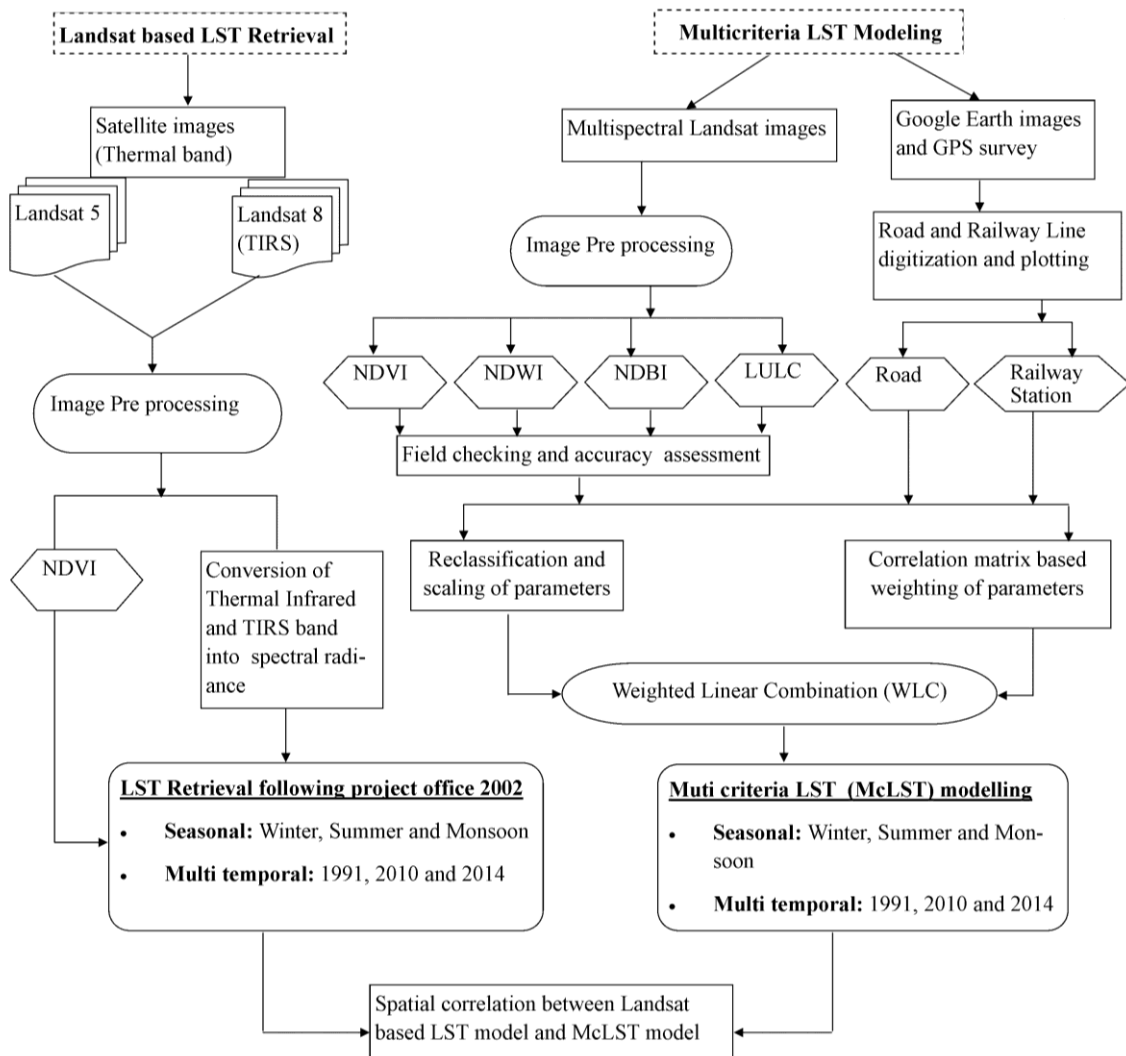


Fig. 2 Flow chart showing methodological workflow



Table 2 Selected proxy parameters and associated sources of data set

Name of the parameters	Source(s)
1) Land use	Sensor: Imageries of Landsat 5, Nov., 2013 (Path/Row:139/43; Band used: G, R, NIR; Spatial resolution: 30m. ), Land use map, 2014 of Land reform Deptt., West Bengal
2) NDBI	Extracted from Landsat 5 and 8 images
3) NDVI	Satellite image of Landsat 5 and 8 based on Townshend and Justice, 1986
4) NDWI	Satellite image of Landsat 5 and 8 based on McFeeters, 1996
5) Major Road	Extracted from Google image, DST map, Malda district
6) Railway Station	Extracted from Google image and field check through GPS
7) Land surface temperature	TIRS 1 & TIRS 2 band of Landsat 8 and Thermal Infrared band of Landsat 5

#### LST extraction and modeling

Approach 1 deals with extraction of LST from thermal band of the selected sensors is well discussed with a good number of merits and demerits by the Xiong et al. (2012), Zhang et al, (2013), Li et. al. (2014). It is multistep methods i.e. Conversion of the Digital Number (DN) to Spectral Radiance, conversion of spectral radiance to at satellite brightness temperature, LST extraction, conversion of LST from Kelvin to degree Celsius. This method is quite different for each sensor (Landsat 5, 7 etc.). All these things are well defined in the respective guidelines published by Landsat Project Science Office (2002). In this present work, guidelines of the same have been followed for working out LST from Landsat imageries.

Approach 2 deals with six proxy data layers (Table 3). These layers are (1) Landuse/landcover, (2) Normalized differential Vegetation Index (NDVI) map, (3) Normalized differential water index (NDWI) map, (4) Normalized differential built up index (NDBI), (5) Major roads and (6) railway station. Here some other factors theoretically can be adopted like relief, rainfall etc. But these layers are not taken here because of their minimal influence within such a small spatial area.

As WLC process executes on the basis of raster based weighted linear combination (WLC), it is required to convert each with an equal. NDWI, NDVI, NDBI, landuse/landcover layers have been extracted as raster layers, so there is no need for conversion for these four layers. But other two layers i.e. major roads and railway station layers are in vector forms and these are needed to be converted into raster layers. For this, proximity maps have been constructed from these layers. It is assumed that the area nearer to the roads or railway lines or stations will be affected more by increased LST and gradually it will decrease with increasing distance from roads or railway lines. After converting the selected layers to raster format, each attribute (map layer) is categorized into 10 classes ranking 1 to 10, where a higher rank reflects a potentiality higher LST. Landuse/landcover classes have been ranked

based on the potential contribution toward LST. For example, built up class has assigned maximum weight. Here relative ranking of the landuse/landcover class is done based on subjective priority. To fulfill this purpose, all the attributes have been reclassified into 10 classes following natural break method and ranked accordingly. The logic behind ranking to intra attribute classes from 1-10 is described in Table 3. Weightage of each attribute has been defined objectively (Table 4) considering the degree of correlation of each driving factor with land surface temperature generated for different years. The logic behind this consideration is that highly correlated parameters maximally explain the spatial variation of temperature. Normalization of respective weights (values of  $r$  for respective parameters) based on dimension index have been performed for frame it in a scientific scale. It is calculated for distributing relative weight of all the parameters. Here total normalized weight is 1. The parameter shares maximum out of 1 is emerged as dominant parameter. The result of each normalized value is called attribute weight. Weights of the parameters for different seasons in respective years are different due to having some dynamic variables like landuse/landcover, built up area, water bodies, canopy coverage etc. Therefore nine models have been articulated for different seasons in the selected years.

Table 3 Modes of ranking of the intra sub class of parameters

Name of the attribute (j)	Highest rank indicates at 10 point scale	Logic behind
1) Land use	10 rank at built up land	Concrete area has high temperature emissivity
2) NDBI	10 rank at highest intensity class	High intensity built up land emits maximum temperature
3) NDVI	10 rank at '0' value	Above and below 0 value canopy cover and water availability increases which may reduce temperature
4) NDWI	10 rank at lowest NDWI value	It does indicate water concentration; more concentration of water bodies mean less temperature and vice versa
5) Major Road	10 rank at road adjacent zone	Highly dense traffic in all roads concerned specifically National High Way 34 insists temperature rise
6) Railway Station	10 rank at near to the railway station	Being a nodal centre, a good number of trains ups and down and huge number of passengers uses this station as nodal point

Expression of weight calculation is as follows (Eq. 1):

$$w_j = \frac{a_{j_r}}{\sum_{j=1}^n j_r} \quad (\text{Eq. 1})$$

where  $w_j$ =weight of  $j$ th parameter;  $a_{j_r}$ = correlation coefficient of  $j$ th attribute;  $\sum_{j_r}$  = summation of correlation of all  $j$ th variable.

Rank of all sub classes under each attribute is then multiplied by the defined weight of each individual attribute. This function can be presented using Equation 2:

$$WLC = \sum_{j=1}^n a_{ij} w_j \quad (\text{Eq. 2})$$

where,  $a_{ij}$ = ith rank of jth attribute;  $w_j$ = weightage of jth attribute. This weighted linear combination has been done using raster calculator tool in ArcGIS environment.

Weight of the attributes for different other periods has been calculated based on their respective correlation coefficient values. See table 6 for calculated weights of the parameters for different time phases. Calculation of the entire process is represented in Table 4 showing the case of January, 2014.

Table 4 Pattern of reclassification of the parameters, ranking and weighting of the parameters of January, 2014

Parameters	Sub-class	Rank	Weight of parameters
1) NDBI	natural breaks	1-10	0.382
2) NDVI	natural breaks	1-10	0.042
3) NDWI	natural breaks	1-10	0.064
4) Land use/ Land cover	Water Bodies & Water Hyacinth	1	0.336
	Mango Orchard	3	
	Agricultural Land	6	
	Fallow Land	8	
	Built up Land	10	
5) Major Road (Distance from major road)	natural breaks	1-10	0.154
6) Railway Station (Distance from station)	natural breaks	1-10	0.022

After preparing the multicriteria spatial LST model based on controlling factors and the Landsat TIR based LST model(s), spatial correlation coefficient between them has been calculated to judge the level of spatial association. Strong correlation coefficient (r) does mean higher level of spatial coincidence and vice-versa. Chen et al (2006) and Ogashwara and Brum Bastos (2012) focused on the quantitative relationship between LST and temperature controlling factors by using correlation coefficient analysis. In this present work, their line of thinking has been followed.

#### Methods for framing data layers used for multicriteria LST modeling

This section describes how NDVI, NDWI, NDBI and others have been prepared for constructing multicriteria LST models. For NDVI extraction, method of Townshend and Justice, (1986) is used.

$$NDVI = \frac{(NIRband - Rband)}{(NIRband + Rband)} \quad (\text{Eq. 3})$$

where, NIR=near infrared band (band 4 of MSS and TM), R=red band (MSS band 2, TM band 3). Values ranges from -1 to +1, where negative values normally are associated with water and where positive values indicate vegetation mass. In principle, higher values are linked with higher vegetation density.

For extracting NDWI, equation presented by McFeeters (1996) is used:

$$NDWI = \frac{(Greenband - NIRband)}{(Greenband + NIRband)} \quad (\text{Eq. 4})$$

where Green is the green band (MSS band 1, TM band 2) and NIR is the near infrared band (band 4 of MSS and TM). This value ranges from -1 to 1. Value nearer to 1 indicate greater possibility of low LST.

Normalized differential built up index (NDBI) has been calculated following Zha et al (2003):

$$NDBI = \frac{(MIRband - NIRband)}{(MIRband + NIRband)} \quad (\text{Eq. 5})$$

where, MIR is the mid infrared band (TM band 5, OLI band 6) and NIR is the near infrared band (TM band 4, OLI band 5). NDBI value ranges from -1 to 1. Value nearer to 1 means greater possibility of high LST.

The land use data set has been prepared from Landsat imageries of the respective periods mentioned in Table 2. Supervised image classification techniques (non-parametric rule: maximum likelihood) have been used for landuse/land-cover (LULC) classification. Accuracy assessment has been done by cross checking 139 sites through GPS survey and Google Earth images. From this assessment, it was found that the accuracy assessment generated from the supervised classification technique showed an overall classification accuracy of 84.45% with Kappa statistic of 0.829, which indicates a very good agreement (Monserud and Leemans, 1992) between thematic maps generated from image and the reference data.

Road and railway lines have been digitized from Google Earth image, toposheet of Survey of India and those vector layers have been converted into raster layers through proximity or distance mapping. Actually, ten equidistance buffer classes have been made both from roads and railway line individually.

#### Method for spatial association between Landsat based LST model with multicriteria LST (McLST) model

Most of the previous work across India in this field have extracted surface temperatures but these were not validated with any reference standard datasets collected from meteorological monitoring stations. As only one meteorological station is available over the present study area, it is difficult to validate the spatio-temporal data with meteorological data available there on. Authors here attempted to compare their models with some Multicriteria LST models created based on major locally dominant temperature driving factors. After extracting LST from TIRS of Landsat and constructing multicriteria LST model, simple

correlation coefficient ( $r$ ) between these two layers for different seasons in the selected years has been calculated. It is being considered that higher degree of  $r$  value means strong spatial association. Student's 't' test has been carried out for assessing degree of significance level of the calculated correlation at 95% and 99% confidence levels. A strong spatial relation would indicate that multicriteria LST models can be used for assessing relative LST pattern over the study area.

For finding out dominant factor of LST, correlation coefficient of the selected factors with surface temperature layers of the respective periods have been calculated. Strongly correlated parameters are considered as dominant factors. This is calculated during Multicriteria LST model building.

## RESULTS AND DISCUSSION

### *Results extracted from data layers*

Earlier it is mentioned that six data layers have been prepared for constructing multicriteria LST modeling. In this section result of the individual layers has been depicted. Through supervised image classification, six number of major landuse/landcover classes have been identified with an accuracy level of 84.45% with Kappa statistic of 0.829. Out of total area (~5500 ha), 42.24% is covered with built up land followed by mango orchard (24.15%). The core part of the study area is composed of built up land and it spreads along the major roads and railway line outside the core. If only core area is considered, more than 78% of the area is built up area. Such built up area concentration is highly effective for enhancing LST. The NDBI pattern shows that the maximum intensities (NDBI score: 0.160-0.179) of built up area are found at the core part and also it increases even in the peripheral land. Over time, greater proportion of study area comes under this intensity of NDBI. NDVI value is recorded maximum (0.292-0.487) in the north western part of the study area where one denser mango orchard is located. Such value is only found in the peripheral part of the study area. This value decreases over time over the major parts, especially in the core parts. From this result it can be stated that there is a negative relation between NDBI and NDVI. NDWI values with maximum intensity are only (0.288-0.422) found in the river Mahananda at the eastern side and Chatra wetland at the western side of the study area.

### *Landsat image based LST change*

Seasonal temperature dynamics (winter, pre-monsoon and monsoon) in 1991

Usually, temperature is confined within the range of 14.41-20.34°C during January, 1991 (Fig. 3A). Out of total area, 32.83% area represents temperature from 16.18 - 16.77°C followed by 24.8% area is represented by 16.77 - 17.37°C temperature. More than 83% is characterized by the temperature ranges from 16.18-18.55°C. Mean temperature of this study area in this time was 17.24°C and the coefficient of variation (CV) was 4.04%. Core urban area is sensitive to high temperature.

April and May of this year show that the maximum air temperature was 40°C or more. But at present case surface temperature ranges from 23.99°C to 34.64°C (Fig. 3B). Low antecedent moisture and lack of rainfall triggered by nor wester (a kind of local storm with rain) might enhanced temperature a little bit. Within this temperature spectrum, 29.31 - 30.37°C temperature covers 20.97% of the total area followed by 30.37 - 31.44°C temperature in 20.66% of the area. More than 81% area possesses temperature between 27.18-32.5°C. North western and south eastern part of the study area exhibit relatively low range of temperature due to the Bagbari mango orchard and Chatra wetland. Only in April, the wetland area is prominent due to its distinct oceanicity factor. Expectedly, areal coverage of high temperature is maximum in this time. From temperature condition, it is also clear that urban spread is maximum in the eastern part of the main town following river Mahananda and north western part of the main town along main concrete road (National High way) which connects the western and north western part of the Malda district with district town (English Bazar Municipality).

In October of the monsoon month, due to frequent rainfall, despite having high temperature potential, temperature is self regulated. In this year temperature ranges from 21.66°C to 28.09°C (Fig. 3C). About 89% spatial extent is characterized by 22.30°C to 24.87°C temperatures. Spatial character of moisture availability regulates temperature over space. In temperature distribution, there is no such continuity as exhibited in figure 3C. Except main town most part of the peripheral area shows quite lower temperatures. Within main town variation of temperature is 27.64% and it is about 64.25% in the peripheral area.

Seasonal temperature dynamics (winter, pre-monsoon and monsoon) in 2010

In winter season, 2010 range of temperature was 16.72°C to 22.98°C (Fig. 3D), which is 2-2.5°C higher both from lower and upper limits than 1991 of the same season. Out of total area, 75% area is characterized by temperature level ranges from 19.22°C to 21.10°C. Mean and CV of temperature of this phase are respectively 19.97°C and 4.11%. Temperature spread is high both in western and eastern periphery of the main urban land. In the peripheral area rising trend of surface temperature is also identical with core urban area.

In pre monsoon or summer season, 2010 temperature was within the range of 26.83°C to 36.98°C which is 3.20°C higher than 1991. This LST is about 7°C lower than mean air temperature of the same period (Fig. 3E).

Increasing trend of temperature is also reflected in air temperature. Out of the total area, 77% was characterized by a temperature ranged from 28.86°C to 33.93°C. Mean temperature in this period was 31.47°C. and coefficient of variation (CV) was 5.32% which was 0.99% higher than in 1991. The northern part of the main urban area recorded the maximum temperature. This area is characterized by one of the main dense market (Netaji market), busiest traffic node and garlands of hard ware shops.

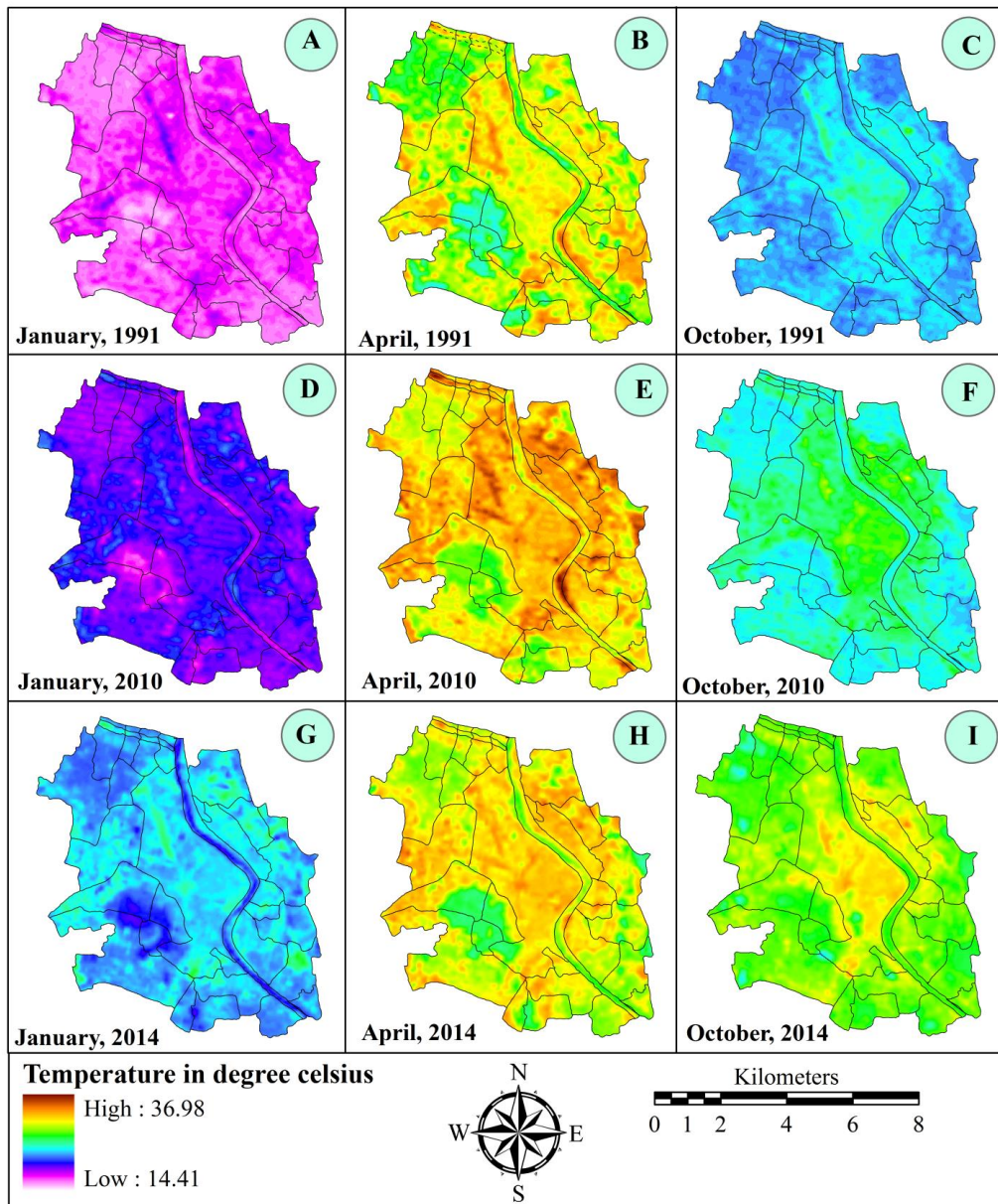


Fig. 3 Land surface temperature A) January 1991 B) April 1991 C) October 1991 D) January 2010 E) April 2010 F) October 2010 (G) January 2014 (H) April 2014 (I) October 2014 based on LANDSAT images

The mean LST was  $1.98^{\circ}\text{C}$  higher than in 1991 in the monsoon season. In 2010, the LST was in range of  $22.98^{\circ}\text{C}$  to  $30.58^{\circ}\text{C}$  (Fig. 3F). Out of total area, 86.08% was characterized by temperatures ranging from  $23.73^{\circ}\text{C}$  to  $26.01^{\circ}\text{C}$ . The mean temperature was  $25.37^{\circ}\text{C}$  and the CV is 4.70% (Table 5).

Seasonal temperature dynamics (winter, pre-monsoon and monsoon) in 2014

In the winter period of 2014, the LST ranged from  $20.17^{\circ}\text{C}$  to  $27.30^{\circ}\text{C}$  and the mean temperature was  $23.39^{\circ}\text{C}$  which was  $3.42^{\circ}\text{C}$  higher compared to 2010 (Fig. 3G). The CV values in this season in all phases establish the fact that there was marginal increase of LST (Table 5).

In the summer season of 2014, the LST varied from  $25.22^{\circ}\text{C}$  to  $34.60^{\circ}\text{C}$  and mean temperature was  $30.36^{\circ}\text{C}$  which was  $1.11^{\circ}\text{C}$  lower than during the previous phase

(Fig. 3H). Actually, 4 days antecedent moisture caused by nor wester lowered surface temperatures. Out of the total area, 87% was characterized by temperatures between  $28.03^{\circ}$  to  $32.72^{\circ}\text{C}$ .

In the monsoon of 2014, the LST ranged from  $23.63^{\circ}\text{C}$  to  $33.66^{\circ}\text{C}$  and the mean temperature was  $28.70^{\circ}\text{C}$  which was  $3.33^{\circ}\text{C}$  higher than in 2010 (Fig. 3I). The lowest temperature limit had increased by  $0.65^{\circ}\text{C}$  and the upper temperature limit with  $3.08^{\circ}\text{C}$  compared to the same period in 2010. Out of total area, 87.75% was characterized by temperatures between  $26.63^{\circ}\text{C}$  and  $30.65^{\circ}\text{C}$ .

The present work shows that not only the metropolitan city, but small urban centre like EBM are also gaining temperatures, which is not a good sign for the ambient living conditions. Figure 4 clearly displays the comparative pattern of areal proportion under different

range of temperature since 1991 to 2014 both for summer and winter periods. From this diagram, it can be observed that a larger proportion of the area has shifted to higher temperature classes. For example, only 2.3% area was under the LST above 33°C in 1991 but it is raised to almost 5% in 2014. Such trend is also noticed for other classes also during summer period. Similarly, in winter time, in 1991, no such area was found where LST was 20°C but in 2014 29% area was found where LST is above 23°C.

Table 5 Coefficient variation of temperature in selected time periods

Season	Year	Tmin (°C)	Tmax (°C)	Tmean (°C)	SD	CV (%)
January	1991	14.41	20.34	17.24	0.70	4.04
	2010	16.72	22.98	19.97	0.82	4.11
	2014	20.17	27.30	23.39	1.01	4.33
April	1991	23.99	34.64	29.67	1.94	6.53
	2010	26.83	36.98	31.47	1.67	5.32
	2014	25.22	34.60	30.36	1.64	5.40
October	1991	21.66	28.09	23.40	0.79	3.36
	2010	22.98	30.58	25.37	1.19	4.70
	2014	23.63	33.66	28.70	1.28	4.47

#### Multicriteria Land Surface Temperature (McLST) models

As mentioned before, the McLST models have been calculated based on six data layers (factors) which control temperature variation. The LST models calculated from the Landsat images and the McLST models have been prepared for the same period of time. Such models will help to understand-whether McLST models can explain LST variation.

#### Models for 1991

The WLC values varied from 2.17 to 8.87 during winter, 1.61 to 8.69 in summer and 1.95 to 8.57 in monsoon seasons (Fig. 5A, 5B and 5C). In all seasons, higher WLC

values were noticed in the main urban land and some parts of peripheral urban areas where urban extension has already proliferated.

#### Models for 2010

In 2010, WLC varied from 1.45 to 9.04 in winter, 1.60 to 9.70 in summer and 1.74 to 9.39 in the monsoon or rainy season (Fig. 5D, 5E and 5F). In all seasons, the upper limit of WLC was above 9, while they were below 9 in 1991. This does indicate that LST has raised between 2010 and 2014. The LST trend extracted from multicriteria LST models shows the same pattern as the extracted surface temperature models from Landsat images during the respective seasons. On average surface, the temperature increased with 2.5°C in 2010 compared to 1991.

#### Models for 2014

In 2014, WLC varies from 1.26 to 9.41 in winter, 2.24 to 9.14 in summer, and 2.54 to 9.35 in rainy season (fig. 5G, 5H, 5I). WLC values at the lower end had raised to some extent indicating rise of LST in the relatively low temperature zones. At the same time, the upper limit of WLC values was also consistently high in all seasons pointing out high LST. From the Landsat based LST models, it was clear that, except in pre-monsoon time, the temperature raised by 3 to 3.5°C in comparison to 2010. Mainly, growing urban intensity could explain this trend.

#### Spatial Association between LST and McLST models

Spatial correlation analysis is carried out between the models for the respective periods to bring out the fact that these models are spatially associated. In all seasons and selected seasons, correlation coefficient values vary from 0.44 to 0.81 (Table 6) and all values are significant at 99% confidence level. Therefore, these models can be considered as spatially associated. Moreover, the scholarly works carried out by Kawashima et al. (2000) clearly indicates that the mean air temperature is 7° to 9.6°C higher than surface temperature. If same line of thinking could be followed, such association is existing. For further analysis of the relationship, the correlation is also calculated between the two models based on different landuse/landcover classes. In summer period, this correlation coefficient is very high (0.93) in case of built up land, -0.57 in vegetated land, and -0.52 in case of moist land and water bodies. In the core area,

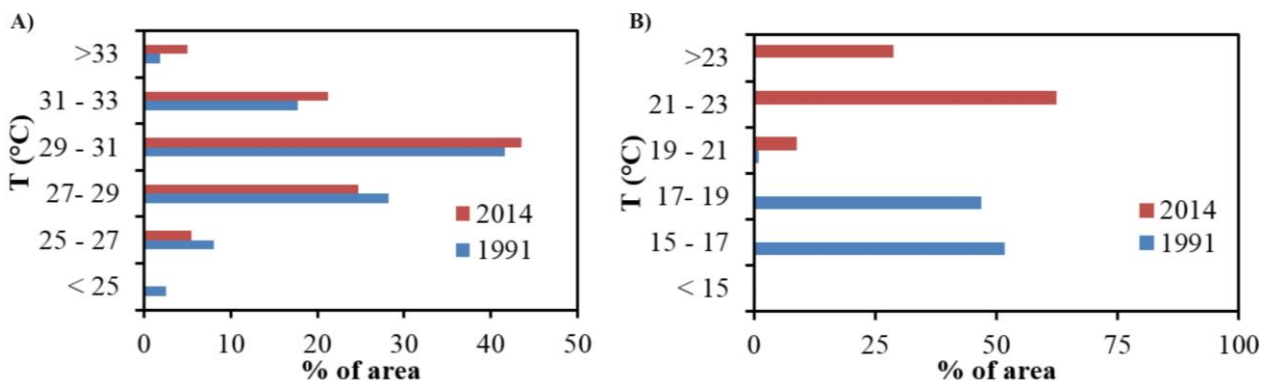


Fig. 4 A) Changing pattern of heat zone (intensity) during April; B) during January in 1991 and 2014

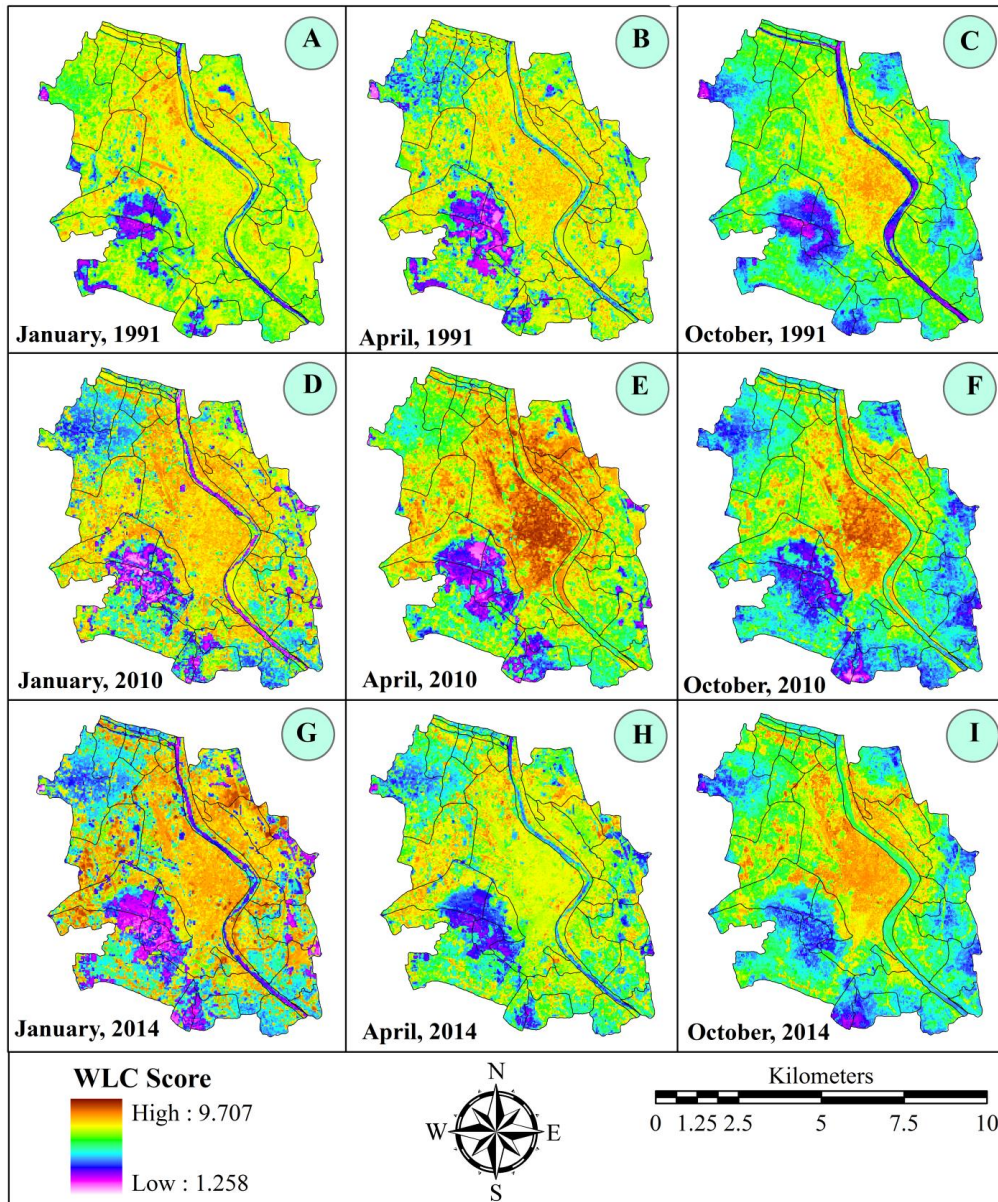


Fig. 5 Multicriteria LST models A) January 1991 B) April 1991 C) October 1991, D) January 2010 E) April 2010 F) October 2010 G) January 2014 H) April 2014 I) October 2014 based on driving factors

this relation is very strong in most of the periods ( $r = 0.86-0.93$ ) while in the peripheral area, the relation is quite weak and varying due to significant differences in landuse/landcover types. In most cases, the strength of the relationship increases over time. Even in the peripheral land, the intensity of temperature rise is mentionable.

Table 6 Degree of correlation between actual and potential temperature models (every correlation coefficient has a significance level of 99%)

Time	Pre-Monsoon	Monsoon	Winter
1991	0.68	0.62	0.51
2010	0.75	0.81	0.60
2014	0.44	0.69	0.68

The McLST models do not directly provide an absolute LST value but the relative temperature differences

can be explored. Relative patterns of WLC values do indicate relative rise or fall of LST. If some random field recording of temperature is made for different sites within the study area and tallying with WLC values, such qualitative McLST models can be quantified.

#### Factorial analysis

From the selected driving factors of temperature in local scale, it was identified that NDBI most strongly affects the surface temperature followed by land use and major roads. The correlation value between NDBI and LST ranges from 0.42 to 0.80 and mean value for all seasons is 0.66 (Table 7). Densely settled building with very narrow inter buildings spacing, high rise building, expanding roads etc. are some triggering vectors behind the trend of rising temperatures in the urban area. Decreasing canopy cover and increasing concrete impervious surface modifies thermal processes in urban regions, thus causing  $2^{\circ}$ -

3.5°C higher temperatures compared to rural areas and this effect is known as urban heat island effect (Ogashawara and Bastos, 2012). Dense mango orchard in the north western part of the study area recorded relatively low LST. But the LST condition is not fixed over time, it also increases. This condition results in confusion regarding the role of local driving factor behind temperature changes. Alteration of the hydrologic cycle represents the most significant urban water quality issue at hand today (DeBusk et al., 2010) because storm water runoff from impervious surfaces creates water quality problems including higher water temperatures and elevated levels of contaminants in surface waters (Davis et al., 2010). This effect can immediately influence the nearby Chatra wetland which is considered as kidney of the town (Kar and Pal, 2012). Lack of impoundments within the town accelerates rain water to run down with a fast rate and it also causes rise of LST even in the monsoon season. Low recharge due to high impervious land reduces moisture availability in pore space of the top and sub soil. So, when incident sun rays strike on surface, they penetrate much deeper into the part of the soil strata and enhance surface temperature. The impact of NDVI is prominent during the pre monsoon season but its impact is less obvious during the monsoon because monotonization of surface in regard to high moisture availability. Major roads, specifically the crowded NH34, enhance temperature levels along their axis and their influence is clearly visible in both the Landsat image based LST models and McLST models created for different seasons. Other roads also influence LST in same trend but not with the same intensity. This sort of result is also found in the work of Weng et al. (2004). The modification of LULC associated with urbanization has altered the thermal properties of land, thereby changing the energy budget, creating the UHI as also reported by Xiong et al. (2012) in his work. Brick kiln factories (15 nos.) in the north western part (Bagbari region) of the study area highly increased temperature. Actually this layer is not separately taken into consideration because of its identical emissivity with built up area. The impact of water bodies on lowering temperature is reflected by the models. Chatra wetland (>4 km<sup>2</sup>), located at south western part of the study area, not only decreases its own temperature but also helps to reduce the temperature of its surroundings. The turbidity level of this wetland has been rising over time and as a result, even in the wetland domain the temperature has also raised up. Related to this, it could

be mentioned that in last 20 years more than 50% of the total wetland area has been converted or will be converted into built up land (Kar and Pal, 2012). Therefore, these areas will also show an increased temperature in the future. The railway station modifies the temperature in an isolated manner, mainly in the station premises. All the discussion imparts to the models prepared from Landsat images and multi criteria approaches and therefore these are comparable.

## CONCLUSIONS

It can be said that surface temperature is rising over time in all seasons and the intensification of concrete surfaces within the urban environment and urban expansion in its peripheral zones increases temperature. Both types of LST models point out the unidirectionality of the temperature change. Land use change in terms of installing brick kiln industries, transforming of wetland into urban land, exchange of land between mango orchard and agricultural land etc. are some prime causes for surface temperature change in the urban fringe area. Expansion of concrete surfaces, intensification of built up land, high rise building etc. are some reasons behind increasing temperature in the urban heart land. Considering this trend, immediately land transformation policies should be reviewed specially regarding transforming mango orchard and wetland into built up land. Wetland and forest land can mediate temperature condition in their surroundings.

Urbanization is the main driving process of land cover changes and consequently of change of LST. However, unless undertaking a radical urban decentralization policy, it is difficult to stop or reverse the urbanization process even to the medium and small cities because their function as facility hub.

Vegetation management policies (e.g., green belt) can be implemented that would contain making space for green belts, can consequently help reducing the UHI effect. In addition, policies must not be limited to horizontal growth management only. Additional consideration to implement new urbanism (e.g., green building) concepts in the planning permission (or development assessment) stage of development would also help reducing the LST. English Bazaar Municipality, a small town is so congested in its core part, it is quite difficult make more space available for greening and reducing land surface temperature,

Table 7 Average and range of degree of correlation between LST and selected factors in different seasons

Parameters	Range of winter season	Average of winter season	Range of pre-monsoon	Average of pre-monsoon	Range of monsoon	Average of monsoon
Landuse	0.06-0.59	0.38	0.22-0.41	0.32	0.07-0.07	0.07
NDBI	0.61-0.68	0.65	0.42-0.80	0.67	0.62-0.74	0.66
NDVI	0.07-0.17	0.12	0.25-0.65	0.41	0.23-0.41	0.29
NDWI	0.05-0.37	0.17	0.16-0.48	0.31	0.16-0.27	0.24
Major Road	0.17-0.27	0.22	0.26-0.30	0.27	0.39-0.44	0.42
Railway Station	0.04-0.13	0.07	0.07-0.21	0.11	0.13-0.38	0.27

but further growth should be happening using the new urbanism concepts. Existing roof area can be surfaced with horticulture based plants. At present, municipal rules regarding keeping space between two buildings is only 1 foot but this is too narrow. So, this inter building space policy should be reconsidered. One of the valuable environmental limbs is Chatra wetland located in the south western part of this city that should be intensively preserved. Unfortunately, this wetland is rapidly reclaimed by built up area through urban sprawl. At any cost, it should be protected. Association of such wetland can to some extent decelerate the rise of temperature. Dispersion of urban population through expanding urban structure toward peripheral areas can also reduce temperature. Keeping vacant space with less concrete structures can help to reduce the rising temperature effect. So it is inferred that there is a dire need for continuous monitoring of city's landuse/landcover dynamics and to devise scientific and sustainable urban landuse policies with the purpose to monitor the phenomenon of intensification of UHI.

## References

- Alavipannah S., Wegmann, M., Qureshi, S., Weng, Q., Koellner, T. 2015. The Role of Vegetation in Mitigating Urban Land Surface Temperatures: A Case Study of Munich, Germany during the Warm Season, *Sustainability*, 7, 4689–4706; DOI: 10.3390/su7044689.
- Buyantuyev, A., Wu, J. 2010. Urban heat islands and landscape heterogeneity: linking spatiotemporal variations in surface temperatures to land-cover and socioeconomic patterns. *Landscape Ecology* 25: 17–33. DOI: 10.1007/s10980-009-9402-4
- Carver, S. J. 1991. Integrating multi-criteria evaluation with geographical information systems. *International Journal of Geographical Information Systems* 5 (3), 321–339. DOI: 10.1080/02693799108927858
- Central Ground Water Board, Ministry of Water Resources, Government of India 2010. Ground Water Scenario of India 2009-10, 8–10.
- Chen, X.L., Zhao, H. M., Li, P. X., Yin, Z. Y. 2006. Remote sensing image-based analysis of the relationship between urban heat island and land use/cover changes, *Remote Sensing of Environment* 104, 133–146. DOI: 10.1016/j.rse.2005.11.016
- Choudhury, B. J. 1987. Relationships between vegetation indices, radiation absorption and net photosynthesis evaluated by a sensitivity analysis. *Remote Sensing of the Environment* 22, 209–233. DOI: 10.1016/0034-4257(87)90059-9
- Dai, X., Zhongyang, G., Zhang, L., Li, D. 2010. Spatiotemporal exploratory analysis of urban surface temperature field in Shanghai, China. *Stochastic Environmental Research & Risk Assessment* 24, 247–257. DOI: 10.1007/s00477-009-0314-2
- Davis, A. P., Traver, R. G., Hunt, W. F. 2010. Improving urban stormwater quality: Applying fundamental principles. *J. Contemp. Water Res. Educ* 146, 3–10. DOI: 10.1111/j.1936-704x.2010.00387.x
- DeBusk, K., Hunt, W. F., Hatch, U., Sydorovych, O. 2010. Watershed retrofit and management evaluation for urban stormwater management systems in North Carolina. *J. Contemp. Water Res. Educ*, 146, 64–74. DOI: 10.1111/j.1936-704x.2010.00392.x
- Deosthali, V., 2000. Impact of rapid urban growth on heat and moisture islands in Pune City, India. *Atmospheric Environment* 34, 2745–2754. 10.1016/s1352-2310(99)00370-2
- Ding, H., Shi, W. 2013. Land-use/land-cover change and its influence on surface temperature: A case study in Beijing city. *Int. J. Remote Sens.*, 34, 5503–5517. DOI: 10.1080/01431161.2013.792966
- Eastman, J. R. 1997. Idrisi for Windows, Version 2.0: Tutorial Exercises, Graduate School of Geography—Clark University, Worcester, MA.
- Essa, W., Verbeiren, B., van der Kwast, J., van de Voorde, T., Batelaan, O. 2012. Evaluation of the DisTrad thermal sharpening methodology for urban areas. *Int. J. Appl. Earth Obs. Geoinf.* 19, 163–172. DOI: 10.1016/j.jag.2012.05.010
- Gémes, O., Tobak, Z., Leeuwen, B. V. 2016. Satellite based analysis of surface urban heat island intensity, *Journal of environmental geography* 9 (1–2), 23–30. DOI: 10.1515/jengeo-2016-0004
- Giridharan, R., Ganesan, S., Lau, S. S. Y. 2004. Daytime urban heat island effect in high-rise and high-density residential developments in Hong Kong. *Energy and Buildings* 36(6), 525–534. 10.1016/j.enbuild.2003.12.016
- Grover, A., Singh, R. B., 2015. Analysis of Urban Heat Island (UHI) in Relation to Normalized Difference Vegetation Index (NDVI): A Comparative Study of Delhi and Mumbai, *Environments* 2015, 2, 125–138.
- Gulácsi, A., Kovács, F. 2015. Drought Monitoring with Spectral Indices Calculated from Modis Satellite Images in Hungary, *Journal of Environmental Geography* 8 (3–4), 11–20, DOI: 10.1515/jengeo-2015-0008.
- Jalan, S., Sharma, K. 2014. Spatio-Temporal Assessment Of Land Use/Land Cover Dynamics And Urban Heat Island Of Jaipur City Using Satellite Data, The International Archives of the Photogrammetry, Remote Sensing and Spatial Information Sciences, Volume XL-8, 767–772.
- James, M. M., Charles, N. M. 2014. Dynamism of Land use Changes on Surface Temperature in Kenya: A Case Study of Nairobi City, *International Journal of Science and Research* 3 (4), 38–41.
- Kar, S., Pal, S. 2012. Changing Land use Pattern in Chatra Wetland of English Bazar Town: Rationale and Flaws. *International Journal of Humanities and Social Sciences* 2(2), 201–206.
- Kawashima, S., Ishida, T., Minomura, M., Miwa, T. 2000. Relations between Surface Temperature and Air Temperature on a Local Scale during Winter Nights. *Journal of Applied Meteorology* 39, 1570–1779. DOI: 10.1175/1520-0450(2000)039<1570:rbstaa>2.0.co;2
- Keller, C. F. 2008. Global warming: a review of mostly settled issue. *Stochastic Environmental Research & Risk Assessment*, DOI: 10.1007/s00477-008-0253-3.
- Khatun, S., Pal, S. 2016. Identification of Prospective Surface Water Available Zones with Multi Criteria Decision Approach in Kushkaran River Basin of Eastern India, *Archives of Current Research International* 4(4): 1–20, DOI:10.9734/ACRI/2016/27651.
- Kibert, C. J. 2012 *Sustainable Construction: Green Building Design and Delivery*; 3rd ed.; John Wiley and Sons, Inc: Hoboken, NJ, USA, p. 236.
- Kuang, W., Dou, Y., Zhang, C., Chi, W., Liu, A., Liu, Y., Zhang, R., Liu, J. 2015a. Quantifying the heat flux regulation of metropolitan land use/land cover components by coupling remote sensing modeling with in situ measurement. *J. Geophys. Res. Atmos.* 120, 113–130. DOI: 10.1002/2014jd022249
- Kuang, W., Liu, Y., Dou, Y., Chi, W., Chen, G., Gao, C., Yang, T., Liu, J., Zhang, R. 2015b. What are hot and what are not in an urban landscape: Quantifying and explaining the land surface temperature pattern in Beijing, China. *Landsc. Ecol.* 30, 357–373. DOI: 10.1007/s10980-014-0128-6
- Landsat Project Science Office 2002. Landsat 7 Science Data User's Handbook. URL: [http://ltpwww.gsfc.nasa.gov/IAS/handbook/handbook\\_toc.html](http://ltpwww.gsfc.nasa.gov/IAS/handbook/handbook_toc.html), Goddard Space Flight Center, NASA, Washington, DC (last date accessed: 10 September 2003).
- Landsberg, H. E. 1981 *The Urban Climate*. New York: Academic Press.
- Li, L., Tan, Y., Ying, S., Yu, Z., Li, Z., Lan, H. 2014. Impact of land cover and population density on land surface temperature: case study in Wuhan, China. *Journal of Applied Remote Sensing* 8, DOI: 1117/1.JRS.8.084993.
- Li, Y. Y., Zhang, H., Kainz, W. 2012. Monitoring patterns of urban heat islands of the fast-growing Shanghai metropolis, China: Using time-series of Landsat TM/ETM+ data. *Int. J. Appl. Earth Obs. Geoinf.* 19, 127–138. DOI: 10.1016/j.jag.2012.05.001
- Liu, L., Zhang, Y. 2011. Urban heat island analysis using the Landsat TM data and ASTER data: A Case study in Hong Kong. *Remote Sens.* 3, 1535–1552. DOI: 10.3390/rs3071535
- Liu, Y., Hiyama, T., Yamaguchi, Y. 2006. Scaling of land surface temperature using satellite data: A case examination on ASTER and MODIS products over a heterogeneous terrain area. *Remote Sensing of Environment*, 105, 115–128. DOI: 10.1016/j.rse.2006.06.012
- Malczewski, J. 2004 GIS-based land-use suitability analysis: a critical overview. *Progr. Plann.* 62 (1), 3–65. DOI: 10.1016/j.progress.2003.09.002
- McFeeters, S. K. 1996. The use of normalized difference water index (NDWI) in the delineation of open water features. *International*



- Journal of Remote Sensing* 17(7), 1425–1432. DOI: 10.1080/01431169608948714
- McMillin, L.M. 1975 Estimation of sea surface temperature from two infrared window measurements with different absorptions. *Journal of Geophysical Research* 80, 5113–5117. DOI: 10.1029/jc080i036p05113
- Monserud, R. A., Leemans, R. 1992. Comparing global vegetation maps with the Kappa statistic, *Ecological Modelling* 62, 275–293. DOI: 10.1016/0304-3800(92)90003-w
- Neteler, M. 2010. Estimating daily land surface temperatures in mountainous environments by reconstructed MODIS LST Data. *Remote Sensing* 2, 333–351. DOI: 10.3390/rs1020333
- Nichol, J. E., Hang, T. P. 2012. Temporal characteristics of thermal satellite images for urban heat stress and heat island mapping, *ISPRS Journal of Photogrammetry and Remote Sensing* 74, 153–162. DOI: 10.1016/j.isprsjprs.2012.09.007
- Nieuwolt, S. 1966. The urban microclimate of Singapore. *The Journal of Tropical Geography* 22, 30–37.
- Ogashawara, I., Bastos, V. S. B. 2012. A quantitative approach for analyzing the relationship between urban heat islands and land cover. *Remote Sens.* 4, 3596–3618. DOI: 10.3390/rs4113596
- Park, H. S. 1986. Features of the heat island in Seoul and its surrounding cities. *Atmos. Environ.* 20, 1859–1866. DOI: 10.1016/0004-6981(86)90326-4
- Peng, S., Piao, S., Ciais, P., Friedlingstein, P., Otle, C., Bréon, F., Nan, H., Zhou, L. 2012. Myneni, R. Surface Urban Heat Island Across 419 Global Big Cities. *Environ. Sci. Technol.* 46, 696–703. DOI: 10.1021/es2030438
- Saaty, T.L. 1980. *The Analytic Hierarchy Process*, New York: McGraw Hill. International. Translated to Russian, Portuguese, and Chinese, Revised editions, Paperback (1996, 2000), Pittsburgh: RWS Publications.
- Schwarz, N., Lautenbach, S., Seppelt, R. 2011. Exploring indicators for quantifying surface urban heat islands of European cities with MODIS land surface temperatures, *Remote Sens. Environ.* 115, 3175–3186. DOI: 10.1016/j.rse.2011.07.003
- Sharma, R., Joshi, P.K. 2013. Monitoring urban landscape dynamics over Delhi (India) using remote sensing (1998–2011) inputs, *J. Indian Soc. Remote Sens.* 41, 641–650. 10.1007/s12524-012-0248-x
- Singh, R. B., Grover, A., Zhan, J. 2014 Inter-seasonal variations of surface temperature in the urbanized environment of Delhi using Landsat thermal data. *Energies* 7, 1811–1828. DOI: 10.3390/en7031811
- Stathopoulou, M., Cartalis, C. 2009. Downscaling AVHRR land surface temperatures for improved surface Urban Heat Island intensity estimation. *Remote Sensing of Environment* 113, 2592–2605. DOI: 10.1016/j.rse.2009.07.017
- Townshend, J. R., Justice, C. O. 1986 Analysis of the dynamics of African vegetation using the normalized difference vegetation index. *International Journal of Remote Sensing*, 7(11), 1435–1445. DOI: 10.1080/01431168608948946
- UNFPA 2007. *The state of world population 2007: Unleashing the potential of urban growth*. United Nations Population Fund, United Nations Publications.
- Wan, Z., Dozier, J. A. 1996. Generalized split-window algorithm for retrieving land-surface temperature from space. *IEEE Trans Geosci Remote Sens*, 34, 892–905. DOI: 10.1109/36.508406
- Weng, Q. 2001. A remote sensing-GIS evaluation of urban expansion and its impact on surface temperature in the Zhujiang Delta, China. *International Journal of Remote Sensing*, 22, 1999–2014.
- Weng, Q., Lu, D., Schubring, J. 2004 Estimation of land surface temperature-vegetation abundance relationship for urban heat island studies, *Remote Sensing of Environment* 89, 467–483. DOI: 10.1016/j.rse.2003.11.005
- Weng, Q., Yang, S. 2004. Managing the adverse thermal effects of urban development in a densely populated Chinese city. *J. Environ. Manag.* 70, 145–156. DOI: 10.1016/j.jenvman.2003.11.006
- Xiao, R. B., Ouyang, Z. Y., Zheng, H., Li, W. F., Schienke, E. W., Wang, X. K. 2007. Spatial patterns of impervious surfaces and their impact on land surface temperature in Beijing, China. *J. Environ. Sci.* 19, 250–256. DOI: 10.1016/s1001-0742(07)60041-2
- Xiong, Y., Huang, S., Chen, F., Ye, H., Wang, C., Zhu, C. 2012. The impacts of rapid urbanization on the thermal environment: A remote sensing study of Guangzhou, South China. *Remote Sens.* 4, 2033–2056. DOI: 10.3390/rs4072033
- Yuan, F., Bauer, M. E. 2007. Comparison of impervious surface area and normalized difference vegetation index as indicators of surface heat island effects in Landsat imagery. *Remote Sensing of Environment* 106, 375–386. DOI: 10.1016/j.rse.2006.09.003
- Zha, Y., Gao, J., Ni, S. 2003. Use of normalized difference built-up index in automatically mapping urban areas from TM imagery. *International Journal of Remote Sensing* 24(3), 583–594. DOI: 10.1080/01431160304987
- Zhang, H., Qi, Z. F., Ye, X.Y., Cai, Y. B., Ma, W. C. 2013. Analysis of land use/land cover change, population shift, and their effects on spatiotemporal patterns of urban heat islands in metropolitan Shanghai, China. *Appl. Geogr.* 44, 121–133. DOI: 10.1016/j.apgeog.2013.07.021



## WATER QUALITY SURVEY OF STREAMS FROM RETEZAT MOUNTAINS (ROMANIA)

Mihai-Cosmin Pascariu<sup>1,2</sup>, Tiberiu Tulucan<sup>3,4</sup>, Mircea Niculescu<sup>5</sup>, Iuliana Sebarchievici<sup>2</sup>,  
Mariana Nela Ștefănuț<sup>2\*</sup>

<sup>1</sup>Vasile Goldiș” Western University of Arad, Faculty of Pharmacy, 86 Liviu Rebreanu, RO-310414, Arad, Romania

<sup>2</sup>National Institute of Research & Development for Electrochemistry and Condensed Matter – INCEMC Timișoara, 144 Dr. Aurel Păunescu-Podeanu, RO-300569, Timișoara, Romania

<sup>3</sup>Vasile Goldiș” Western University of Arad, Izoi-Moneasa Center of Ecological Monitoring, 94 Revoluției Blvd., RO-310025, Arad, Romania

<sup>4</sup>Romanian Society of Geography, Arad subsidiary, 2B Vasile Conta, RO-310422, Arad, Romania

<sup>5</sup>University Politehnica Timișoara, Faculty of Industrial Chemistry and Environmental Engineering, 6 Vasile Pârvan Blvd., RO-300223, Timișoara, Romania

\*Corresponding author, e-mail: mariana.stefanut@gmail.com

Research article, received 3 July 2016, accepted 14 November 2016

### Abstract

The Retezat Mountains, located in the Southern Carpathians, are one of the highest massifs in Romania and home of the Retezat National Park, which possesses an important biological value. This study aimed at the investigation of water quality in creeks of the Southern Retezat (Piule-Iorgovanul Mountains) in order to provide information on pollutants of both natural and anthropogenic origin, which could pose a threat for the human health. Heavy metal and other inorganic ion contents of samples were analyzed with on-site and laboratory measurements to estimate water quality. The samples were investigated using microwave plasma - atomic emission spectrometry to quantify specific elements, namely aluminium, cadmium, cobalt, chromium, copper, iron, magnesium, manganese, molybdenum, nickel, lead and zinc. The results were compared with the European Union and Romanian standards regarding drinking water and surface water quality. The studied heavy metals have been found to be in very low concentrations or under the method's detection limit. Thus, in the microbasin corresponding to the sampling points, there seems to be no heavy metal pollution and, from this point of view, the samples comply as drinking water according to the European Union and Romanian recommendations. Our findings confirm that the Retezat Mountains are still among the least contaminated regions in Europe and that the ecosystem and the human health is not negatively influenced by water quality problems.

**Keywords:** water chemical analysis, surface water quality, heavy metals, MP-AES, Retezat National Park

### INTRODUCTION

Heavy metals are considered common pollutants of the environment, having both natural and anthropogenic origins (Tchounwou et al., 2012; Bradl et al., 2005). The rapid development of modern world has accelerated their release into the biosphere (Mosa et al., 2016; Panagos et al., 2013). Some of the chemical species that contain heavy metals can be highly toxic when inhaled or ingested. They can have an impact on almost every organ and system in a living organism, posing a serious threat to the stability of the ecosystems and a danger for the human health (Jaishankar et al., 2014; Bradl et al., 2005). They constitute the main contaminant category that affects Europe, contributing to around 30-35% in soil and groundwater contamination (Panagos et al., 2013). Besides air pollution, heavy metals have been regarded, in the last decades, the greatest immediate health threat in Central and Eastern Europe (Fitzgerald et al., 1998). The influence of metal pollution on the river ecological status in Europe is evaluated according to the Water Framework Directive (Roig et al., 2016).

The Retezat National Park is located in the western part of the Southern Carpathian Mountain Range (Romania, Hunedoara County). It possesses a high biological value and has thus been added to the UNESCO's Man and the Biosphere reserves network. The park includes 19 peaks above 2000 m elevation and it has been proposed as a model for the conservation efforts in Romania and other countries (Bytnerowicz et al., 2005). While several studies from the scientific mainstream literature have dealt with the geology and hydrogeology of the area (Povară and Ponta, 2010) or the composition of mountain lake sediments (Catalan, 2015; Camarero et al., 2009; Rose et al., 2009), studies regarding the composition of surface creeks seem to be scarce or non-existent.

In this work, several springs and streams from the Southern Retezat were analyzed for the presence of heavy metals and other ions (cations and anions). The tested cations include ammonium ( $\text{NH}_4^+$ ), arsenic ( $\text{As}^{3+}$ ), calcium ( $\text{Ca}^{2+}$ ), iron ( $\text{Fe}^{2+}/\text{Fe}^{3+}$ ) and other heavy metals (e.g., lead  $\text{Pb}^{2+}$ ), while the anions that were searched for

include halides (chloride  $\text{Cl}^-$ , bromide  $\text{Br}^-$ , iodide  $\text{I}^-$ ), nitrite ( $\text{NO}_2^-$ ) and sulfate ( $\text{SO}_4^{2-}$ ), all of them being determined according to the chemical methods stipulated in the Romanian Pharmacopoeia (1993) or by using test strips. The results were supplemented by microwave plasma - atomic emission spectrometry (MP-AES) determinations for some metals, i.e. aluminium, cadmium, cobalt, chromium, copper, iron, magnesium, manganese, molybdenum, nickel, lead and zinc. Most of these species are included in the category of heavy metals (Duffus, 2002).

## STUDY AREA

The studied area (Fig. 1) belongs to the southern part of the Retezat Mountains (Bytnerowicz et al., 2005), also known as Southern Retezat ("Retezatul Sudic" in Romanian), and is located on the southern slope of the Piule-Iorgovanu Mountains (Ardelean, 2010; Povară and Ponta, 2010), between 1529 and 1871 m of altitude. The stream water samples (Fig. 1) were collected at six sampling points at Scorota cu Apă and Scorota Seacă (the headwaters of Scorota River) in the upper part of the Jiul de Vest River basin (Iordache et al., 2015;

Ujvári, 1972). The microbasins corresponding to the sampling points contain active streams with lengths which vary between 100 and 500 m, and with a discharge usually between 2 and 5 L/s. The sampling points were allocated by considering these short lengths and their relative position to the Scorota sheepfold: near the sheepfold, which is also the lowest part of the grazing area, and in the higher limit of this area, with approximately 100 m of altitude between the different sample points.

From geological point of view, mostly sedimentary rocks cover the surface, like quartz sandstones, marl and marl-limestones, with patches of schists and limestones. The most important soil types are humus-iron-illuvial podzols, humus-silicate soils, brown podzols and brown acidic soils. These mountains are characterized by a rich flora and fauna. Subalpine meadows (grassland) predominate, being in contact with the upper limit of the coniferous domain, composed mainly of Norway spruce (*Picea abies*). *Carex* and *Festuca* meadows alternate with mountain pine, juniper shrubs and dwarf shrubs composed of *Vaccinium vitis-idaea* and *Vaccinium myrtillus* (Bytnerowicz et al., 2005; Kern and Popa, 2009; Măciu

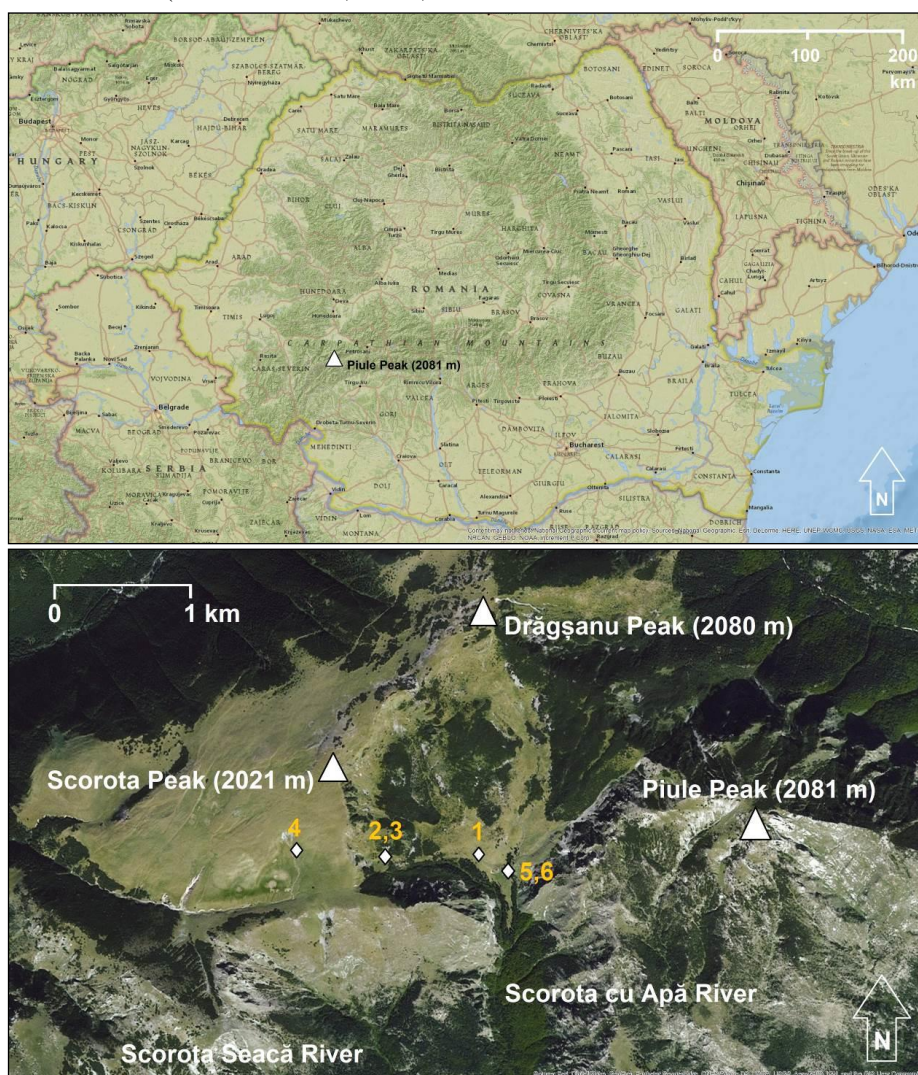


Fig. 1 Location of the sampling points



Fig. 2 Environment of the sampling sites (left side: juniper forest and *Festuca* meadows, characteristic for samples 1, 2, 3, 5 and 6; right side: eroded mountain slopes in the case of sample 4)

et al., 1982; Tulucan et al., 1999), as can be seen in Fig. 2 (left). The climate is continental and typical for high mountain areas (Povară and Ponta, 2010). Prior to sampling, weather was stable with constant atmospheric pressure. There was no record of rainfall or snowfall that could have produced signs of indirect contamination (e.g., acid rain or residual grazing waste).

The list of analyzed samples, together with time, location and on-site measured parameters, are given in Table 1. Samples 1-3 come from springs which originate in fluvial deposits from non-karst rocks (sandstones). For samples 2 and 3, the measurements were taken near a confluence of two very short creeks, which combine to form a right tributary of Scorota cu Apă stream. Sample 4, corresponding to the highest measured point, comes from a spring localized in non-calcareous detrital rocks; the sampling was done in a ravine with erosional slopes (Fig. 2, right). Samples 5 and 6 were collected near Scorota sheepfold from two creeks that flow over Holocene detrital deposits. The catchment is located in the *Festuca* meadows perimeter; sampling sites corresponding to samples 1-3, 5 and 6 are located in the juniper floor, where juniper clusters alternate with *Festuca* meadows.

Due to the fact that the sampling was performed at the beginning of November, any organic pollution that might have appeared because of grazing should have been washed by precipitations in the two months that have passed since the ending of the grazing period.

## METHODS

### *Sampling and in situ measurements*

Geographic coordinates and altitudes were established using a Magellan Meridian Platinum Mapping GPS receiver, while air temperature and pressure were recorded with a portable Auriol weather station. Sample temperature, pH and electrical conductivity (EC) were registered with a portable Hanna HI 98130 Combo pH&EC measuring device. Nitrites and sulfates were measured *in situ* using Merck test strips (Merckoquant® Nitrit-Test and Merckoquant® Sulfat-Test) (Table 1).

We have generally followed ISO 5667-3 guidelines for sampling. To prevent contaminations, thoroughly cleaned plastic recipients were used (Bradl et al., 2005; Ogoyi et al., 2011), prepared in the laboratory by protracted soaking with 2 M nitric acid followed by rinsing with double distilled water. They were also conditioned *in situ* with several aliquots of the water to be

Table 1 Sampling parameters

Parameter / Sample	1	2	3	4	5 <sup>a</sup>	6 <sup>a</sup>
Date (day/month/year)	01/11/2014	01/11/2014	01/11/2014	01/11/2014	02/11/2014	02/11/2014
Time (UTC+2 hours)	12:00	13:00	13:10	16:00	09:00	09:10
Geographic coordinates	45°17'57''N 22°53'23''E	45°17'55''N 22°52'57''E	45°17'55''N 22°52'57''E	45°17'57''N 22°52'30''E	45°17'53''N 22°53'33''E	45°17'53''N 22°53'35''E
Altitude [m]	1620	1759	1759	1871	1533	1529
Air pressure [mbar]	842.8	828.3	828.3	817.6	<sup>b</sup>	<sup>b</sup>
Air temperature [°C]	25	22	22	15	<sup>b</sup>	<sup>b</sup>
Sample temperature [°C]	4.8	5.4	5.9	4.9	5.0	4.0
pH [pH units]	8.40	7.92	8.02	8.00	8.13	8.18
EC [μS/cm]	~ 10	< 10	< 10	< 10	< 10	< 10

<sup>a</sup> geographic coordinates and altitude were established using Google Earth (2015) software;

<sup>b</sup> not measured.

sampled. After completing this protocol a volume of 350 mL of water was collected. To avoid the loss of elements by adsorption on the walls of the storage recipients, the samples were stabilized by acidification to pH ~ 1 by adding 20 mL of 10% nitric acid (Pascariu et al., 2013).

#### Laboratory analysis

All glassware needed for analysis was washed with 2 M nitric acid and thoroughly rinsed with double distilled water just prior of being used. Preliminary analyses were performed on filtrated samples the day after they were collected according to the general procedures stated by the Romanian Pharmacopoeia (1993). A blank solution (350 mL double distilled water with 20 mL 10% nitric acid) was also prepared in an identical plastic container and tested for comparison. The following aqueous reagents were used: Nessler's reagent (potassium tetraiodomercurate (II),  $K_2HgI_4$ , and potassium hydroxide, KOH) for ammonium, sodium hypophosphite ( $NaH_2PO_2$ ) in hydrochloric acid (HCl) for arsenic, ammonium oxalate ( $(NH_4)_2C_2O_4$ ) for calcium, silver(I) nitrate ( $AgNO_3$ ) for halides, potassium hexacyanoferrate(II) ( $K_4[Fe(CN)_6]$ ) for iron, sodium sulfide ( $Na_2S$ ) for heavy metals (e.g., lead) and barium chloride ( $BaCl_2$ ) for sulfates. The chemical reactions that use these reagents are stated to have the following detection limits: 0.3 ppm for ammonium, 1 ppm for arsenic, 3.5 ppm for calcium, 0.5 ppm for chlorides, 0.5 ppm for iron, 0.5 ppm for lead and 3 ppm for sulfates (Romanian Pharmacopoeia 1993).

For MP-AES, an Agilent 4100 with web-integrated Agilent MP Expert software was used. The instrument was adjusted using as calibration standard the provided Wavelength Calibration Concentrate for ICP-OES & MP-AES (Al, As, Ba, Cd, Co, Cr, Cu, Mn, Mo, Ni, Pb, Se, Sr, Zn 50 mg/L, K 500 mg/L) and also an AAS standard solution for Ca, Fe and Mg. The following wavelengths (in nm) were measured: Al 396.152, Cd 228.802, Co 340.512, Cr 425.433, Cu 324.754, Fe 259.940, Mn 403.076, Mg 285.213, Mo 379.825, Ni 352.454, Pb 405.781, and Zn 213.857. In contrast to atomic absorption spectrometry (AAS), which is based upon the absorption of a characteristic radiation, atomic emission spectrometry (AES) uses the emission of a characteristic wavelength for the

determination of the analyte element. Plasma emission spectrometry utilizes a plasma as the excitation source for atomic emissions, which, in MP-AES, is formed via the use of a microwave field source. AES belongs to the most useful and commonly used techniques for the analysis of heavy metals, providing rapid and sensitive results in a variety of sample matrices, although the detection limits are higher than those of AAS (Bradl et al., 2005; Higson, 2006).

## RESULTS AND DISCUSSION

The average water temperature was 5.0 °C, the mean pH value was 8.11, while the measured EC value was around or below 10  $\mu S/cm$  for all samples (Table 1). The in situ tests using test strips did not indicate the presence of nitrites or sulfates (nitrite ion concentration less than 1 mg/L, sulfate ion concentration less than 200 mg/L, according to test strips instructions). Also, the very low measured EC indicates that the total dissolved solids (TDS) must be under 10 ppm (Lenntech, 2016).

The samples were tested for the presence of ammonium, arsenic, calcium, halides (chloride, bromide, and iodide), iron, heavy metals (e.g., lead) and sulfates. Except for a very faint opalescence obtained when sample 1 was tested for calcium, all these tests were negative, an observation that supports the very low measured EC for all samples (Table 1).

MP-AES results are summarized in Table 2, while the drinking water standards from EU (1998) and Romanian "Law no. 311 from June 28, 2004" (Romanian Government 2004) are given in Table 3 for comparison with the analyzed samples. As can be seen, except for a somewhat increased iron content in sample 1 (probably due to the humus-iron-illuvial podzols, which are present in the area), the studied streams are within the limits specified for drinking water (Brad et al., 2015) by all specified standards. The metal contents are generally low and there is no observable trend downstream on any of the elements.

The Romanian environmental legislation regarding surface water quality, stipulated in "Order no. 161 from February 16, 2006" (Romanian Government 2006), is summarized for the considered ions in Table 4. This surface water quality classification is useful in order to establish the ecological status of all marine and continental

Table 2 MP-AES cation content results, in mg/L

Sample	Concentration											
	Al	Cd	Co	Cr	Cu	Fe	Mg	Mn	Mo	Ni	Pb	Zn
1	*	*	0.03	*	*	1.61	0.53	*	0.03	*	0.01	*
2	*	*	0.03	*	*	0.05	1.10	*	0.02	*	0.01	*
3	*	*	0.02	*	*	0.13	1.84	*	0.02	*	*	*
4	0.01	*	0.02	*	*	0.08	0.18	*	0.02	*	*	*
5	0.01	*	0.02	*	*	0.14	0.88	*	0.02	*	*	*
6	*	*	0.02	*	*	0.05	0.54	*	0.02	*	*	*

\* under detection limit (< 0.005 mg/L).

Table 3 Drinking water standards comparative table; all values are in units of mg/L unless stated otherwise (European Union, 1998; Romanian Government, 2004)

Parameter	EU standards 1998	Romanian law no. 311/2004
pH [pH units]	6.5-9.5	6.5-9.5
EC [mS/cm]	2.500	2.500
TDS	#	#
Temperature [°C]	#	#
Aluminium (Al <sup>3+</sup> )	0.200	0.200
Ammonia/ammonium (NH <sub>3</sub> +NH <sub>4</sub> <sup>+</sup> )	0.50	0.50
Cadmium (Cd <sup>2+</sup> )	0.0050	0.0050
Calcium (Ca <sup>2+</sup> )	#	#
Chromium (Cr <sup>3+</sup> +Cr <sup>6+</sup> )	0.050	0.050
Cobalt (Co <sup>2+</sup> +Co <sup>3+</sup> )	#	#
Copper (Cu <sup>2+</sup> )	2.0	0.1*
Iron (Fe <sup>2+</sup> +Fe <sup>3+</sup> )	0.200	0.200
Lead (Pb <sup>2+</sup> )	0.010	0.010
Manganese (Mn <sup>x+</sup> )	0.050	0.050
Magnesium (Mg <sup>2+</sup> )	#	#
Molybdenum (Mo <sup>x+</sup> )	#	#
Nickel (Ni <sup>2+</sup> )	0.020	0.020
Zinc (Zn <sup>2+</sup> )	#	5.000
Chloride (Cl <sup>-</sup> )	250	250
Nitrite (NO <sub>2</sub> <sup>-</sup> )	0.50	0.50
Sulfate (SO <sub>4</sub> <sup>2-</sup> )	250	250

# not mentioned;

\* is allowed as 2.0 mg/L if the distribution piping material contains copper.

Table 4 Surface water quality classes depending on cation content, as stated in Romanian "Order no. 161 from February 16, 2006"; units are in mg/L, unless stated otherwise

Parameter	Order no. 161 (2006)				
	I	II	III	IV	V
pH [pH units]	6.5 – 8.5				
EC [mS/cm]	No guideline				
TDS	Not mentioned				
Temperature [°C]	No guideline				
Aluminium (Al <sup>3+</sup> )	Not mentioned				
Cadmium (Cd <sup>x+</sup> )	0.0005	0.001	0.002	0.005	>0.005
Chromium, total (Cr <sup>3+</sup> +Cr <sup>6+</sup> )	0.025	0.050	0.100	0.250	>0.250
Calcium (Ca <sup>2+</sup> )	50	100	200	300	>300
Cobalt (Co <sup>3+</sup> )	0.010	0.020	0.050	0.100	>0.100
Copper (Cu <sup>2+</sup> )	0.020	0.030	0.050	0.100	>0.100
Iron, total (Fe <sup>2+</sup> +Fe <sup>3+</sup> )	0.3	0.5	1.0	2	>2
Lead (Pb <sup>x+</sup> )	0.005	0.010	0.025	0.050	>0.050
Magnesium (Mg <sup>2+</sup> )	12	50	100	200	>200
Manganese, total (Mn <sup>2+</sup> +Mn <sup>7+</sup> )	0.05	0.1	0.3	1	>1
Nickel (Ni <sup>x+</sup> )	0.010	0.025	0.050	0.100	>0.100
Zinc (Zn <sup>2+</sup> )	0.100	0.200	0.500	1.000	>1.000
Chloride (Cl <sup>-</sup> )	25	50	250	300	>300
Sulfate (SO <sub>4</sub> <sup>2-</sup> )	60	120	250	300	>300

aquatic ecosystems, including rivers and lakes, both natural and artificial. The evaluation of the considered quality elements, like chemical and physical-chemical parameters, can indicate the presence of certain natural environments, minor alterations of these or the degree of anthropic impact, and, respectively, the status of water bodies quality in a certain amount of time. There are five ecological states being defined for natural rivers and lakes: very good (I), good (II), moderate (III), poor (IV) and bad (V). According to Table 4, the streams corresponding to samples 3-6 belong to class I. An exception could be the stream that provided sample 1, which belongs to class IV according to the iron content. Also, according to the lead content, the streams that provided samples 1 and 2 could belong to class II or III, but these low measured lead levels may more realistically be accounted for by the MP-AES precision limit.

Our findings support the previous studies which state that the Retezat Mountains are among the least contaminated regions in Europe (Catalan, 2015; Catalan et al., 2009). Regarding the studied parameters and considering the low levels of dissolved ions, water quality was found to be good or very good. Thus, heavy metals do not pose any ecological or human risk in the studied area.

## CONCLUSIONS

MP-AES, alongside some classical analytical procedures, were used to analyze the water quality of springs and creeks from the Retezat National Park. For all tested samples, heavy metals were at very low levels or under the detection limit for the chemical reactions employed and the MP-AES method applied. From this point of view, the samples comply as drinking water according to the EU and Romanian recommendations. The average water temperature was 5.0 °C, the mean pH value was 8.11, while the measured EC value was around or below 10 µS/cm for all samples, the later also confirming the very small ion content present in the analyzed mountain streams. In the microbasin corresponding to the sampling points, there seems to be no heavy metal pollution. Also, no other potential sources of chemical pollution was recorded in the studied perimeter during our survey.

## Acknowledgements

Part of this paper was presented at The 17<sup>th</sup> DKMT Euroregional Conference on Environment and Health, June 5-6, 2015, Szeged, Hungary. Some of the research was done at the Center of Genomic Medicine of the "Victor Babeş" University of Medicine and Pharmacy of Timișoara, POSCCE 185/48749, contract 677/09.04.2015.

## References

- Ardelean, M. 2010. Piule-Iorgovanu Mountains – Geomorphologic study (PhD thesis). "Babeş-Bolyai" University of Cluj-Napoca, Faculty of Geography, Cluj-Napoca, Romania.
- Brad, T., Fekete, A., Șandor, M.S., Purcărea, C. 2015. Natural attenuation potential of selected hydrokarst systems in the Carpathian Mountains (Romania). *Water Sci. Technol.: Water Supply* 15(1), 196–206. DOI: 10.2166/ws.2014.092.

- Bradl, H., Kim, C., Kramar, U., Stüben, D. 2005. Interactions of Heavy Metals. In: Bradl, H.B. (ed.) *Heavy Metals in the Environment: origin, interaction and remediation*. Elsevier Academic Press, Amsterdam, Netherlands, 28–164. DOI: 10.1016/S1573-4285(05)80021-3.
- Bytnerowicz, A., Badea, O., Popescu, F., Musselman, R., Tanase, M., Barbu, I., Frączek, W., Gembasu, N., Surdu, A., Danescu, F., Postelnicu, D., Cenusa, R., Vasile, C. 2005. Air pollution, precipitation chemistry and forest health in the Retezat Mountains, Southern Carpathians, Romania. *Environ. Pollut.* 137, 546–567. DOI:10.1016/j.envpol.2005.01.040.
- Camarero, L., Botev, I., Muri, G., Psenner, R., Rose, N., Stuchlik, E. 2009. Trace elements in alpine and arctic lake sediments as a record of diffuse atmospheric contamination across Europe. *Freshwater Biol.* 54(12), 2518–2532. DOI: 10.1111/j.1365-2427.2009.02303.x.
- Catalan, J. 2015. Tracking Long-Range Atmospheric Transport of Trace Metals, Polycyclic Aromatic Hydrocarbons, and Organohalogen Compounds Using Lake Sediments of Mountain Regions. In: Blais, J.M. et al. (eds.) *Environmental Contaminants, Developments in Paleoenvironmental Research 18*. Springer Netherlands, 263–322. DOI: 10.1007/978-94-017-9541-8\_11.
- Catalan, J., Curtis, C.J., Kernan, M. 2009. Remote European mountain lake ecosystems: regionalisation and ecological status. *Freshwater Biol.* 54(12), 2419–2432. DOI: 10.1111/j.1365-2427.2009.02326.x.
- Duffus, J.H. 2002. “Heavy metals” – a meaningless term? (IUPAC Technical Report). *Pure Appl. Chem.* 74(5), 793–807. DOI: 10.1351/pac200274050793.
- European Union 1998. Council Directive 98/83/EC of 3 November 1998 on the quality of water intended for human consumption, <http://eur-lex.europa.eu/legal-content/EN/TXT/?uri=URISERV:128079> (accessed July 2, 2016).
- Fitzgerald, E.F., Schell, L.M., Marshall, E.G., Carpenter, D.O., Suk, W.A., Zejda, J.E. 1998. Environmental Pollution and Child Health in Central and Eastern Europe. *Environ. Health Perspect.* 106(6), 307–311.
- Google Earth (v. 7.1.5.1557). © 2015 Google Inc., <https://www.google.com/earth/>.
- Higson, S. 2006. *Analytical Chemistry*. Oxford University Press, New York, p. 201.
- Iordache, M., Popescu, L.R., Pascu, L.F., Iordache, I. 2015. Environmental Risk Assessment in Sediments from Jiu River, Romania. *Rev. Chim. (Bucharest)* 66(8), 1247–1252.
- Jaishankar, M., Tseten, T., Anbalagan, N., Mathew, B.B., Beeregowda, K.N. 2014. Toxicity, mechanism and health effects of some heavy metals. *Interdiscip. Toxicol.* 7(2), 60–72. DOI: 10.2478/intox-2014-0009.
- Kern, Z., Popa, I. 2009. Assessing temperature signal in X-ray densitometric data of Norway spruce and the earliest instrumental record from the Southern Carpathians. *Journal of Env. Geogr.* 2(3-4), 15–22.
- Lenntech, 2016. Conductivity convertor, <http://www.lenntech.com/calculators/conductivity/tds-engels.htm> (accessed July 2, 2016).
- Măciu, M., Chioreanu, A., Văcaru, V., Posea, G., Ielenicz, M., Pătrosescu, M., Velcea, I., Pișota, I. 1982. Romania's Geographic Encyclopedia. “Editura Științifică și Enciclopedică” Publisher, Bucharest, Romania (in Romanian).
- Mosa, K.A., Saadoun, I., Kumar, K., Helmy, M., Dhankher, O.P. 2016. Potential Biotechnological Strategies for the Cleanup of Heavy Metals and Metalloids. *Front. Plant Sci.* 7:303. DOI: 10.3389/fpls.2016.00303.
- Ogoyi, D.O., Mwita, C.J., Nguu, E.K., Shiundu, P.M. 2011. Determination of heavy metal content in water, sediment and microalgae from Lake Victoria, East Africa. *Open Environ. Eng. J.* 4, 156–161. DOI: 10.2174/1874829501104010156.
- Panagos, P., Van Liedekerke, M., Yigini, Y., Montanarella, L. 2013. Contaminated Sites in Europe: Review of the Current Situation Based on Data Collected through a European Network. *J. Environ. Public Health* 2013:158764. DOI: 10.1155/2013/158764.
- Pascariu, M.C., Ciobotaru, A.L., Tulucan, T., Ștefănuț, M.N., Cătă, A., Fițișău, I.F., Ienașcu, I. 2013. Romanian Pharmacopoeia versus atomic spectrometry as analysis tools for heavy metal content in some water sources from the western and south-western part of Romania. *Arad Medical Journal* XVI(1-4), 91–99.
- Povară, I., Ponta, G. 2010. Geology and hydrogeology of the Jiul de Vest – Cernișoara Basins, Romania. *Carbonates Evaporites* 25, 117–126. DOI: 10.1007/s13146-010-0017-2.
- Roig, N., Sierra, J., Moreno-Garrido, I., Nieto, E., Pérez Gallego, E., Schuhmacher, M., Blasco, J. 2016. Metal bioavailability in freshwater sediment samples and their influence on ecological status of river basins. *Sci. Total Environ.* 540, 287–296. DOI: 10.1016/j.scitotenv.2015.06.107.
- Romanian Government. 2004. Law no. 311 from June 28, 2004, [http://www.rowater.ro/dacrisuri/Documente%20Repository/Legislatie/gospodarirea%20apelor/LEGE%20311\\_28.06.2004.pdf](http://www.rowater.ro/dacrisuri/Documente%20Repository/Legislatie/gospodarirea%20apelor/LEGE%20311_28.06.2004.pdf) (accessed July 2, 2016) (in Romanian).
- Romanian Government. 2006. Order no. 161 from February 16, 2006, [http://www.rowater.ro/dacrisuri/Documente%20Repository/Legislatie/gospodarirea%20apelor/ORD.%20161\\_16.02.2006.pdf](http://www.rowater.ro/dacrisuri/Documente%20Repository/Legislatie/gospodarirea%20apelor/ORD.%20161_16.02.2006.pdf) (accessed July 2, 2016) (in Romanian).
- Romanian Pharmacopoeia, 10<sup>th</sup> edition. 1993. Bucharest, Romania (in Romanian).
- Rose, N.L., Cogălniceanu, D., Appleby, P.G., Brancelj, A., Fernández, P., Grimalt, J.O., Kernan, M., Lami, A., Musazzi, S., Quiroz, R., Velle, G. 2009. Atmospheric contamination and ecological changes inferred from the sediment record of Lacul Negru in the Retezat National Park, Romania. *Adv. Limnol.* 62, 319–350. DOI: 10.1127/advlim/62/2009/319.
- Tchounwou, P.B., Yedjou, C.G., Patlolla, A.K., Sutton, D.J. 2012. Heavy Metal Toxicity and the Environment. In: Luch, A. (ed.) *Molecular, Clinical and Environmental Toxicology*. Volume 3: Environmental Toxicology. Springer Basel, 133–164. DOI: 10.1007/978-3-7643-8340-4\_6.
- Tulucan, A.D., Tulucan, T.N., Beke, L. 1999. Alpine Karst in Romania. *Acta carsologica* 28(1), 139–147.
- Ujvári, I. 1972. *The Geography of Romanian Waters*. “Editura Științifică” Publisher, Bucharest, Romania, p. 371 (in Romanian).



## RISK MANAGEMENT AS A BASIS FOR INTEGRATED WATER CYCLE MANAGEMENT IN KAZAKHSTAN

**Burghard Meyer<sup>1\*</sup>, Lian Lundy<sup>2</sup>, John Watt<sup>2</sup>, Iskandar Abdullaev<sup>3</sup>, Jose E. Capilla Roma<sup>4</sup>**

<sup>1</sup>Leipzig University, Institute of Geography, Johannisalle 19a, 04103 Leipzig, Germany

<sup>2</sup>Middlesex University, Department of Natural Sciences, The Burroughs, Hendon, London NW4 4BT, UK

<sup>3</sup>CAREC, Regional Environmental Centre for Central Asia, 40 Orbita 1, Almaty, 050043, Republic of Kazakhstan

<sup>4</sup>Technical University of Valencia, Research Institute of Water and Environmental Eng. Camino de Vera, s/n, 46022 Valencia, Spain

\*Corresponding author, e-mail: e-mail: burghard.meyer@olanis.de

Research article, received 30 September 2016, accepted 15 November 2016

### Abstract

Integrated Water Cycle Management (IWCM) aims to bring together a diversity of social, environmental, technological and economic aspects to implement sustainable water and land management systems. This paper investigates the challenges and opportunities facing Kazakhstan as it its efforts to move towards a more sustainable approach to managing its finite and highly stressed water resources. The use of a strategic-level risk governance framework to support a multi-disciplinary Kazakh-EU consortium in working collaboratively towards enhancing capacity and capability to address identified challenges is described. With a clear focus on addressing capacity building needs, a strong emphasis is placed on developing taught integrated water cycle management programmes through communication, stakeholder engagement and policy development including appropriate tools for managing the water issues including hydraulic models, GIS-based systems and scenario developments. Conclusions on the benefits of implementing an EU-style Water Framework Directive for Central Asia based on a risk management approach in Kazakhstan are formulated.

**Keywords:** risk management, capacity building, water management, stakeholder engagement

### INTRODUCTION

Kazakhstan is facing important challenges in water resource management from a variety of perspectives, including climate change and melting glaciers (Salnikov et al., 2011; Smith et al., 2005; Chen et al., 2013) over usage of river water resources and groundwater systems for irrigation (Dostay, 2012), water pollution by industry and agriculture, and increasing water consumption (Qadier et al., 2009). As a result, ecological crises including the drying out of large terminal lakes such as Aral lake and, more recently, Balkhash Lake are reported (Zavialov, 2005; Turzunov et al., 1997; Dostay, 2009). Figure 1 shows the main Kazakh river catchments, with seven of the eight river catchments identified as being transboundary and thus requiring the establishment of an international water management agreement to peacefully address water distribution conflicts which have been reported (Wegerich, 2008).

Integrated Water Cycle Management (IWCM is a term used in Kazakhstan, which is synonymous with Integrated Water Resource Management) aims to bring together a diversity of social, environmental, technological and economic aspects to implement sustainable water and land management systems (Global Water Partnership, GWP, 2010). It is widely promoted as international best

practice with regard to water resources planning to meet the needs of both current and future generations (e.g. Bunting, 2009; EU WFD, 2000; Meyer et al., 2014). The central concept is the development and application of objectives in the form of regional and national catchment-based goals for water management based on each catchment's natural conditions and water usage patterns. It includes the development of knowledge about ground and surface water quality and quantity, evaluation of water resource policy over a long-term perspective, implementation of plans and actions that have been developed collaboratively by all water users to address problems identified, and the on-going monitoring and evaluation of management processes including the development of simulation models and decision support systems as supporting tools for IWCM (Meyer et al., 2014). Any implementation of IWCM also includes the protection of the environment by avoiding overexploitation and/or the deterioration of water resources. It requires the development and modernization of institutional structures, methods, legislation and norms including a range of management skills for building capability, capacity and impact in IWCM and working in partnerships.

The need to strengthen partnerships between business, regulatory and academic sectors at a national and international level was identified by the Kazakh Govern-



ment, with the areas of environmental protection and water management recognised as priority areas requiring action (Nazarbayev, 2010). It is within this context that the nurturing of a collaborative cross-sector approach to developing capability and capacity of Kazakh graduates in the field of IWCM was the specific challenge targeted by the EU-TEMPUS funded project I-WEB (Integrating Water cycle Management: Capability, Capacity and Impact in Education and Business). In addition to its recognition at a national level, Kazakh members of I-WEB were able to further clarify the scale and impact of the major water resource issues currently impacting Kazakhstan, demonstrating recognition of its importance at a local and sub-regional level. These include increasing levels of water consumption by agriculture, industry (especially the gas and oil industries) and urban areas. For example, whilst modernisation of agriculture is strongly encouraged, it is often linked to increasing water consumption. This is leading to reduction in water levels in both surface and groundwater bodies, the most notable example of which is the Aral Sea (Kostianoy and Kosarev, 2010; Micklin et al., 2014).

Increasing demand for water resources within Kazakhstan is driven by intensifications of agriculture irrigation, industrialisation and urbanisation. Together with the transboundary nature of the majority of its river basins, the need for IWCM plans to balance demands on water resources across economic sectors but also across national boundaries is clear. A further crucial aspect is the need to mitigate the impacts of climate change (current scenarios indicate continuing falling levels of precipitation and glacier run-off with the latter imparticular a key source of

drinking water supply within Almaty (the largest city in Kazakhstan). Water pollution is also a major national concern, with water quality in many of its surface and ground waters identified as 'unsatisfactory'. Discharges of untreated effluents from chemical industries and petroleum processing are identified as principal sources with devastating environmental impacts reported (Lundy, 2014).

A common issue in managing environmental resources at a national or regional level is that it requires inputs from a wide range of stakeholders, each with very different capabilities, agendas, mandates and resources. It also requires an evidence-based assessment of the risks associated with adopting any changes in practice proposed, in association with an assessment of the risks of any 'business as usual' scenario. The complexity of implementing such legislative requirements within and across national boundaries and sectors requires a strategic level risk management approach that utilises the best scientific and technical evidence to prioritise sustainable decisions but also has the flexibility to respond meaningfully to variations in stakeholder perceptions of what is acceptable or tolerable (Ecologic Institute and SERI, 2010).

As a contribution to addressing this 'wicked problem' of water management in a Kazakh context, this paper, maps a strategic risk management approach to developing management capacity. It identifies key methodologies and supporting tools for assisting in the implementation of IWCM and discusses the current status of transboundary basins of Kazakhstan and its neighbours. Finally conclusions on the benefits of implementing a Water Framework Directive for Central Asia based on a risk management approach in Kazakhstan are developed.



Fig. 1 Map of Main River Basins and Rivers in Kazakhstan (Water Resources Committee of the Ministry of Agriculture of the Republic of Kazakhstan, Anonymous, 2004; Map after Duskeyev & Minzhanova 2014, changed)

## STUDY AREA- CURRENT STATUS OF TRANSBOUNDARY BASINS OF KAZAKHSTAN AND ITS NEIGHBOURS

Water resources are a key for the sustainable economic development of Central Asian states, with Kazakhstan being an exceptionally transboundary- dependent state. Almost all sectors of the economy in these countries are water dependent, requiring huge amounts of water for development. Most of the water resources in the region are transboundary, formed and flowing in from the territory of neighbouring states. Almost 60% of water resources of the country are transboundary and Kazakhstan is downstream almost in all transboundary basins (Table 1). The transboundary water management became a uniquely important aspect of water management in Kazakhstan after the collapse of Soviet Union.

Table 1 Transboundary Basins of Kazakhstan (see also Fig. 1)

Name of the river	Catchment area (km <sup>2</sup> )	Riparian states
Irtish	1.643.000	Kazakhstan, Russian Federation, People Republic of China
Tobol	426.000	Kazakhstan, Russian Federation
Ural	237.000	Kazakhstan, Russian Federation
Syr Darya	219.000	Kazakhstan, Kyrgyzstan, Tajikistan, Uzbekistan
Ishim	177.000	Kazakhstan, Russian Federation
Ili	140.000	Kazakhstan, People Republic of China
Shu	67.500	Kazakhstan, Kyrgyzstan
Talas	52.700	Kazakhstan, Kyrgyzstan

Other smaller transboundary catchments (not shown in Fig. 1) are the Big Uzen (14.300 km<sup>2</sup>); the Small Uzen (13.200 km<sup>2</sup>) and the Burla (12.800 km<sup>2</sup>) of Kazakhstan and Russian Federation; the Aspara catchment (1.210 km<sup>2</sup>) of Kazakhstan and Kyrgyzstan and the Ugam catchment (870 km<sup>2</sup>) of Kazakhstan and Uzbekistan. With Russia (Ural River basin and others), Kazakhstan has agreed "least problematic" relations on transboundary river systems, enforcing the Soviet era agreements through water commissions. The abundance of water, resources and a less dry climate made it possible to continue the agreements between Kazakhstan and Russia made within Soviet times (Table 2). However, water quality is a current concern and measures to improve the environmental situation in both in the Urals and Siberia are planned between two countries. Being part of Eurasian Economic Union, the two countries have a strong legislative basis for water cooperation (Abdullaev and Rakhmatullaev, 2013). China, on the other hand, is a major problematic riparian state for Kazakhstan. Although having major economic interests in Kazakhstan, China has made no efforts to improve water cooperation. Despite having Soviet era agreements in force with China, no technical or institutional enforcement mechanisms are in place to monitor their implementation.

Kazakhstan has Transboundary Rivers flowing in from China, Russia, Uzbekistan, Kyrgyzstan and flowing out to the same neighbouring states (Table 1). Two examples from Central Asia show different options of transboundary water cooperation where Kazakhstan is involved. In both cases, Kazakhstan is a downstream country but has applied different approaches in order to receive its water shares from the Transboundary Rivers. Former Soviet Central Asian states have been using water resources of the two largest rivers and many smaller ones since historical times (Abdullaev and Rakhmatullaev, 2013). The Central Asian neighbours of Kazakhstan are linked with Kazakhstan through Syr Darya River, which supplies water Southern part of Kazakhstan. Around 700,000 ha land and around 1 million people depend from the water of Syr Darya River.

Soviet era water agreements and regulations in Central Asia were arranged and monitored by Moscow. The centrally administered and financed water management system has been built to enforce the water agreements among Central Asia states (then Soviet republics). However, frequent water related disputes emerged even in the Soviet period, which was arbitrated by the Central Ministry of Water and Amelioration of the USSR. The Soviet era water agreements were regulated by "normative" documents - decrees of Cabinet of Ministries, assigning water shares to the production system and not to the specific country (state), although national states then translated these allocations into water sharing percentages.

Although, national states (republics) did not openly contest decisions of the centre, in most of the cases arrangements were made in order to sustain own water shares. Therefore, in the mid-1980's the Soviet government felt pressure from the national states and prepared new basin plans for both rivers of the region and launched new institutions - River Basin Organizations (BVO's) for Syr Darya and Amu Darya. These were two serious interventions focused on de-centralizing the transboundary water management in Central Asia. Basin plans clearly predicted development scale and pressure on the river systems of the region and described measures to be implemented in order to balance water situation in the region, including the balancing of the Aral Sea levels. The basin plan included water-sharing percentages among the riparian states. Moreover, the plan proposed measures on improving water efficiency in both basins for the long-term. The plan was a part of the centralized, top-down principles of water (natural) resources management in the Soviet Union. After the collapse of the Soviet Union, newly emerged Central Asian countries agreed to keep this system unchanged and signed an agreement in 1992 (Abdullaev and Rakhmatullaev, 2013).

Since then, countries of the region have made a few attempts to replace the old Soviet water agreement with new one, either for the region as a whole or each for river basin. However, these attempts have not achieved any success. The water allocation in the region is set up through bi-annual meetings of Interstate Coordination

Table 2 Transboundary River agreements of Kazakhstan

Title of the agreement	Place and date of signing the agreement	Agreed bodies and countries	Focus of the agreement
Statement of heads of water economy organizations of Central Asian Republics and Kazakhstan	10-12 October 1991 meeting in Tashkent	State committee on water resources of Kazakhs SSR, Ministry of Water Resources of Kyrgyzstan, Ministry of Water Resources of Tajikistan, Ministry of Water Resources of Uzbekistan, Ministry of Water Resources of Turkmen SSR	Lack of water resources, ecological tension in Aral Sea basin <a href="http://icwc-aral.uz/statute2">http://icwc-aral.uz/statute2</a>
Statement between Republic of Kazakhstan, Kyrgyz Republic, Republic of Uzbekistan, Republic of Tajikistan and Turkmenistan on cooperation in the fields of joint management, using and protection of water resources of intergovernmental sources	Almaty, 18 <sup>th</sup> of February, 1992	Republic of Kazakhstan, Kyrgyz Republic, Republic of Uzbekistan, Republic of Tajikistan and Turkmenistan	Regulation, protection of water resources, water supply, irrigation Related to all transboundary watersheds and lakes
Agreement between Government of Russian Federation and Government of Republic of Kazakhstan on joint use and protection of transboundary water bodies (and Protocol decision on prolongation of the Agreement)	Orenburg, 27 <sup>th</sup> of August, 1992 (Pavlodar, 26 <sup>th</sup> of June, 1997)	Republic of Kazakhstan, Russian Federation	Protection of water resources, water supply, irrigation, floods, regulation; Related to all surface and ground water resources, including transboundary rivers such as Ishim, Irtish, Ural, Tobol and Volga <a href="http://base.spinform.ru/show_doc.fwx?rgn=31129">http://base.spinform.ru/show_doc.fwx?rgn=31129</a>
Statement on joint actions to address the problems of Aral Sea Basin and Aral Sea Region, ecological recovery and providing of socio-economic development of the Aral Sea Region	Kyzyl Orda, 26 <sup>th</sup> of March, 1993	Republic of Kazakhstan, Kyrgyz Republic, Republic of Uzbekistan, Republic of Tajikistan and Turkmenistan	Problems of Aral Sea Basin The Inter-State Council on Aral Sea Basin Problems and its Commission has been established <a href="http://on-line.zakon.kz/Document/?doc_id=1045205">http://on-line.zakon.kz/Document/?doc_id=1045205</a>
Statement between Republic of Kazakhstan and People's Republic of China on Kazakh-Chinese State Border	Almaty, 26 <sup>th</sup> of April, 1994	Republic of Kazakhstan, People's Republic of China	Identification of location of boundary watersheds, middle of boundary rivers or its main streams, belonging of islands on boundary rivers <a href="http://on-line.zakon.kz/Document/?doc_id=1016993">http://on-line.zakon.kz/Document/?doc_id=1016993</a>
Statement on using of fuel-power and water resources, construction and maintenance of gas pipe line in Central Asian region	Tashkent, 5 <sup>th</sup> of April, 1996	Government of Republic of Kazakhstan, Government of Kyrgyz Republic, Government of Republic of Uzbekistan	Effective using of the hydro resources of Syr Darya river for irrigational purposes. Regulation of working practices of Naryn – Syr Darya cascade of water reservoirs

Water Commission (ICWC), which consists of water ministers of the Central Asian states. Kazakhstan, represented by the deputy Minister of Agriculture in the commission, receives its shares for Syr Darya in the meeting of this body. The decisions are made based on water allocation percentage of the flow and water availability forecasts for the given season (6 month). This agreement retains internationally known historical

rights principles. However, currently upstream countries, Kyrgyzstan and Tajikistan, are not happy and are contesting this agreement. The need for energy and abundance of the water resources formed in their territories are arguments used by the two upstream countries to change the pattern of the water use more towards energy generation (Abdullaev and Atabaeva, 2012; Wegerich, 2013).

Kazakhstan has been facing the consequences of the change of water use in the Syr Darya basin, having floods in winter and water shortages in summer due to the energy generation regime in the river. In order to reduce negative impacts of such changes, Kazakhstan has promoted regional energy trade and tried to promote energy exchange with Kyrgyzstan and other riparian states. This was a short-lived strategy and only worked for a short time. Then Kazakhstan took a unilateral approach and built counter-regulations for capturing the water in winter, and strengthened the river bed of the Syr Darya within its territory. In order to enhance its water security in summer Kazakhstan has worked out bi-lateral and mostly informal agreements with Kyrgyzstan and Uzbekistan.

Kazakhstan has also developed a different approach utilising exemplary agreements with Kyrgyzstan on the Chu-Talas basin (Abdullaev and Atabaeva, 2012). In this smaller basin, two sides agreed to work out the agreement on joint management and maintenance of the water infrastructure, which are transboundary. Kazakhstan, being the downstream country, has put funds for rehabilitation and maintenance of water infrastructure located in Kyrgyzstan. The joint basin organization has been set up by two sides in order to institutionalize the water cooperation.

In spite of existing legal and institutional instruments for transboundary cooperation Kazakhstan is facing a serious risk on water security. Moreover, current setting of transboundary system does not respond to environmental and water quality issues, mainly concentrating only quantity aspects. Therefore, inclusion of major stakeholders, namely local – riparian communities into the process of transboundary cooperation will reduce the risk of failure. Application of more integrative and inter-sectoral principles would help to include issues of water quality and environmental maintenance into the transboundary negotiations.

## METHODOLOGY

A scoping study and the creation of a project advisory board to facilitate the development of a common understanding of current working practices and emerging challenges was undertaken for clarification of the major risks with regard to water cycle management. Representatives of Kazakh academic, practice, policy and student organisations were interviewed to identify current working practices and emerging challenges. The results of this process are detailed in (NIREAS, 2013) and were used to identify and frame IWCM needs from multiple perspectives.

Building on the initial assessment, the concept of risk governance (IRGC, 2005; Renn, 2008; Renn and Walker, 2008) was identified as a useful framework to link identified strategic and applied components together in a manner that integrated the various functions and showed the relationship between them. Watt (2014a) discusses the origin of such approaches and introduces the first major feature that can be used to begin to understand the relationship between the roles of different actors (stakeholders). This reflects a development that emerged in the USA in the 1980s (NAS, 1983) that:

*“Regulatory agencies should take steps to establish and maintain a clear conceptual distinction between assessment of risks and the consideration of risk management alternatives; that is, the scientific findings and policy judgments embodied in risk assessments should be explicitly distinguished from the political, economic, and technical considerations that influence the design and choice of regulatory strategies”.*

In this context, risk governance can be presented as a conversation between two ‘sides’ (risk management and risk assessment), which facilitates evaluation of the functions of those responsible for any given task. Policy makers and regulators can be presented as general managers undertaking a risk management function, which may require evidence from scientists and engineers, who are specialists.

## RESULTS AND DISCUSSION

The first challenge identified during the interviewing of stakeholders was the need to support stakeholders in developing a strategic vision – a way of looking at the IWCM challenges faced from the top down that would support recognition of how the various components/activities of stakeholders fit together. A further challenge within this was recognition that many individuals come to the practice of IWCM from different disciplines and backgrounds and also may go on to a variety of roles in their professional life. A strategic approach needs to integrate data from specialists, for example engineers and analytical chemists, operating across a range of sectors that can appear remote from each other, and which require very different types of education and training, and yet each has an important role in different parts of IWCM. For example, whilst policy makers may never undertake a technical role, they will be called on to set objectives or develop policy that technical teams will have to implement and which need to be underpinned by high quality science and engineering.

*A strategic risk management approach to developing management capacity*

A framework for the evaluation of IWCM in Kazakhstan was developed by Watt, 2014b based on the International Risk Governance Council (IRGC) Risk Governance Framework (IRGC, 2005, Renn, 2008, Renn and Walker, 2008; see Fig. 2). The framework separates the process of risk governance into a number of different elements that make the process easier to understand.

The first stage of the IRGC framework, known as ‘pre-assessment’, highlights the importance of context for anchoring the subsequent risk management to the aims and objectives of the organisation mandated to manage the risk, and discuss ways that the local context can be established with a clear recognition of the benefits of the water being managed. Pre-assessment is undertaken by both managers and technical specialists together, and can be framed in many different ways – physical (e.g. hydrology, climate, ecology) and human (e.g. sustainability, economy, use to which resources are devoted). Pre-assessment also evaluates

constraints placed on options for risk management by scientific conventions utilised, the law and regulatory arrangements. Within I-WEB, this pre-assessment process involved interviewing a range of stakeholders including policy-makers, practitioners, industry representatives and academics to understand their current working practices, challenges and ambitions (see NIREAS, 2013). This initial needs assessment supported the identification of a broad set of skills required in teaching and practice, encompassing social, environmental, technological and economic aspects of sustainable water-land management. Specific topics identified included water indicators and monitoring (including statistical methods and modelling), geo-information and water treatment technologies and methods to the strengthen cooperative working between diverse actors (e.g. public authorities, universities and research institutes, NGOs, governmental and international organisation), including the relevant laws, finances and management approaches pertaining to surface and ground waters both nationally and internationally (NIREAS, 2013).



Fig. 2 Framework of the functions of the risk governance at strategic level (Adapted from Bunting, 2009)

The second stage, risk appraisal, involved gathering and sharing data from scientific assessments of the water supply and its quality undertaken by several disciplines e.g. hydrologists, climate change scientists, agricultural scientists and economists. Within I-WEB, this stage took the form of a specialist workshop on IWCM methodologies and practices where representatives from a range of Kazakh and EU organisations presented research methodologies, current scenarios and future challenges from a range of organisational perspectives. The outputs of this workshop formed the basis of the development of the 'IWCM in Kazakhstan' handbook (Meyer and Lundy, 2014) which includes concepts of IWCM, methodologies and supporting tools for IWCM, management skills for building capability, capacity and impact, best practice examples for water treatment, basics on the sustainable use of water resources in KZ, a concept of IWCM for KZ and transboundary catchment issues and future integrated management. In the current model, this stage is an extension of the risk assessment referred to by the NAS (1983) in the quotation above to include evaluation of

public (or other stakeholder) concerns, which may impact on the way that management options can be evaluated.

The third stage, characterisation and evaluation is the core of the process, best undertaken by all involved, where the evidence from the risk appraisal is evaluated in the light of the organisational values set out in the first stage. This is where a judgement is made on the acceptability of a risk and leads to one of three possible management actions – do nothing, ban some proposed or current activity or manage the risk. Within the I-WEB programme this stage took the form of presenting the results of the pre-assessment process to members of the I-WEB International Activity Board (IAB) for their comment and feedback on data collected and its interpretation. The I-WEB IAB currently consists of over 20 members from a range of academic, policy, and professional/industry backgrounds who voluntarily participate in annual meetings to share knowledge on IWCM challenges within their sectors and comment on I-WEB outputs as they develop to collectively take forward best practice within IWCM in Kazakhstan. This IAB approach is a co-owned mechanism to facilitate the development of closer links between academia and practice for mutual benefit; enhancing the skill sets of graduates and hence graduate employability (through ensuring graduates have the skills employers need) as well as an awareness of the challenges they face.

The fourth stage, risk management, shows how policy or management options can be developed based on the judgement made and implications from the technical evidence. A number of generic approaches were presented taking into account the extent to which stakeholder concerns needed to be incorporated. As an example, if scientific uncertainty was very high, a risk management decision might be required to be made by the government or a regulator to address public concern. In the absence of scientific data this might be made on the basis of a risk philosophy such as the precautionary principle with some form of stakeholder agreement (or societal endorsement) needed on the level of precaution required. Within I-WEB, the management options developed were three-fold involving staff re-training, the development of Bologna-compliant academic programmes and the re-working of programme material to additionally form short continued professional development (CPD) courses. More specifically, using outputs of the stage 1 and stage 2 activities, and following input and refinement of the stage 3 activities, findings derived were used to develop a bespoke intensive re-training programme for 30 Kazakh academics. New knowledge developed was shared both horizontally, through seminars at each participating institution, and vertically through the subsequent development of learning materials for MSc and PhD teaching and research programmes as well as the more vocational CPD courses.

The fifth element of the risk governance framework highlights the importance of communication (both internal and external), by positioning it in the centre of all of the other activities. A number of approaches have been developed depending on the nature of the risk, which is tasked with dealing with it and their relationship to other

stakeholders. In I-WEB, communication was both a central challenge (language, cultural and experiential) and a core area of activities, which was addressed through multiple routes with particular focus on developing strong partnership working approaches. The wider context for this is that, together with many other sectors, communication and partnership working is now fundamental to water resource management legislation in many EU and Central Asian countries as its recognised that there are practical limits to the application of a top-down legislative approach as it is often difficult to enforce. It is increasingly appreciated that the existence of legislation alone is not enough to ensure environmental protection, because when water pollution occurs, it is often the result of ignorance and neglect rather than deliberate acts (Chatfield and Lundy, 2016). Over the last twenty years a range of alternative cross-sector partnership approaches have been developed to protect the water environment, involving regulators, industry partners and communities, working together to promote good practice and improved standards. In recognising the success of such, often voluntary, partnership initiatives, legislative frameworks increasingly include a requirement for partnership working as a core element. These include, for example, the EU Water Framework Directive (EU WFD, 2000), the EU Floods Directive (2007), the Integrated Pollution Prevention and Control Directive (EU, 2008) and Strategic Environmental Assessment Directive (SEA, 2001).

Whilst actual data on the benefits of a partnership working approach is hard to source (Slater et al., 2007, Reed, 2008), the literature identifies a range of reasons for collaborative working. The development of a forum where industry, regulators and communities can work together provides a constructive arena for those affected by decisions to influence those decisions which may affect their activities (e.g. industry) and or quality-of-life (local communities). It can facilitate the breakdown of legislative, institutional and social barriers to changes, supporting the development of novel options which are workable and acceptable within national and local regulatory and operating contexts (van Herk et al., 2011). Partnership approaches can raise awareness of environmental issues, making use of the knowledge and expertise held by a wider range of stakeholders and generating approaches which have higher levels of regulator, organisational, sectoral and wider public acceptance, commitment and support (CIS, 2003). Within an I-WEB context, the IAB was the forum that brought individuals from a range of sectors together with a common goal of enhancing water resource management within not only Kazakhstan but the Central Asian region as whole. The IAB activities commenced with Kazakh partners pro-actively identifying and contacting a range of environmental protection specialists, water managers, policy makers and users to join discussions on enhancing the management of Kazakhstan's water resources. With national government recognition of the challenges being faced, there was interest in the IWEB IAB from a range of sectors, although bringing all interested parties together was a time-consuming process. It is well recognised that

partnership working is a long process, that successful partnerships grow incrementally and evolve through the building of trust and shared experiences (Slater et al., 2007). The role of a 'local champion' – a person who is known by all parties, and is passionate and enthusiastic about the initiative in hand - is critical in the early stages of partnership building to both bring on board other partners and strengthen commitment to the process (Morris, 2006). Within I-WEB each of the local Kazakh university partners took the role of 'local champion', often using a combination of local knowledge and personal contacts to bring relevant stakeholders to the table together.

#### *Methodologies and supporting tools for supporting implementation of IWCM*

In implementing IWCM in practice, it is widely recognised that water resource (WR) systems are among the most complex systems to cope with when analysed from a risk management perspective. Risk management of WR systems has to include the identification, assessment, and prioritization of risks in order to implement coordinated actions to reduce, monitor and control the probability and/or the impact of any plausible events. A short list of the type of events that are usually of concern includes climate change, hydrological events, infrastructure safety, system management policies, effects of management policies in trans-boundary basins, accidental spills and incidents arising from other natural hazards. Alone or combined, these events define scenarios to be addressed by the risk management strategy. Ideally, any integrated WR strategic risk management platform should rely on a set of interconnected subsystems:

1. Events: Determination of plausible events and their probabilities.
2. Impacts: Assessment of every event impact.
3. Monitoring: System monitoring to anticipate events and to support the quantification of associated impacts.
4. Control: Mathematical models of the WR system – frequently based on a GIS platform – to predict and quantify the evolution of relevant parameters and variables of the system.
5. Actions: WR system protocols and procedures to make decisions in real time, and for the short and mid-terms.

The above subsystems are also connected through a loop because any taken action changes the probabilities and impacts of events. The whole platform has to be conceived and managed embedding the fundamental policy guidelines of the responsible organisation, and the participation of the stakeholders.

In general, most basin authorities and administrations, mainly in developed and populated regions, run different institutional programs or units that address the above subsystems. These programmes have usually focused on the most plausible events, many of them of hydrological origin, with droughts and floods often being the main concerns. However, risk associated to infrastructure failures or to the accidental introduction of pollutants into the water bodies should be also

prioritized. A situation that requires special consideration is that of trans-boundary basins / WR systems. In this case, with different areas of the basin managed by different authorities, the existence of supra-national or supra-regional organisation to coordinate the basic policy objectives of the WR system is fundamental. This should be the “layer 0” underlying the participation of stakeholders and the existing risk management platforms in every sub-basin or subsystem. Without this basic coordination, risk management has to be based on partial treaties and slow and limited mechanisms; this situation would call for the use of specific tools such as the methods developed in games theory to support the decision-making process in the absence of ability to control sub-parts of the system. Madani (2010) reviews the applicability of game theory to water resources management and conflict resolution through a series of non-cooperative water resource games. The study includes case studies all over the world, including central Asia conflict on the legal status of Caspian Sea waters.

The implementation of a strategic risk management platform requires the availability and integration of data, models and networks, including at least the following:

- Historical records of the WR system to support conceptual models of subsystems, the analysis of trends in selected variables, extreme hydrological events estimations, and the calibration of mathematical models - both deterministic and statistical. These records should at least include data series of: runoff at selected control points along rivers, reservoirs storage and operation, piezometric levels in selected points in the main groundwater bodies, rainfall and other meteorological variables, basic quality parameters in surface water and groundwater at selected points, water consumption for irrigation, energy production and urban use, evapotranspiration, and series of any other relevant information regarding the characteristics of the WR system. The length of the series is relevant and if no information is available, or the series are very short, data series from similar locations might be useful.
- A complete and sound hydrological and hydrogeological description of the system.
- Monitoring networks to increase the length of existing historical records, and real-time networks connected to feed alert systems. The latter might require rainfall and rainfall intensity, river and/or channel flows, reservoirs levels, critical quality parameters, etc.
- Conceptual and qualitative models to understand the main subsystems flows and interactions, including surface water and groundwater.
- Rainfall – runoff sub basin models.
- Mathematical flow models of the main groundwater bodies.
- Flood simulation models for the main basins / sub basins with higher flood risks.
- Basin / sub basin models that integrate both surface water and groundwater systems with capabilities to simulate both flows and water quality.

Geographical information systems are basic tools to organize the basin information and in many cases they support the use of models for different purposes. There can be other types of water resources like water imported from other basins, desalinated water or treated water. In this case, the proper parameters to characterize these resources have to be also included in the above listing. Note that this is a basic list of required data, monitoring networks and modelling tools to build a strategic RM platform. In practice, it is necessary to develop Decision Support Systems (DSSs) that help the decision-maker to analyse and understand the dynamics of the system, foresee short and mid-term evolution, and to assess the impact of alternative decisions. DSSs are tools specifically designed for a given system and specific purposes (although the software platform can be design to be adapted to different basins). They usually integrate several mathematical models of the system, and stochastic simulators for hydrological inflows, that can cope with WR system operation under drought or flooding conditions, simulating short, mid and long term scenarios to remediate water scarcity or pollution problems, etc. The use and development of DSSs has historically run in parallel with the development of graphical capabilities in computers. An early DSS, under continuous development and well described in scientific and technical literature, is AQUATOOL, see Andreu et al. (1996). This tool has been evolving since the first releases and includes simulation and optimization of WR management accounting for the uncertainty of hydrological inflows in the system and many other features. It has been applied in many basins around the world (Spain, Argentina, Brazil, Italy, Mexico, Bosnia, Chile, Morocco, Algeria, Ecuador, Peru, etc.), and is supported by a friendly Graphic User Interface (GUI), spatially referenced, that allows its use by personnel with a low levels of training in the use of computers.

The use of risk as a criterion to manage a water resource (WR) system – risk based WR management - was described and applied by Capilla et al. (1998). Other authors, e.g. Roust and Araghinejad (2015), illustrate how to incorporate multi-criteria decision making into a DSS using objective functions that include multiple goals. These goals or objectives can be as diverse as the fulfilment of ecological flows, the satisfaction of minimum levels of water demands, the maintenance of levels in lakes and reservoirs, the amount of energy generated in hydropower plants or maintenance of thresholds in the exploitation of groundwater bodies, etc. Note that the mathematical formulation of the multiple objectives optimization requires the definition of weights to be applied to reflect the importance to be apportioned to a prior decision reflecting the fundamental management policy.

Integrated water cycle management also requires working with scenarios that account for future climate change. In this case it is necessary to work with scenarios that are downscaled from General Circulation Model (GCM) results. The reports issued by the Intergovernmental Panel on Climate Change (IPCC), see IPCC (2014) are the primary source of information.

However, for specific geographical regions and basins, it is necessary to analyse which GCM best reproduces the local conditions, and to downscale the low resolution data provided to a scale that allows more accurate determination of impacts on water resources. Chirivella et al. (2015) show the results and methodology of a study in which dynamic and statistical downscaling methodologies are compared.

## CONCLUSION ON THE BENEFITS OF IMPLEMENTING A WFD RISK MANAGEMENT APPROACH IN KAZAKHSTAN

Whilst both the EU and Kazakhstan are moving towards implementing an IWCM approach, the launch and phased implementation of the EU WFD has greatly accelerated progress towards its full implementation throughout Europe. As a single piece of legislation that all European Member States must implement, it requires the collection of data, involvement of all stakeholders and the development and implementation of science-based programmes of measures via the use of common methodologies and processes. All data collected is freely available with the use of common methodologies promoting the harmonization of management approaches both within and, crucially, between Member States. As such, this transparent approach facilitates transboundary dialogue with the development of common goals, languages and tools identified here as a strong mechanism for intra-regional co-operation irrespective of national boundaries. Therefore risk management is applied from strategic to local application scales.

Whilst the adoption of legislation such as the Kazakh Water Code indicates the recognition of, and priority placed on IWCM within Kazakhstan, no single country which shares transboundary waters can fully implement an IWCM approach in isolation. Whilst arguably not a short-term objective, the need for a Central Asian Water Framework Directive approach - which would co-ordinate and harmonize the emerging activities taking place across the region - is identified as a priority requirement. In developing such an over-arching framework, the current transboundary river basin agreements (Table 2) can be considered as an initial agenda for discussions to further develop and strengthen partnerships between business, regulatory and academic sectors at a national and international level to face the common need to implement robust approaches to water resource management in the face of a changing climate. Furthermore key aspects on the adaptation to climate change have to be considered including establishment of core principles and approaches, international commitments, policy, legislation and institutional frameworks, information and monitoring needs for adaptation strategies design and implementation, scenarios and models for impact assessment and water resource management, adaptation strategies and measures for financial matters and evolution purposes (UN ECE, 2009).

In developing and implementing approaches to ensuring water resources are available to meet the needs of current and future generations, Europe and Central

Asian are facing many common challenges. The opportunity for closer collaboration between regions is highlighted here, with regard to both the need to develop a regional approach to IWCM and the role that individual countries can play in contributing to its delivery. With a specific focus on supporting the development of IWCM within Central Asia, key challenges identified by Lundy and Meyer (2014) included:

- Persuading neighbouring upstream countries that it is in their interest to work on a catchment basis
- Developing increased collaboration as opposed to competition over use of water resources within catchments e.g. to address tensions between agriculture and energy production
- Compliance with state legislative controls and facilitating stakeholder participation
- Scoping and developing a Central Asian Water Framework Directive; what can be learned from international best practice and mistakes?
- Developing the institutions and their capacities to successfully develop and deliver an IWCM approach which can respond to the challenges of a changing climate

By prioritising IWCM and investing strongly in their education system, Kazakhstan is now well positioned to take a leading role in supporting Central Asia's transition to a region with a strong economy based on the sustainable management of its resources.

## Acknowledgements

The authors gratefully acknowledge the support of the EU TEMPUS IWEB (Integrating Water cycle management: building capability, capacity and impact in Education and Business) consortium. This project has been funded with support from the European Commission. This publication reflects the views only of the authors, and the Commission cannot be held responsible for any use which may be made of the information contained therein.

## References

- Abdullaev, I., Atabaeva, S. 2012. Water sector in Central Asia: slow transformation and potential for cooperation. *Int. J. Sustainable Society* 4 (1/2), 103–112. DOI: 10.1504/ijssoc.2012.044668
- Abdullaev, I., Rakhmatullaev, S. 2013. Transformation of water management in Central Asia: from State-centric, hydraulic mission to socio-political control. *Environmental Earth Sciences* 73, 849–861. DOI: 10.1007/s12665-013-2879-9
- Andreu, J., Capilla, J., Sanchis, E. 1996. AQUATOOL, a generalized decision-support system for water-resources planning and operational management. *Journal of Hydrology* 177, 3-4: 269–291. DOI: 10.1016/0022-1694(95)02963-x
- Anonymous, 2004. Water Resources of Kazakhstan in the new millennium. Publication Series of UNDP in Kazakhstan 7, Almaty.
- Bunting, C. 2009. An introduction to the IRGC Risk Governance Framework. IRGC, Geneva. 24 p.
- Capilla, J.E., Andreu, J., Solera, A., Quispe, S.S. 1998. Risk based water resources management. In Hydraulic Engineering Software VII, Blain, W.R. (Ed.). WIT Transactions on Ecology and the Environment, Wessex Institute of Technology, UK, 427–436.
- Chatfield, P., Lundy, L. 2016 (in press). Beyond legislation - Working together to protect the water environment. In: D'Arcy B.J. (ed) Wealth creation without pollution: Industry, Ecobusiness Parks & Industrial Estates. IWA publishing, London.
- Chen, X., Bai, J., Li, X., Luo, G., Li, J., Li, B.L. 2013. Changes in land use/land cover and ecosystem services in Central Asia during



- 1990–2009. *Current Opinion in Environmental Sustainability* 5 (1), 116–127. DOI: 10.1016/j.cosust.2012.12.005
- Chirivella, V., Capilla, J.E., Perez-Martín, M.A. 2015. Dynamical versus statistical downscaling for the generation of regional climate change scenarios at a Western Mediterranean basin: The Jucar river district. *Journal of Water and Climate Change* 11/2015; DOI: 10.2166/wcc.2015.207.
- CIS, 2003. Common Implementation Strategy for the Water Framework Directive (2000/60/EC) Guidance document n.o 8 Public Participation in relation to the Water Framework Directive. Available at: [https://circabc.europa.eu/sd/a/0fc804ff-5fe6-4874-8e0d-de3e47637a63/Guidance%20No%208%20-%20Public%20participation%20\(WG%202.9\).pdf](https://circabc.europa.eu/sd/a/0fc804ff-5fe6-4874-8e0d-de3e47637a63/Guidance%20No%208%20-%20Public%20participation%20(WG%202.9).pdf)
- Dostay, Z.D. 2009. Management of Hydroecosystems of the Balkhash Lake Basin. Institute of Geography; Almaty Kazakhstan. 236 p.
- Dostay, Z.D. 2012. Natural Waters of Kazakhstan: Resources, Hydroregime, Quality and Forecast. [Природные воды Казахстана: ресурсы, режим, качество и прогноз] Almaty: Institute of Geography, 335 p.
- Duskayev, K., Minzhanova, G. 2014. Water resources and sustainable Development. In: Meyer, B.C., Lundy, L. (Eds.) Integrated water cycle management in Kazakhstan. Al-Farabi Kazakh National University Publishing House, Almaty, 157–162.
- Ecologic Institute and SERI, 2010. Establishing Environmental Sustainability Thresholds and Indicators. Final report to the European Commission's DG Environment, November 2010, 138 p.
- EU Floods Directive, 2007. Directive 2007/60/EC on the assessment and management of flood risks Available at: [http://ec.europa.eu/environment/water/flood\\_risk/index.htm](http://ec.europa.eu/environment/water/flood_risk/index.htm)
- EU WFD, 2000. Directive 2000/60/EC of the European Parliament and of the Council of 23 October 2000 establishing a framework for Community action in the field of water policy Water Framework Directive. Available at: <http://eur-lex.europa.eu/LexUriServ/LexUriServ.do?uri=CELEX:32000L0060:EN:HTML>
- GWP, 2010. What is IWRM? Available at: <http://www.gwp.org/The-Challenge/What-is-IWRM/>
- EU, 2008. Directive 2008/1/EC of the European Parliament and of the Council of 15 January 2008 concerning integrated pollution prevention and control. Available at: <http://eur-lex.europa.eu/LexUriServ/LexUriServ.do?uri=OJ:L:2008:024:0008:0029:en:PDF>
- IPCC, 2014. Summary for policymakers. In: Field, C.B., Barros, V.R., Dokken, D.J., Mach, K.J., Mastrandrea, M.D., Bilir, T.E., Chatterjee, M., Ebi, K.L., Estrada, Y.O., Genova, R.C., Girma, B., Kissel, E.S., Levy, A.N., MacCracken, S., Mastrandrea, P.R., White L.L. (eds.) Climate Change 2014. Impacts, Adaptation, and Vulnerability. Part A: Global and Sectoral Aspects. Contribution of Working Group II to the Fifth Assessment Report of the Intergovernmental Panel on Climate Change Cambridge University Press, Cambridge, United Kingdom and New York, NY, USA, 1–32.
- IRGC, 2005. White paper on Risk Governance: Toward an integrative framework, IRGC, Geneva. 156 p.
- Kostianoy, A.G., Kosarev, A.N. (Eds.) 2010. The Aral Sea. Environment Springer, 355 p.
- Lundy, L., Meyer B.C. 2014. Application of a Water Framework Directive approach in Kazakhstan. In: In Meyer, B.C., Lundy, L. (Eds.) Integrated water cycle management in Kazakhstan. Al-Farabi Kazakh National University Publishing House, Almaty, 250–255.
- Madani, K. 2010. Game theory and water resources. *Journal of Hydrology* 381, 225–238. DOI: 10.1016/j.jhydrol.2009.11.045
- Meyer, B.C., Lundy, L. (Eds.) 2014. Integrated water cycle management in Kazakhstan. Al-Farabi Kazakh National University Publishing House, Almaty, 304 p. [https://www.researchgate.net/publication/270818634\\_Integrated\\_Water\\_Cycle\\_Management\\_in\\_Kazakhstan](https://www.researchgate.net/publication/270818634_Integrated_Water_Cycle_Management_in_Kazakhstan)
- Meyer, B.C., Lundy, L., Watt, J. 2014. Integrated Water Cycle Management in Kazakhstan – introduction in content and use. In Meyer, B.C., Lundy, L. (Eds.) Integrated water cycle management in Kazakhstan. Al-Farabi Kazakh National University Publishing House, Almaty, 1–3.
- Micklin, P., Aladin, N., Plotnikov, I. (Eds.) 2014. The Aral Sea. The Devastation and Partial Rehabilitation of a Great Lake. Springer Earth System Sciences, 254 p.
- Morris, M. 2006. Learning Alliance Briefing Note No 1: An introduction to learning alliances. Available at: [http://www.switchurbanwater.eu/outputs/pdfs/WP6-2\\_BRN\\_1\\_Intro\\_to\\_LAs.pdf](http://www.switchurbanwater.eu/outputs/pdfs/WP6-2_BRN_1_Intro_to_LAs.pdf)
- NAS, 1983. Risk Assessment in the Federal Government: Managing the Process. National Academy Press. Washington D.C., 206 p.
- Nazarbaev, N. 2010. Strategy Kazakhstan 2050. Available at: <http://www.kazakhembus.com/content/address-kazakhstan-president-nursultan-nazarbayev-strategy-kazakhstan-2050>
- NIREAS, 2013. Evaluation of current IWC, educational and quality assurance practices. Deliverable 3.1 of the EU TEMPUS I-WEB project. Available at: <http://iwebtempus.kz>
- Qadir, M., Noble A.D., Qureshi, A. S., Gupta, R.K., Yuldashev, T., Karimovet, A. 2009. Salt-induced land and water degradation in the Aral Sea basin: A challenge to sustainable agriculture in Central Asia. *Natural Resources Forum, A United Nations Sustainable Development Journal* 33 (2), 134–149. DOI: 10.1111/j.1477-8947.2009.01217.x
- Reed, M.S. 2008. Stakeholder participation for environmental management: A literature review. *Biological Conservation* 141: 2417–2431. DOI: 10.1016/j.biocon.2008.07.014
- Renn, O. 2008. Risk Governance: Coping with Uncertainty in a Complex World. Earthscan, London 455 p.
- Renn, O., Walker, K. 2008. Global risk governance. Concept and practice using the IRGC framework, Springer, Dordrecht, The Netherlands, 367 p.
- Rousta, B.A., Araghinejad, S. 2015. Development of a Multi Criteria Decision Making Tool for a Water Resources Decision Support System. *Water Resources Management* 29 (15), 5713–5727. DOI: 10.1007/s11269-015-1142-4
- Salnikov, V.G., Turulina, G.K., Talanov, E.A., Polyakova S.E., Dolgih S.A., Petrov E.E. 2011. The climate of Kazakhstan - the basis for formation of water resources. *Water Resources of Kazakhstan: assessment, forecast, management* V. 5, 348 p.
- SEA. 2001. Directive on Strategic Environmental Impact Assessment (Directive 2001/42/EC). Available at <http://ec.europa.eu/environment/eia/sea-legalcontext.htm>
- Slater, R., Frederickson, C., Thomas C., Wiold, D. and Potter, S. 2007. A critical evaluation of partnerships in municipal waste management in England. *Resources, Conservation and Recycling* 51: 643–664. DOI: 10.1016/j.resconrec.2006.11.008
- Smith, L. C., Sheng, Y., MacDonald, G. M., Hinzman, L. D. 2005. Disappearing Arctic Lakes. *Science* 308 (3), 1429. DOI: 10.1126/science.1108142
- Tursunov, A.A. and others, 1997. Environmental Problems of Drainage Water Basins in Central Asia. Publishing House “Gylym”, Kyzylorda 320 p.
- UN ECE, 2009. Guidance on Water and Adaptation of Climate change. Geneva, 127p.
- van Herk, S., Zevenbergen, C., Ashley, R., Rijke, J. 2011. Learning and Action Alliances for the integration of flood risk management into urban planning: a new framework from empirical evidence from The Netherlands. *Environmental science and policy* 14: 543–554. DOI: 10.1016/j.envsci.2011.04.006
- Watt, J. 2014a. Strategic risk management. In Meyer, B.C., Lundy, L. (Eds.) Integrated water cycle management in Kazakhstan. Al-Farabi Kazakh National University Publishing House, Almaty p 41–45.
- Watt, J. 2014b. An introduction to water management in Kazakhstan in the context of integrated risk management. In Meyer, B.C., Lundy, L. (Eds.) Integrated water cycle management in Kazakhstan. Al-Farabi Kazakh National University Publishing House, Almaty, 4–9.
- Wegerich, K. 2008. Passing over the conflict. The Chu Talas Basin agreement as a model for Central Asia? In M.M. Rahaman and O. Varis (eds.) Central Asian Waters, Water & Development Publications – Helsinki University of Technology, Espoo, 117–131.
- Wegerich, K. 2013. Politics of water in post-Soviet Central Asia. In Europa Publications. (Ed.) Eastern Europe, Russia and Central Asia 2014. 14th Ed. Abingdon, UK, Routledge, 30–35.
- Zavialov, P.O., 2005. Physical Oceanography of the Dying Aral Sea. Springer-Verlag, Praxis, Chichester, UK, 15.



## ESTIMATION OF THE CHANGES IN THE RAINFALL EROSIIVITY IN HUNGARY

Gábor Mezósi\*, Teodóra Bata

Department of Physical Geography and Geoinformatics, University of Szeged, Egyetem u. 2-6, H-6722 Szeged, Hungary

\*Corresponding author, e-mail: mezosi@geo.u-szeged.hu

Research article, received 1 September 2016, accepted 15 November 2016

### Abstract

According to the forecasts of numerous regional models (eg. REMO, ALADIN, PREGIS), the number of predicted rainfall events decreases, but they are not accompanied by considerably less precipitation. It represents an increase in rainfall intensity. It is logical to ask (if the limitations of the models make it possible) to what extent rainfall intensity is likely to change and where these changes are likely to occur in the long run. Rain intensity is considered to be one of the key causes of soil erosion. If we know which areas are affected by more intense rain erosion, we can identify the areas that are likely to be affected by stronger soil erosion, and we can also choose effective measures to reduce erosion. This information is necessary to achieve the neutral erosion effect as targeted by the EU. We collected the precipitation data of four stations every 30 minute between 2000 and 2013, and we calculated the estimated level of intensity characterizing the Carpathian Basin. Based on these data, we calculated the correlation of the measured data of intensity with the values of the MFI index (the correlation was 0.75). According to a combination of regional climate models, precipitation data could be estimated until 2100, and by calculating the statistical relationship between the previous correlation and this data sequence, we could estimate the spatial and temporal changes of rainfall intensity.

**Keywords:** rainfall intensity, regional differences of R, data of REMO and ALADIN models

### INTRODUCTION

Soil erosion is one of the greatest environmental threats, which causes significant environmental damage in Hungary. Its extent has been estimated lots of times, and it affects about 2 million hectares (Stefanovics, 1992). In order to prepare long-time estimations concerning the regional change tendencies of soil erosion, we have to pre-estimate dynamic parameters and factors. (In 2015, the EU set an ambitious goal to reduce the extent of soil erosion to zero.) The aim of the present analysis is to pre-estimate the temporal changes of rainfall erosion potential of the dynamic parameters. By doing so, we will receive information about one of the most important factors of soil erosion. Even if it is all about tendencies, detecting temporal and spatial changes in rainfall intensity may serve as important information to take extended-range measures to reduce the effects of erosion. In addition to geomorphological and soil data, dynamic (land cover) as well as numerous static factors may also be required to estimate the extent of soil erosion. Our study aims at revealing major changes of the R value in the present study. There are lots of uncertainties that result from using the data of the applied regional climate models, and, besides these, we also have to take into account that such social and economic changes may happen in the next few decades that may also change climate and land cover data predicted earlier. Our results must be interpreted within these limitations.

Soil erosion processes are characterized by a lot of theoretical and empirical models. However, the parameters of the processes can be well-defined. For example, rainfall

intensity and land cover (C) are dynamic parameters in the Universal Soil Loss Equation (USLE), while the others are static ones. It is a complex task to calculate rainfall intensity and the erosion potential associated with it. Rainfall erosivity factor (R) is expressed by summarizing the energy values of each rainfall event in a given period (Wischmeier - Smith, 1978, Wischmeier, 1959). The rainfall erosivity factor is calculated by multiplying the kinetic energy of precipitation (E) by the maximum rainfall intensity during a period of 30-minutes for each rainstorm (ExI<sub>30</sub>). Rainfall erosivity (R) expresses the collective erosivity value of locally occurring rainstorms (Table 1). The logic of the calculation dates back to the 1961s (Wischmeier, 1959), but it gained wide recognition when the Universal Soil Loss Equation became commonly used (1978) as it was one of its parameters.

Table 1 Calculating the rainfall erosivity factor

Rainfall erosivity factor (R) (MJ/ha.cm/h)	$R = E \times I_{30} / 100$ , where $I_{30}$ – maximum rainfall intensity during a period of 30-minutes for each rainstorm (cm/h), $E$ – total kinetic energy of precipitation (J/m <sup>2</sup> )
Total kinetic energy of precipitation (E) (J/m <sup>2</sup> )	$E = \sum_{i=1}^n E_i$ , where $E_i$ - the kinetic energy of the $i$ segment of precipitation ( $n$ is the number of segments) $E_i = (206 + 87 \log I_{si}) \times H_{si}$ , where $I_{si}$ – the intensity of the $i$ segment of precipitation (cm/h), $H_{si}$ – the amount of the $i$ segment of precipitation (cm)

In Hungary, R factor values vary between 360 and 1,000 (Panagos et al., 2015), and they are characterized by small-scale variance as a result of the homogeneous environmental features of the country. (The calculation is based on the ten-minute precipitation data of 30 rain gauges between 1998 and 2013.) It has an average value compared to other European data, and it is also far below the great, 4,000 to 6,000 MJ/ha rainfall intensity values of the continent. Former Hungarian local test results usually recorded data in this interval (Kertész and Richter, 1997: 49-59 MJ/ha; Centeri, 2002: 76 MJ/ha; Jordán et al., 2004: 809 MJ/ha; Szűcs, 2012: 60-512 MJ/ha). Homogeneity is expressed in the elevation, the climate type, and the general water balance, although different soil conditions would require different land use in order to reduce soil erosion. Despite the relative homogeneity of the environmental factors, territorial differences are visible (if not otherwise, then their impact is). We also aimed at estimating this spatial difference concerning the future periods.

Rainfall intensity can be calculated by two different methods. One of them operates with great temporal resolution using a minimum of 30-minute precipitation data. The other one does not have such high temporal resolution data, it calculates intensity with more easily accessible precipitation data by employing parameters which are significantly correlated with R. The frequent use of the latter method also shows that there is no widely accepted and widely applied method for calculating rainfall intensity. The different precipitation data and their correlations can only be used with quantitative (eg. with <12.7 mm of rainfall - otherwise

at EI default event) and qualitative (e.g. fixed drop size ratio) prerequisites, and they can be converted to  $\text{MJha}^{-1}\text{cmh}^{-1}$  value. A weakness of the commonly used empirical formula is that it presupposes the existence of precipitation data series dating back to several decades, and the correlation was tested on plot-sized areas. The erosion factor (R) is usually the average value of the data collected during several years.

There are usually not any data (which would be detailed enough) available to calculate the rainfall erosivity factor, so a lot of alternative parameters were developed by using daily and annual precipitation data to substitute the value of the R factor. These parameters are typically such indices that are related to smaller areas, and they are used at the maximum of meso-level. They often show as good correlation with soil erosion as the R index (eg. Fournier  $p^2/P$  index, REM index Lal's Aim index,  $P/S_t$  universal index) (Fournier, 1960; Arnoldus, 1980; Daidato, 2007; Onchev, 1985; Sauerborn et al., 1999; Renard et al., 1994 - Table 2). These indices also show at least as strong a correlation with the rainfall erosivity index as the  $E_{xI_{30}}$  calculated by Wischmeier. The rainfall erosivity factor (R) was also estimated by using other precipitation data, but they usually did not live up to the expectations (eg. Deumlich et al., 2006).

The result of the large number of measurements is that there is not a one and only sure method of calculating the rainfall erosivity factor due to the large number of active components and their plot-specific nature (although it would be important in order to estimate soil erosion, for example). Measuring soil

Table 2 A compilation of alternative methods of calculating rainfall erosivity

Authors	Alternative methods of calculating rainfall erosivity	Remarks
Fournier, 1960	$F = p^2/P$ , where p is mean monthly precipitation, and P is mean annual precipitation	Fournier Index
Arnoldus, 1980	$MFI = \sum_{i=1}^{12} p_i^2/P$ , where $p_i$ is mean monthly precipitation, and P is mean annual precipitation	Modified Fournier Index
Onchev, 1985	$R = P/S_t$ , where P is > 9.5 mm rainfall intensity, $S_t$ is the time of a > 0.18mm/min rainstorm	Universal Precipitation Event Index / Universal Index for Calculating Rainfall Erosivity
Renard – Freimund, 1994	$R = 0.07397 F^{1.847}$ $R = 95.77 - 6.08 F + 0.477 F^2$	$F < 55\text{mm}$ $F > 55\text{mm}$
Sauerborn et al., 1999	$R_s = -33.2 + 2 \times FIM_s$ ( $r^2 = 0.64$ )	Fournier Index with summer months
FAO – Colotti, 2004	$R = a \times MFI + b$	a and b are two regionally defined parameters
Deumlich et al., 2006	$R = -12.98 + 0.0783 \times P$ , where P is annual precipitation	Mean annual precipitation
Diodato – Bellocchi, 2007	$R_m = b_0 \times [p_m(f(m) + f(E, L))]^{b_1}$	$R_m$ is based on monthly precipitation
Eltaif et al., 2010	$R = 4 \times 10^{-6} \times F^{3.5874}$	Monthly precipitation data
Hernando – Romana, 2015	$R = 0.15 P$ , where P is annual precipitation data $R = 2.51 F$ , where F is the Fournier Index $R = 1.05 MFI$ , where MFI is the Modified Fournier Index	>5-year-long simulation > 10-year-long simulation >10-year-long simulation

erosion requires an extensive collection of both spatial and temporal data (eg. 10-to-30-minute precipitation data, and a sufficient number of rain gauges, or pluviographs). As they often were and/or are available, a lot of methods were developed to estimate this factor by employing easily obtainable data (Table 2). The R factor was often introduced as an index that significantly correlates to soil erosion (Wischmeier, 1959; Wischmeier and Smith, 1978; Lo et al., 1985). Several alternative indices were also connected to rainfall erosivity. Most of these indices had a strong correlation with the Fournier Index that uses monthly and annual mean precipitation data (1960), which index assesses the extent of erosion by using the  $p^2/P$  (average monthly/annual rainfall) correlation. The subsequent modification of the Fournier Index (MFI) defined an even stronger correlation, and it eventually showed its connection with soil erosion.

Preparing soil erosion models requires such precipitation information that is very time-consuming and cost-intensive to obtain, and it is often without measurable benefits. The R value often correlates well with other readily available rainfall data in the long run. Of course, the result is usually also true: high erosivity rainfalls result in high R values. From the alternative calculations, the readily available monthly/annual precipitation data were investigated, a lot of researchers also used these data for extreme values, e.g. for >100 mm precipitation. Other researches preferred to have a greater number of rain gauges (>100) or excluded extreme values (eg. >1,000 mm, exclusion of winter precipitation) in order to secure a strong correlation between the MFI and the R index (typically 0.8) (Renard, 1997; van Dijk et al., 2002; Hernando 2015).

## STUDY AREA AND METHODS

In our study the major changes of R were evaluated in Hungary, as study area. The method we applied consisted of the following steps:

**Step 1:** We calculated the R value on the basis of the 10-minute rainfall data of 4 meteorological stations in Hungary (Szeged, Agárd, Pécs, Debrecen) as shown in Table 1, and we used the available data series from 1999 to 2014. We calculated the Modified Fournier Index on the basis of mean monthly and mean annual precipitation data as shown in Table 2 for the same period. Then we calculated the correlation between the rainfall intensity (R) and the Modified Fournier Index (MFI) data series.

**Step 2:** We calculated monthly and annual precipitation data by averaging the daily data of this century on the basis of the REMO and ALADIN regional models (Mezősi et al., 2013). These models did not provide detailed data on rainfall events, which could have helped to estimate the spatial and temporal changes of rainfall intensity. These average values were the raw data of the MFI values concerning certain intervals of this century.

**Step 3:** We used the so-gained correlation between the R and the MFI to do the calculations for this century. By employing it as a linear relationship, we could estimate the R values as we also had knowledge of the

MFI values of this century. In addition to the linear nature of the relationship calculated by FAO (which is also used in the study), other relationships can also be interpreted (Table 2).

**Step 4:** We calculated the R values for the periods of 2021-2050, and 2071-2100. For both the near and the distant future, we prepared the average results as the average of every five years, then we visualized these data on maps. We edited the maps by kriging which was based on the data relating to the given settlements. The small number of data limits the preparation of statistical maps. This disadvantage is reduced by the nature of the results which were created to raise awareness about both time periods. It could not be calculated for the target data model limited of uncertainty, respectively. We did not aim at preparing a more accurate spatial and temporal estimation of rainfall intensity as it was restricted by the limitations and uncertainty of the computed model data, and the limited possibilities of the applied calculation. Applying the Gaussian process regression slightly improved the geostatistical method that had been based on little data. Practically it meant that elevation (despite the study area having relatively small elevation differences) as a supportive parameter was included in generating the pattern of the R factor when the maps were being produced (Goovaerts, 1999).

## RESULTS

We calculated the correlation of the R factor with the data measured for the 1999-2014 period by applying the Modified Fournier Index (MFI) for a linear relationship, (Figure 1). More than three dozens of such rainfall events occurred during that period which were characterized by >12.7 mm of rainfall. The correlation was 0.74 which indicates a significant relationship between the two parameters as the limit is 0.4 with a 1% probability. Hernando and Romana (2015) studied a smaller Spanish area with eight stations for a longer time period, and calculated a >0.8 correlation. It further strengthens the relationship between the R and the F/MFI/P that had already been proven by numerous researches earlier, however, it does not exclude further analyses.

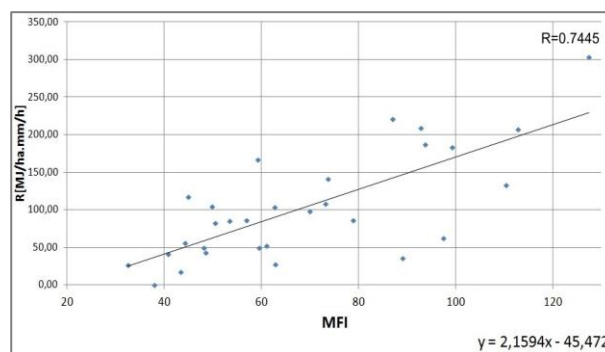


Fig. 1 The correlation between rainfall intensity (R) and the calculated MFI value on the basis of 10-minute data recorded from 1999 to 2014

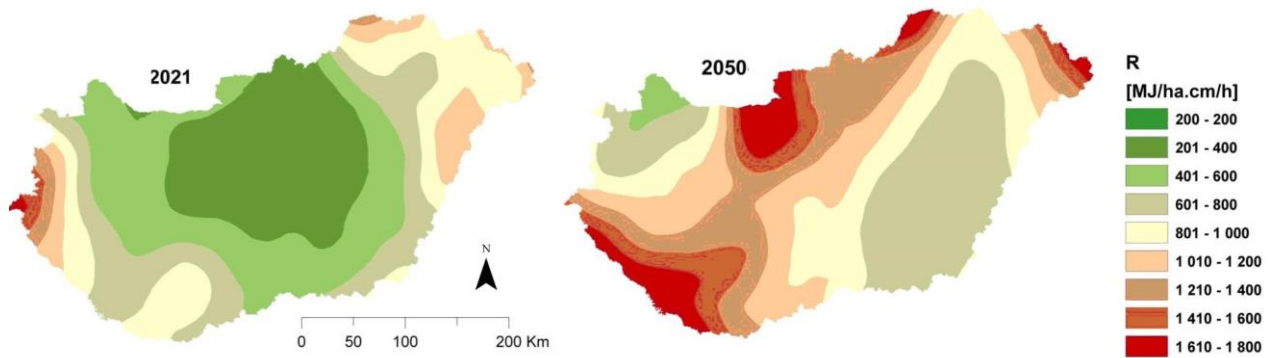


Fig. 2 Rain intensity values in two years of the modeled time period from 2021 to 2050

Changes in rainfall intensity can also be studied annually. The annual results of the R value using simulated data increase in the 30-year time period. We give two examples of our calculations calculated by the average values of the REMO and ALADIN models between 2021 and 2050. These results demonstrate that intensity varies both spatially and temporally (Fig. 2).

The initial values are characterized by 750 MJ/ha intensity, which is characteristic of the average values of the past 25 years (Panagos et al., 2014), and their increase is clearly observable from 2021 to 2050. Changes in the pattern of the R often follow the changes of relief (even if elevation differences are modest) and the changes in the amount of rainfall. The deviation of the R data shows a more significant change which is greater than the increase in the R values. Figure 2 represents the annual data displaying this change. The uncertain, simulated basic data can be evaluated on the basis of the average values of longer time periods.

Figure 3 displays the R values modeled for a nearer time period broken down by five years. The average figures for the short period support the fact that these data are not sufficient enough to reach an easily recognizable and well-established conclusion. However, when comparing to the average raw data of the 1961-1990 interval that served as the base of our study, we can see that the R value usually differs positively. The changes do

not exhibit regional trends though. Therefore, the average data of longer periods provide more reliable information.

Changes in rainfall intensity can be obtained by using average model values. The comparison was related to the average value calculated for the years between 1961 and 1990 which served as raw data. The regional climate models used in our study do not give the same known results when calculating the quantity of rain. The results of the models are, therefore, separately included (Table 3), but regional conclusions were drawn on the basis of the average values. The rate of growth both in the proximal and distant intervals is significant, it is more than 50% of the current value.

Compared to the raw data, the R value can as well be doubled, but it is not extremely high concerning European data. Other European peak values of the R index exceed 4,000, while the maximum mean value is 1,500 in Hungary. In addition, the environmental features and economic conditions of the Carpathian Basin are also remarkably different. This increase is in line with the projected growth of heavy rainfalls of >30 mm of rainfalls in the 21<sup>st</sup> century as the model results indicate. The increase of the mean R value can also be estimated locally. The joint calculations of the REMO – ALADIN models show the changes of mean values in Figure 4. The biggest change can be seen in the central and north-western parts of the Carpathian Basin in this period.

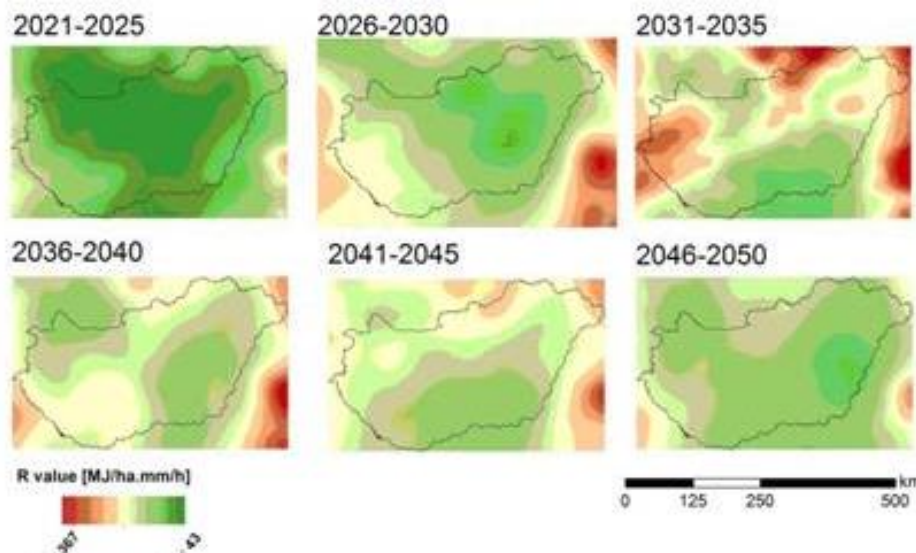


Fig. 3 Changes in the R value compared to the raw data of the 1961-1990 period

Table 3 Changes in the R value compared to the base period (1961-1990)

	ALADIN		REMO	
	2021- 2050	2071-2100	2021- 2050	2071-2100
<b>Mean</b>	+60.45 %	+50.99 %	+51.93 %	+53.17 %
<b>Minimum</b>	+41.38 %	+28.79 %	+27.86 %	+29.81 %
<b>Maximum</b>	+90.37 %	+72.61 %	+82.11 %	+86.19 %

**DISCUSSION AND CONCLUSION**

According to earlier analyses, the rainfall intensity index of the Carpathian Basin increased in the summer over the past 100 years (Lakatos et al., 2011). Based on the modeled characteristics of different climate change scenarios (eg. the number of rainy days, >30 mm of rainfalls), the previously mentioned growth characterizing the summer is not likely to continue, but the annual intensity is likely to increase due to fewer but heavier, more intense rainfall events (Tables 4 and 5). The amount of precipitation will not become less, but its annual distribution will be rearranged. The 20% reduction in summer precipitation will be compensated by the increase in winter precipitation, but the growing number of more intensive rainfalls indicates an increase in rainfall intensity.

In order to estimate the R value for this century, we used the Modified Fournier Index. We could reveal a significant correlation between the R and the MFI by using the precipitation data of the past nearly 30 years. By applying this trend and the data provided by the model results, we calculated a 50-80% increase in rainfall intensity for this century. Yet, the estimated 1,000-1,500 MJ/ha increase in intensity significantly lags behind the maximum values (5,000 to 6,000 MJ/ha) of certain regions in Italy, Croatia, or Slovenia (as well as western Scotland and southern Spain) (Panagos et al., 2014). The estimated value of R concerning Hungary comes near to the contemporary mean R values (1,300-1,600 MJ/ha) of the

previously mentioned countries. Of course, it must be taken into account that the Carpathian Basin is characterized by very different environmental features and land use.

One of the most obvious effects is how the increasing precipitation intensity influences agriculture. In order to measure it (either on model or standard Hungarian levels), versions of the Wischmeier-Smith formula (EPIC, USLE, RUSLE, etc.) are used the most. Although they operate with 5-7 variables, rainfall intensity (R) is the one that affects the extent of soil erosion the most. In terms of the extent of soil erosion, slope length, steepness, soil type are also sensitive parameters, but they can be considered stable at this scale. Land cover is also susceptible to the extent of soil erosion. In our case, however, the change should be a consequence rather than the cause of soil erosion growth. A change in land cover/land use could be a point of intervention which could help reduce the extent of erosion. Calculating the extent of soil erosion is not easy because the critical period from May to September. The climate data provided by the models predict greater R values and greater erosivity values in the long run despite decreasing summer precipitation. Apart from the rainfall erosivity factor, the extent of soil erosion is also regulated by terrain-, soil-, and land-cover-related data. The complexity of the system means that the conclusions drawn from the R data can only be considered as the mean values of longer periods, but the consequences of their possible effect may be useful to provide support for regional development.

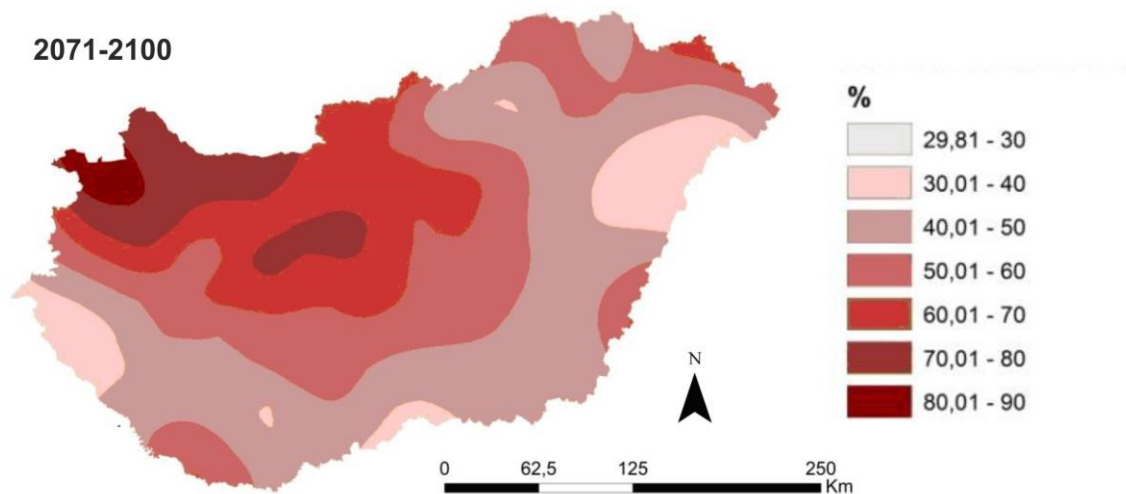


Fig. 4 The increase of the mean R value for the years 2071-2100 as calculated with REMO-ALADIN data

Table 4 Changes in the amount of annual precipitation in mm compared to the base data of the 1961-1990 period as calculated by the REMO and ALADIN models (Szabó et al., 2011)

Period	Annual mean	Spring	Summer	Autumn	Winter
2021-2050	-1 to 0	-7 to +3	-5	+3 to +14	-10 to +7
2071-2100	-5 to +3	-2 to +2	- 26 to -20	+10 to +19	-3 to +31

Table 5 Changes in precipitation and temperature compared to the base data of the 1961-1990 period as calculated by the REMO and ALADIN models (Blanka et al., 2013)

Parameter	The extent of change compared to the mean values of the 1961-1990 period			
	REMO 2021-2051	ALADIN 2021-2051	REMO 2071-2100	ALADIN 2071-2100
Precipitation (mm/year)	-42.6 – 58.5	-31.6 – 53.1	-16.5 - 101	-21.4 - (-84.2)
Temperature (°C/year)	1.2 – 1.5	1.7 - 2	3.4 – 3.7	3.4 – 3.7
RR> 30 mm (day/year)	0.7 – 1.0	0.6 – 1.2	1.0 – 1.5	0.9 – 1.3

On the basis of our results, it is necessary to provide more reliable and accurate raw data to define the R value (eg. using the ENSEMBLES model), and to further investigate soil erosion by applying vegetation change scenarios.

## References

- Arnoldus, H.M.J. 1980. An approximation of the rainfall factor in the Universal Soil Loss Equation. In: De Boodt, M., Gabriels, D. (Eds.): Assessment of Erosion. John Wiley & Sons, Chichester, 127–132.
- Blanka, V., Mezősi, G., Meyer, B. 2013. Projected changes in the drought hazard in Hungary due to climate change, Időjárás, J.Hungarian Meteorol. Serv., 117, 219–237.
- Borrelli, P., Diodato, N., Panago, P. 2016. Rainfall erosivity in Italy: a national scale spatio-temporal assessment. International Journal of Digital Earth, 2016 (online first) DOI: 10.1080/17538947.2016.1148203
- Centeri, Cs. 2002. Az általános talajvesztés becslési egyenlet (USLE) K tényezőjének vizsgálata. PhD dissertation. Szent István University. Gödöllő
- Deumlich D, Funk R, Frielinghaus M.O., Schmidt, W.A., Nitzsche. O. 2006. Basics of effective erosion control in German agriculture. *Journal of Plant Nutrition and Soil Science*, 169, 370–381. DOI: 10.1002/jpln.200621983
- van Dijk AI, Bruijnzeel LA, Rosewell CJ 2002 Rainfall intensity – kinetic energy relationships: a critical literature appraisal. *J. Hydrol* 261, 1–23. DOI: 10.1016/S0022-1694(02)00020-3
- Diodato, N., Bellochi. G. 2007. Estimating monthly (R)USLE climate input in a Mediterranean region using limited data. *J. Hydrol.*, 345, 224–236. DOI: 10.1016/j.jhydrol.2007.08.008
- Eltaiif, N.I., Gharaibeh, M.A., Al-Zaitawi, F., Alhamad, M.N. 2010. Approximation of rainfall erosivity factors in North Jordan. *Pedosphere* 20 (6): 711–717. DOI: 10.1016/S1002-0160(10)60061-6
- FAO 2004 <http://www.fao.org/docrep/006/y5160e/y5160e00.htm>
- Fournier, F. 1960. Climat et érosion. La relation entre l'érosion du sol par l'eau et les précipitations atmosphériques. [Relationship between soil erosion by water and rainfall]. Presses Universitaires de France, Paris. (In French.)
- Goovaerts, P. 1999. Geostatistics in soil science: state-of-the-art and perspectives. *Geoderma* 89 (1–2), 1–4. DOI: 10.1016/S0016-7061(98)00078-0
- Hernando, D., Romana, M.G. 2015. Estimating the rainfall erosivity factor from monthly precipitation data in the Madrid Region (Spain). *J. Hydrol. Hydromech.*, 63 (1), 55–62. DOI: 10.1515/johh-2015-0003
- Jenece, M., Kubatova, E., Tripl, M. 2006. Revised Determination of the Rainfall-runoff Erosivity Factor R for Application of USLE in Czech Republic. *Soil and Water Res.* 2, 65–71.
- Jordán, Gy., van Rompey, A., Szilassi, P., Csillag, G. 2004. Digitális domborzatmodell alkalmazása GIS környezetben a Káli-medence talaj-erózió vizsgálatában. HUNDEM, Miskolc. <http://www.uni-miskolc.hu/~fkt/hundem/Cikkek/Jordan%20Gy%20-%20A%20von%20Rompey%20-%20Szilassi%20P%20-%20Csillag%20G.pdf>
- Kertész Á., Richter, G. 1997. Results. Soil loss in the Örvényesi watershed In: The Balaton project. ESSC Newsletter 1997. 2-3. Bedford. European Society for Soil Conservation, 22–26.
- van der Knijff, J.M., Jones, R.J.A., Montanarella, L. 2000. European Commission directorate general JRC joint research centre Space Applications Institute European Soil Bureau Soil Erosion Risk Assessment. p.38 [http://www.unisdr.org/files/1581\\_ereurnew2.pdf](http://www.unisdr.org/files/1581_ereurnew2.pdf)
- Lakatos, M., Szentirmai, T., Bihari, Z. 2011. Application of gridded daily data series for calculation of extreme temperature and precipitation indices in Hungary. *Időjárás* 115 (1-2), 99–109.
- Lo, A., El-Swaify, S.A., Dangler, E.W., Shinshiro, L. 1985. EI30 as an erosivity index in Hawaii. In: El-Swaify S.A., Moldenhauer W.C. & Lo A. (eds), Soil erosion and conservation. Soil Conservation Society of America, Ankeny, 384–392.
- Mezősi, G., Meyer, B.C., Loibl, W., Aubrecht, Ch., Csorba, P., Bata, T. 2013. Assessment of regional climate change impacts on Hungarian landscapes. *Regional Environmental Change* 13, 4 797–811. DOI: 10.1007/s10113-012-0326-1
- Onchev, N.G. 1985. Universal index for calculating rainfall erosivity. In: El-Swaify, S.A., Moldenhauer, W.C., Lo, A. (Eds.): Soil erosion and conservation. Soil Conservation Society of America, Ankeny, 424–431.
- Panagos, P., Ballabio, C., Borrelli, P., Meusburger, K., Klik, A., Rouseva, S., Tadić, M.P., Michaelides, S., Hrabalíková, M., Olsen, P., Aalto, J., Lakatos, M., Rymaszewicz, A., Dumitrescu, A., Beguería, S., Alew, Ch. 2015. Rainfall erosivity in Europe. *Science of the Total Environment* 511, 801–814. DOI: 10.1016/j.scitotenv.2015.01.008
- Renard, K.G., Freimund, J.R. 1994. Using monthly precipitation data to estimate the R-factor in the revised USLE. *J. Hydrol.*, 157, 287–306. DOI: 10.1016/0022-1694(94)90110-4
- Sauerborn, P., Klein, A., Botschek, J., Skowronek, A. 1999. Future rainfall erosivity derived from large-scale climate models — methods and scenarios for a humid region. *Geoderma* 93. 269–27. DOI: 10.1016/S0016-7061(99)00068-3
- Stefanovics, P. 1992. Talajtan. Mezőgazda Kiadó, Budapest.
- Szabó, P., Horányi, A., Krüzselyi, I., Szépszó, G. 2011. The climate modelling at Hungarian Meteorological Survey: ALADIN and REMO. 36. Meteorológiai Tudományos Napok OMSZ, Budapest, 87–101.
- Szűcs, P. 2012. Az erózió lépték függése. PhD dissertation. Pannon Egyetem Keszthely p. 146.
- Wischmeier, W.H. 1959. A rainfall erosion index for a Universal Soil-Loss Equation. *Soil Sci. Soc. Am. Proc.* 23 (3), 246–249. DOI: 10.2136/sssaj1959.03615995002300030027x
- Wischmeier, W.H., Smith, D.D. 1978. Predicting rainfall erosion losses. A guide to conservation planning. Agriculture Handbook No. 537. U.S. Department of Agriculture, Washington, D.C



## IDENTIFICATION AND SPECTRAL EVALUATION OF AGRICULTURAL CROPS ON HYPERSPECTRAL AIRBORNE DATA

**Bálint Csendes\*, László Mucsi**

Department of Physical Geography and Geoinformatics, University of Szeged, Egyetem u. 2-6, H-6722 Szeged, Hungary

\*Corresponding author, e-mail: bcsendes@geo.u-szeged.hu

Research article, received 10 October 2016, accepted 15 December 2016

### Abstract

Hyperspectral remote sensing combined with advanced image processing techniques is an efficient tool for the identification of agricultural crops. In our study we pursued spectral analysis on a relatively small sample area using low number of training points to examine the potential of high resolution imagery. Spectral separability measurements were applied to reveal spectral overlapping between 4 crop species and for the discrimination we also used statistical comparisons such as plotting the PC values and calculating standard deviation of single band reflectance values on our classes. These statistical results were proven to be good indicators of spectral similarity and potential confusion of data samples. The classification of Spectral Angle Mapper (SAM) had an overall accuracy of 72% for the four species where the poorest results were obtained from the test points of garlic and sugar beet. Comparing the statistical analyses we concluded that spectral homogeneity does not necessarily have influence on the accuracy of mapping, whereas separability scores strongly correlate with classification results, implying also that preliminary statistical assessments can improve the efficiency of training site selection and provide useful information to specify some technical requirements of airborne hyperspectral surveys.

**Keywords:** hyperspectral remote sensing, Spectral Angle Mapper, spectral separability measurements, agricultural monitoring

### INTRODUCTION

High resolution aerial and satellite spectrometers opened new horizons for the computer-assisted analysis of land cover. Hyperspectral remote sensing techniques are not only used for identifying minerals, soils and urban surfaces, but they also constitute a powerful tool for the mapping of vegetation and natural habitats. Chlorophyll and other biochemical components have their very specific spectral characteristics, like absorption bands or the red edge in the near-infrared wavelength region, thus reflectance curves can be accurately classified if the spectral sampling of the data is subtle enough to detect these features.

Agricultural parcels are widely used for the calibration and testing of image processing tools as the spatially separated and homogeneous blocks of crops can be easily identified both on the images and in the field surveys.

There are a high number of scientific papers that deal with the spectral analysis of different vegetation parameters, natural habitats and agricultural plants (Visi-Rajczi et al., 2012; Burai et al., 2014; Kertész et al., 2014; Lausch et al., 2015). For example, advanced machine learning algorithms were employed for the detection of mixed pixels of weeds by Moshou et al. (2001), and Liu et al. (2010) were also using vector quantization for the mapping of fungal plant infections. The scope of environmental applications includes floodplains and saline soils (Burai

and Tomor, 2011; Kardeván et al., 2003), laboratory measurements for the estimation of various biochemical parameters (Lausch et al., 2016) and the monitoring of plant diseases (Liu et al., 2010; Visi-Rajczi et al., 2012).

In our study we focused on some basic statistical approaches to estimate the separability and the classification accuracy of crops based on hyperspectral aerial photography. Conclusions derived from our results can be used for the improvement of field surveys, feature and noise reduction and the preliminary planning of aerial photography campaigns.

### BACKGROUND

The so called curse of dimensionality is a significant obstacle to hyperspectral data interpretation, the large number of data bands combined with data noise and limited training areas can lead to poorer classification accuracy (Landgrebe, 2003). A possible way to mitigate this risk is either to improve the ground truth data set or to perform feature reduction (i. e. principal component transformation). In order to test the training pixels we can calculate spectral separability indices that indicate the overlappings between classes. Both Jeffries-Matusita and Transformed divergence algorithms were proven to be efficient tools for the evaluation of vegetation, soil and other land cover training sites (Büttner et al., 1988; Metternicht and Zinck, 1998; Ustin et al., 2009).



Another way to present spectral similarities is to plot image data to a 2 dimensional feature space where pixels are usually arranged in a triangle of soils, water surfaces and vegetation (Tobak et al., 2012).

The elaboration of ground survey is crucial for the agricultural applications of remote sensing, some studies show that adding biochemical and soil parameters increases mapping accuracy on high resolution imagery (Burai, 2006). Hence, the limitation of ground truth data is a serious constrain for the classifications which can be mitigated using non-parametric methods that are less sensitive to small deviations, like the SAM (Burai et al., 2010).

**STUDY AREA**

The geographical region of our study, the flood plain area called Tápai-rét is situated in southeastern Hungary, at the outskirts of the city of Szeged, over the confluence of rivers Tisza and Maros (Fig. 1). The landscape is mainly characterized by cultivated agricultural land and parcels of various sizes and settlements of scattered farmsteads. Due to its small differences of elevation and the remarkable diversity of crops Tápai-rét is an ideal site to examine spectral discrimination techniques.

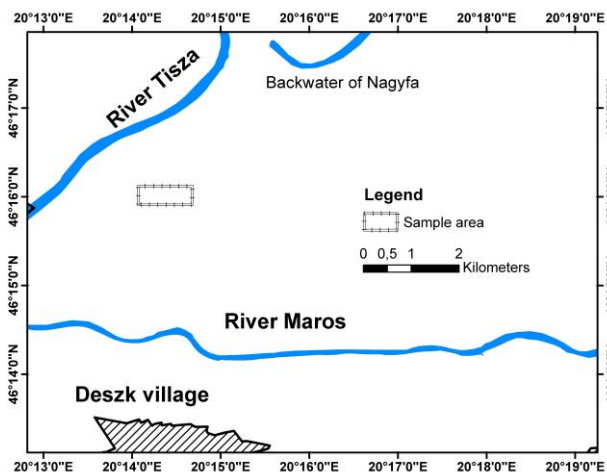


Fig. 1 The geographical location of the study area

Land use in Hungary is usually dominated by smaller agricultural parcels and it is also true for the Tápai-rét area where a great part of the territory belongs

to the irregular network of farm. The mosaic of small and diverse parcels imposes an obstacle to field surveys and significantly limits the number of available training points for the crops.

**DATA AND METHODS**

Hyperspectral imagery were acquired in September 2010 using the airborne spectrometer of AISA. Reflectance values were recorded on 359 spectral bands between the wavelength of 0.4 and 2.4 micrometers with a spatial resolution of 1.5 metres. Some of the bands contained significant amount of noise, the values for these wavelength regions were left blank on the reflectance curve diagram (Fig. 2). Around 120 spectral bands were removed based on their spatial autocorrelation values, however, we kept all the data from the region between 400 and 900 nanometers as these reflectance values are the most informative about vegetation characteristics.

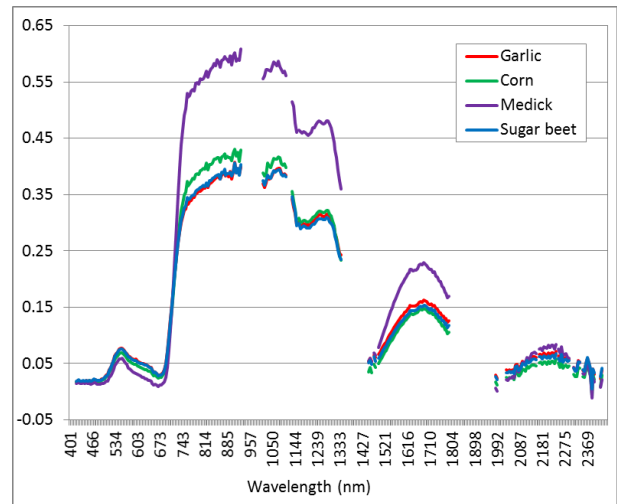


Fig. 2 Average spectra of the four crop species

We used online cadastral maps (Fig. 3) and the expertise of local farmers to collect ground truth data about the crops. The online map contains the 5 digit ID numbers for each parcel that are connected to the ownership information, the database is managed and regularly updated by the Hungarian Cadastral Office.



Fig.3 The online cadastral map of the study area

An accurate method to verify the selection of training points is the calculation of spectral separability. Formulas like the Jeffries-Matusita or the Transformed Divergence distance show index values on a scale of 0 to 2 where 0 refers to complete overlapping and 2 indicates perfect separability. These calculations are based on the comparison of reflectance or other data values within a certain range. However, it is essential to have more training points than the dimensionality, or in other words, the number of the spectral bands. In order to meet this criteria, feature reduction of the hyperspectral imagery is required if the set of data samples cannot be extended. For this purpose, in our study we performed a principal component transformation, where the first few transformed data bands contain most of the spectral information with a reduced degree of noise.

Another important aspect of the training site selection is the spectral homogeneity of the pixels. It can be affected by some possible spatial autocorrelation, the presence of noise, and also the heterogeneity of the examined land cover features. We selected spatially diverse training areas for the better characterization of our classes and to avoid the use of pixels with similar traces of noise. Standard deviation was calculated for single spectral bands both from the visible (550 nm) and the near-infrared region (900 nm).

The Spectral Angle Mapper (SAM) algorithm was applied for the classification which is considered as a relatively simple spectral statistical method as it calculates only the average of the sample spectra and the vector angle deviations of the individual test points, measured by the milliradian. Our goal was to compare the results of this non-parametric classifier with the values obtained from the training site image statistics.

**RESULTS**

*Spectral separability measurements*

To examine the possible spectral overlappings between the classes we performed spectral separability measurements. Jeffries-Matusita (JM) and Transformed Divergence (TD) indices have proven to be powerful tools for the evaluation of training areas (Metternicht and Zinck, 1998; Ustin et al., 2009; Tobak et al., 2013). Since these calculations require more spectral samples than the number of the input bands, we used a principal component transformation to reduce data dimensionality. Separability values were measured on the first two PC bands for the four crop classes (Table 1).

The TD index happened to be less sensitive to the overlappings than the JM, however, the results are in agreement as the ranking of the classes is the same, medick is completely separable from the rest of the species, while a high extent of spectral similarity occurs between the pixels of the other 3 classes, especially in the case of those of garlic and sugar beet.

Table 1 Jeffries-Matusita (JM) and Transformed Divergence (TD) indices based on the values of the first two Principal Component bands

	Medick	Corn	Garlic	Sugar beet	TD
Medick	0	2	2	2	Medick
Corn	2	0	1.08	0.58	Corn
Garlic	2	0.78	0	0.27	Garlic
Sugar beet	2	0.53	0.26	0	Sugar beet
JM	Medick	Corn	Garlic	Sugar beet	

*Scatter plot visualization*

Spectral classes can be visualized by plotting the pixel values of certain image bands, in our study we used the first two principal component bands to illustrate the relative positions of the pixel groups in the spectral space and indicated denser areas with lighter colour shades (Fig. 4). The elements of 2 dimensional plots usually form the shape of a triangle when studying imagery of a natural landscape where the three endmembers are vegetation, water and soil surfaces (Mucsi and Henits, 2011; Tobak et al., 2012). The scatter plot of our study area has the pixels of medick in the upper left corner, separated from the other crops which are closer to the brighter central region where most of the vegetation data points are located, thus confirming the findings of the separability measurements. In comparison, grassland pixels from the external regions of the original aerial photography can be found scattered below the main line of vegetation, water and some shaded surfaces are situated in the upper right corner of the triangle, while soils and concrete are in the bottom (Fig. 4).

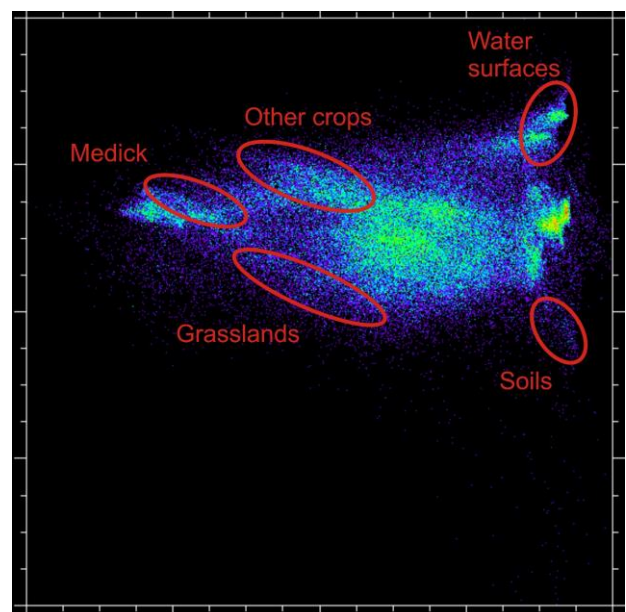


Fig.4 Crops featured on the scatter plot of the first two PC bands

### Homogeneity analysis

The outcome of the supervised classification is affected by the homogeneity of the training areas, therefore we analysed the standard deviation of reflectance values per single spectral bands (Table 2), where data from the visible range (550 nanometres), from the near infrared (900 nm), and one band from the short-wavelength infrared (SWIR) region (2100 nm) were used.

Reflectance values were found more homogeneous in the visible and in the SWIR wavelength regions, while there is a significant increase of the standard deviation at the near infrared light range that can be explained with the individual characteristics of the plants' spectral red edge. Corn shows relatively low heterogeneity compared to the other three species, however, these values depend not only from the spectral features of the vegetation, but also from the spatial distribution and the noise content of pixels.

Table 2 Standard deviation of reflectance values per single bands

Wavelength	Medick	Corn	Garlic	Sugar beet
550 nm	0.0090	0.0031	0.0067	0.0037
900 nm	0.0394	0.0235	0.0357	0.0337
2100 nm	0.0068	0.0041	0.0068	0.0062

### SAM classification

The SAM classification was performed without any spectral angle threshold specified to have more information on misclassifications between our crop classes. Table 3 shows the confusion matrix of the result, where columns represent the ground truth points (15 items per class) and rows display the classified pixels.

The two approaches of classification accuracy measurement (Users' and Producer's Accuracy) show more or less the same results on the reliability of identification. The overall accuracy of the mapping is on an acceptable level (72%), however, significant differences can be observed between the results of certain classes. The worst performance was in the category of sugar beet, where the slight majority of control pixels were misclassified. Also, the highest extent of confusion was registered between sugar beet and garlic.

Figure 5 presents the spatial distribution of the 4 classes on the true colour hyperspectral image. As it can be seen on the picture, the mapping categories of the crops rarely extend beyond the parcels, the SAM classification rather omitted to detect certain pixels of agricultural vegetation. The parcels of corn and medick are easily recognizable, their mapping classes designate more or less homogeneous blocks. On the other hand, in the case of the two western parcels there is a high level of misclassification, especially between the categories sugar beet, garlic, and corn, as it was predicted by the separability measurements.

Table 3 Confusion matrix of the SAM classification, indicating Users' Accuracy (U. A.) and Producer's Accuracy (P. A.)

	Medick	Corn	Garlic	Sugar beet	U. A.
Medick	15				100%
Corn		12	1	3	75%
Garlic			9	5	64%
Sugar beet		3	5	7	47%
P. A.	100%	80%	60%	47%	72%

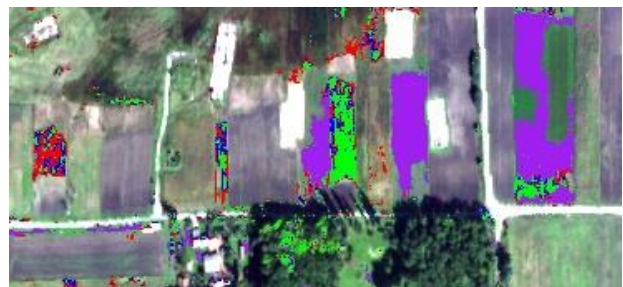


Fig. 5 The four SAM classes placed over the true colour image of the hyperspectral data: sugar beet (blue), garlic (red), corn (green), and medick (purple)

## DISCUSSION

SAM classifier was proven to be an accurate technique for the spectral discrimination of most of the crop species, however, in the cases of spectrally less separable plants (sugar beet and garlic) classification results were significantly poorer. The calculation of spectral angles has also the advantage that the outcome of the analysis is insensitive to the level of illumination of the surface objects, thus shaded pixels will have a lower rate of misclassification (van der Meer, 2004; Lillesand et al., 2004; Kruse et al., 1993). Some papers also suggest that SAM provides acceptable results on hyperspectral data when the number of training points is significantly limited (Burai et al., 2010; Tobak et al., 2012), although an increasing number of authors prefers machine learning algorithms for advanced classifications and land cover mapping (Huang et al., 2002; Lary et al., 2015).

Our finding, that the Jeffries-Matusita distance is more sensitive to spectral similarities than Transformed Divergence has confirmed the same conclusions of Jensen 1986.

In his study Burai (2006) examined the spectral features of similar plants (medick, corn, sugar beet, etc.) in a much larger study area, obtaining an overall mapping accuracy of 85,5%. He argued that the use of an extended and more detailed ground truth database including soil parameters can significantly improve the reliability of classifications, which is in line with our conclusions.

## CONCLUSION

Our main goal was to compare classification results with some spectral statistical analyses we performed on the PC transformed data and on single spectral bands. Using spectral separability measurements we found two classes that show significant overlapping (sugar beet and garlic) what was also confirmed by the SAM accuracy results. Also, it was proven that spectral separability distances correlate with classification results, where a higher degree of spectral overlapping on the PC transformed data can lead to poorer accuracy even in the case of a high resolution hyperspectral dataset. We also examined the spectral homogeneity of training points and we concluded that the standard deviation values of the classes do not show a strong correlation with the classification's outcome.

As the SAM results resembled those of the separability distance calculations, we drew the conclusions that despite the possible data loss, principal component transformation is an applicable tool for the identification and comparison of crops on high resolution imagery even when spectral differences are very subtle and the size of training areas is limited.

## Acknowledgement

This research was supported by the European Union and the State of Hungary, co-financed by the European Social Fund in the framework of TÁMOP 4.2.4. A/2-11-1-2012-0001 'National Excellence Program'.

## References

- Burai, P. 2006. Földhasználat-elemzés és növény-monitoring különböző adattartalmú és térbeli felbontású távérzékelési felvételek alapján (Land use analysis and vegetation monitoring using remote sensed images of different data content and spatial resolution). *Agrártudományi Közlemények* 2006/22 Különszám, 7–12. (In Hungarian)
- Burai, P., Tomor, T. 2011. Hiperspektrális felmérés eredményei az Ipoly Balassagyarmat és Ipolytarnóc közötti szakaszán (The results of the hyperspectral survey along river Ipoly between Balassagyarmat and Ipolytarnóc. In: A Bükk Nemzeti Park Igazgatóság természeti értékeinek kutatása I.: „Az Ipoly–vízgyűjtő vizes élőhelyeinek komplex felmérése, közösségi jegyzékeinek kidolgozása” Felsőtárkány, 2011 (Conference book, in Hungarian). Online at: <https://bnpi.hu/file/45/>.
- Burai, P., Lövei, G. Zs., Lénárt, Cs., Nagy, I., Enyedi, P. 2010. Mapping aquatic vegetation of the Rakamaz-Tiszanagyfalui Nagy-morotva using hyperspectral imagery. *Acta Geographica Debrecina Landscape & Environment*, 4 (1), 1–10.
- Burai, P., Deák, B., Oroly, V., Lénárt, Cs. 2014. Mapping of Grass Species Using Airborne Hyperspectral Data. In: Pfeifer, N., Zlinszky, A. (eds) Proceedings of the International Workshop on Remote Sensing and GIS for Monitoring of Habitat Quality, Vienna, 87–88.
- Büttner, Gy., Csillag, F., Mather, P. M. 1988. Spectral And Spatial Information Content Of Spot Data. In: Geoscience and Remote Sensing Symposium, 1988. IGARSS '88. Remote Sensing: Moving Toward the 21st Century. International; 10/1988 DOI: 10.1109/IGARSS.1988.570172
- Huang, C., Davis, L. S., Townshend, J. R. G. 2002. An assessment of support vector machines for land cover classification. *International Journal of Remote Sensing* 23, 725–749. DOI: 10.1080/01431160110040323
- Jensen, J. R. 1986. Introductory digital image processing: A remote sensing perspective. Englewood Cliffs, NJ: Prentice-Hall.
- Kardeván, P., Vekerdy, Z., Róth, L., Sommer St.–Kemper, Th., Jordan, Gy., Tamás, J., Pechmann, I., Kovács, E., Hargitai, H., László, F. 2003. Outline of scientific aims and data processing status of the first Hungarian hyperspectral data acquisition flight campaign, 3rd EARSeL Workshop on Imaging Spectroscopy in Oberpfaffenhofen, 13–16 May 2003
- Kertész, P., Király, G., Burai, P. 2014. Tree Species Mapping Using Airborne Hyperspectral Remote Sensing. In: Pfeifer, N., Zlinszky, A. (eds) Proceedings of the International Workshop on Remote Sensing and GIS for Monitoring of Habitat Quality, Vienna, 60–62.
- Kruse, F. A., Lefkoff, A. B., Boardman, J. W., Heidebrecht, K. B., Shapiro, A. T., Barloon, J. P., Goetz, A. F. H. 1993. The spectral image processing system (SIPS) - Interactive visualization and analysis of imaging spectrometer data. *Remote Sensing of Environment* 44, 145–163. DOI: 10.1016/0034-4257(93)90013-n
- Landgrebe, D. A. 2003. Signal Theory Methods in Multispectral Remote Sensing. John Wiley & Sons, Inc.
- Lary, D. J., Alavi, A. H., Gandomi, A. H., Walker, A. L. 2015. Machine learning in geosciences and remote sensing. *Geoscience Frontiers* 7, 3–10. DOI: 10.1016/j.gsf.2015.07.003
- Lausch, A., Salbach, C., Doktor, D., Schmidt, A., Merbach, I., Pause, M. 2015. Deriving phenology of barley with imaging hyperspectral remote sensing. *Ecological Modelling* 295, 123–135. DOI: 10.1016/j.ecolmodel.2014.10.001
- Lausch, A., Bannehr, L., Beckmann, M., Boehm, C., Feilhauer, H., Hacker, J. M., Heurich, M., Jung, A., Klenke, R., Neumann, C., Pause, M., Rocchini, D., Schaeppman, M. E., Schmidlein, S., Schulz, K., Selsam, P., Settele, J., Skidmore, A. K., Cord, A. F. 2016. Linking Earth Observation and taxonomic, structural and functional biodiversity: Local to ecosystem perspectives. Ecological indicators. DOI: 10.1016/j.ecolind.2016.06.22 (in press)
- Lillesand, T. M., Kiefer, R. W., Chipman, J. W. 2004. Remote Sensing and Image Interpretation (Fifth Edition). John Wiley & Sons, Inc.
- Liu, Zh-Y., Wu, H-F., Huang, J-F. 2010. Application of neural networks to discriminate fungal infection levels in rice panicles using hyperspectral reflectance and principal components analysis. *Computers and Electronics in Agriculture* 72, 99–106. DOI: 10.1016/j.compag.2010.03.003
- van der Meer, F. D. 2004. Pixel-Based, Stratified and Contextual Analysis of Hyperspectral Imagery. In: de Jong, S. M., van der Meer, F. D. (eds) Remote Sensing Image Analysis: Including the Spatial Domain, Dordrecht, Springer Academic Publishers, 153–180.
- Metternicht, G. I., Zinck, J. A. 1998. Evaluating the information content of JERS-1 SAR and Landsat TM data for discrimination of soil erosion features. *ISPRS Journal of Photogrammetry & Remote Sensing*, 53, 143–153. DOI: 10.1016/S0924-2716(98)00004-5
- Moshou, D., Vrindts, E., De Ketelaere, B., De Baerdemaeker, J., Ramon, H. 2001. A neural network based plant classifier. *Computers and Electronics in Agriculture* 31, 5–16. DOI: 10.1016/S0168-1699(00)00170-8
- Mucsi, L., Henits, L. 2011. Belvízelöntési térképek készítése közepes felbontású űrfelvételek szubpixel alapú osztályozásával (Mapping inland excess water using subpixel classification of middle resolution satellite images) *Földrajzi közlemények* 135(4), 365–378. (In Hungarian).
- Tobak, Z. 2013. Urban surface analyses using high temporal and spectral resolution aerial imagery. PhD theses, University of Szeged, Hungary.
- Tobak, Z., Csendes, B., Henits, L., van Leeuwen, B., Szatmári, J., Mucsi, L. 2012. Városi felszín spektrális tulajdonságainak vizsgálata légifelvételek alapján (Spectral analysis of urban surfaces using aerial photography) In: Lóki, J. (ed) Az elmélet és gyakorlat talákozása a térinformatikában III, Debrecen, 413–420. ISBN:978-963-318-218-5 (In Hungarian:).
- Ustin, L. S., Valko, P. G., Kefauver, S. C., Santos, M. J., Zimpfer, J. F., Smith, S. D. 2009. Remote sensing of biological soil crust under simulated climate change manipulations in the Mojave Desert. *Remote Sensing of Environment* 113, 317–328. DOI: 10.1016/j.rse.2008.09.013
- Visi-Rajczi, E., Burai, P., Király, G., Albert, L. 2012. Ecological Characterization of the green areas in Sopron by Plant Chemical Analysis and Hyperspectral Recording. In: The Impact of Urbanization, Industrial and Agricultural Technologies on the Natural Environment: International Scientific Conference on Sustainable Development and Ecological Footprint. University of West Hungary, Sopron. ISBN 978-963-334-047-9